# Seismic Performance of Steel Plate Shear Walls Using Nonlinear Static Analysis

Moon Moon Dhar

A Thesis in
The Department of
Building, Civil and Environmental Engineering

Presented in Partial Fulfillment of the Requirements
for the Degree of Master of Applied Science (Civil Engineering) at
Concordia University Montreal, Quebec Canada

April, 2015

CONCORDIA UNIVERSITY
School of Graduate Studies

This is to certify that the thesis prepared

By: Moon Moon Dhar

Entitled: Seismic Performance of Steel Plate Shear Walls System Using Nonlinear Static Analysis

and submitted in partial fulfillment of the requirements for the degree of

MASc Civil Engineering

complies with the regulations of the University and meets the accepted standards with respect to originality and quality.

Signed by the final Examining Committee:

Dr. Adel Hanna Chair

Dr. M. Zahangir Kabir Examiner

Dr. Lan Lin Examiner

Dr. Anjan Bhowmick Supervisor

Approved by

Chair of Department or Graduate Program Director

Dean of Faculty

Date

# ABSTRACT

Seismic Performance of Steel Plate Shear Walls Using Nonlinear Static Analysis

Moon Moon Dhar

Unstiffened steel plate shear wall (SPSW) is considered as a primary lateral load resisting system due to its significant post-buckling strength, high ductility, stable hysteretic behaviors and robust initial stiffness. Nonlinear seismic analysis can accurately estimate structural responses, however, the method is very time consuming and may not be suitable for regular engineering practice. On the other hand, traditional pushover analysis method does not consider contributions of higher modes to the structural responses and thus, often do not provide good estimation of seismic responses for taller buildings. Capacity-Spectrum Method (CSM) and modal pushover analysis (MPA) are two simple nonlinear static methods that have been proposed and recently used for seismic performance evaluation of few lateral load-resisting systems. This research further examines the applicability of CSM and MPA methods to assess seismic performance of steel plate shear walls. A nonlinear finite element model was developed and validated with experimental studies. Three different SPSWs (4-, 8-, and 15-storey) designed according to capacity design approach were analysed by subjecting the steel shear walls under artificial and real ground motions for Vancouver. The CSM and MPA procedures were applied to analyse the selected SPSWs and the results were compared with more accurate nonlinear seismic analysis results. It is observed that both CSM and MPA procedures can reasonably predict the peak roof displacements for low-rise SPSW buildings. In addition, MPA procedure, which includes contributions of higher modes when estimating seismic demands of buildings, provides better predictions of critical seismic response parameters for taller SPSWs.

# Acknowledgements

I would like to convey my gratefulness and sincere appreciation to Dr. Anjan Bhowmick for his supervision, guidance and mentorship over the duration of my graduate studies. Special gratitude to my course instructors Dr. Jassim Hassan, Dr. Lucia Tirca and Dr. Ashutosh Bagchi for their support and direction in my graduate classes mainly related to Structural dynamics as well as earthquake engineering, which acted as foundation on my research background.

Faculty of Engineering and Computer Science, Concordia University, Montreal, Canada and the Natural Sciences and Engineering Research Council of Canada are gratefully acknowledged for their support and funding on this project.

Thanks to all my colleagues and friends specially Mona Raissi, Sandip Dey and Arghya Chatterjee for inspiring and supporting me during my graduate studies.

I would also like to thank my parents for their support and encouragement during my studies.

# Table of Contents

# List of Figures

# List of Tables

# List of Symbols

| | |
|---|---|
| $\mu$ | Ductility of the system |
| $A_1$ | Area under the design response spectrum |
| $A_2$ | Area under the ground motion response spectrum |
| $A_b$ | Cross-sectional area of boundary beam |
| $A_c$ | Cross-sectional area of boundary column |
| $B$ | Amplification factor in indirect capacity design approach |
| $c$ | Classical damping of SDOF, Matrix of classical damping of MDOF |
| $D$ | Dead load |
| $D_n$ | Displacement of "$n^{th}$-mode" SDOF system |
| $D_{rno}$ | Maximum displacement of "$n^{th}$-mode" SDOF system |
| $D_{rny}$ | Yield displacement of "$n^{th}$-mode" SDOF system |
| $D_t$ , $U_t$ | Displacement of MDOF system |
| $D_t^*$ | Displacement of SDOF and ESDOF system |
| $D_y^*$ | Yield displacement of ESDOF system |
| $E$ | Earthquake load |
| $F_i$ | Applied lateral forces at $i^{th}$ storey |
| $F_{sn}$ | Lateral force of "$n^{th}$-mode" SDOF system |
| $F_x$ | Storey lateral force |
| $F_y$ | Nominal strength of the infill plate |
| $F_y^*$ | Yield strength of the ESDOF system |

| | |
|---|---|
| $F_{yp}$ | Yield strength of the infill plate |
| $h_i$ | Height above the ground to $i^{th}$ storey |
| $h_n$ | Total building height |
| $h_s$ | Storey Height |
| $\iota$ | Influence vector |
| $I_{bb}$ | Moment of inertia of cross-section of bottom beam |
| $I_c$ | Moment of inertia of cross-section of boundary column |
| $I_E$ | Earthquake importance factor |
| $I_{tb}$ | Moment of inertia of cross-section of top beam |
| $K$ | Lateral stiffness of SDOF and matrix of lateral stiffness of MDOF system |
| $K_{in}$ | Initial Stiffness of "$n^{th}$-mode" SDOF system |
| $L$ | Steel frame width from center to center distance of boundary columns |
| LL | Live load |
| $L_{cf}$ | Clear distance between column flanges |
| $m^*$, $L_n$ | Mass of "$n^{th}$-mode" SDOF system |
| $m_i$ | Storey mass of $i^{th}$ storey |
| $M_n$ | Effective modal mass of $n^{th}$ mode of vibration |
| $M_v$ | Amplification factor to account higher mode effect |
| $P_{eff}$ | Effective earthquake force |
| $P_i$ | Lateral force distribution for inertia force |
| $q_n$ | Modal co-ordinator of $n^{th}$ mode of vibration |
| $R$ | Force reduction factor |
| $R_\mu$ , $R_d$ | Ductility related force reduction factor |

| | |
|---|---|
| $R_o$ | Over-strength related reduction factor |
| $S(T_a)$ | Design Spectral Acceleration for fundamental period of the building |
| $S_a$ | Inelastic spectral acceleration |
| $S_{ae}$ | Elastic spectral acceleration |
| $S_d$ | Inelastic spectral displacement |
| $S_{de}$ | Elastic spectral displacement |
| $S_n$ | Effective lateral force distribution for $n^{th}$ mode of vibration |
| $S_{nL}$ | Snow load |
| $T^*$ | Elastic period of SDOF system |
| $T_a$ | Fundamental period of the system |
| $T_s$ | Characteristics Period of response spectrum |
| $t_w$ | Infill plate thickness |
| $\ddot{u}_g(t)$ | Earthquake ground motion |
| $U_{rno}$ | Maximum roof displacement of MDOF system for $n^{th}$ mode of vibration |
| $U_{rny}$ | Yield displacement at the roof of MDOF system for $n^{th}$ mode of vibration |
| $V_b$ | Design base shear |
| $V_{bn}$ | Base shear for $n^{th}$ mode of vibration of MDOF system |
| $V_{bno}$ | Ultimate base shear at $U_{rno}$ |
| $V_{bny}$ | Yield base shear at $U_{rny}$ |
| $V_e$ | Expected shear strength of SPSW |
| $V_{re}$ | Probable shear resistance of SPSW |
| $V_s$ | Storey shear of SPSW |
| $V_{yp}$ | Storey shear strength of SPSW |

| | |
|---|---|
| $W$ | Seismic weight of the building |
| $W_i$ | Seismic weight of the $i^{th}$ storey |
| $\alpha$ | Angle of inclination of tension field of steel infill plate |
| $\alpha_n$ | Strain hardening of "$n^{th}$ mode" pushover analysis |
| $\Gamma$ | Modal participation factor; Modal transformation factor |
| $\xi_n$ | Damping of "$n^{th}$ mode" SDOF system |
| $\varphi$ | elastic mode shape |
| $\varphi_b$ | Inclination of equivalent brace |
| $\omega_n$ | Natural frequency of vibration of the system |
| $\Omega_s$ | System over-strength factor |

# Abbreviation

| | |
|---|---|
| ADRS | Acceleration displacement response spectrum |
| AISE | American Institute of Steel Construction |
| ASCE | American Society of Civil Engineers |
| ATC | Applied Technology Council |
| CSA | Canadian Standards Association |
| CSM | Capacity spectrum method |
| FEM | Finite Element Model |
| FEA | Finite Element Analysis |
| ESDOF | Equivalent Single degree of freedom |
| FEMA | Federal Emergency Management Agency |
| GMR | Ground motion record |
| HHT | Hilber hughes taylor |
| MDOF | Multi degree freedom system |
| MMPA | Modified modal pushover analysis |
| MPA | Modal pushover analysis |
| NBCC | National Building Code of Canada |
| NTHA | Nonlinear time history analysis |
| PBSD | Performance based seismic design |
| PEER | Pacific Earthquake Engineering Research |
| RET | Reverse energy technique |
| SDOF | Single degree of freedom |
| SPSW | Steel plate shear wall |

## Chapter-One

# Introduction

### 1.1. Background

Steel Plate Shear Wall (SPSW) system is an effective seismic load resisting system for new building and seismic up gradation of existing buildings. Its robust post-buckling strength, large ductility, great initial stiffness and stable hysteretic behaviors have introduced it as an alternative to conventional lateral load resisting systems. The SPSW system is made of a steel plate that is connected as an infill to the structural frame of the building composed of beams and columns. Boundary beams-to-columns connection may be either simple or rigid connections. The steel infill plate is either bolted or welded to these boundary elements using fishplates. SPSW system offers a light-weight structure, increases floor area, decreases foundation cost and better quality control when compared to a conventional reinforced concrete shear wall.

Originally, SPSWs were designed to prevent elastic out-of-plane buckling of plates, so that SPSWs were built either with thick steel plates or with stiffened steel plates. In 1980s, researches established the design philosophy of the use of thin unstiffened infill plates. The shear is primarily resisted by the diagonal tension field that forms in the unstiffened infill plate when they have buckled. Axial coupling of column loads is the main mechanism to resist the overturning moment in the SPSW system. This design philosophy is accepted by the current Canadian (CAN/CSA-S16-09) and American (ANSI/AISC 2010) steel design standards.

Both the American and Canadian design provisions for SPSW are based on the capacity design approach where steel plates and beams ends are designed to dissipate energy as a preliminary ductile fuse. AISC 2010 has provided provisions for three different capacity design approaches they are, nonlinear pushover analysis; indirect capacity design approach; and combined linear elastic computer programs and capacity design concepts. The prescriptive strength and deflection limitations of both Canadian and American design standard cannot provide actual performance evaluation of SPSWs. Performance-based seismic design (PBSD) is the new concept of design where the design procedure certifies the probable level of performance of a structure under a given level of hazard. PBSD requires a precise performance assessment of the structure at various stages in the design. Several studies have been performed under real seismic loading to evaluate different design procedures as well as performance evaluation of the SPSW systems. Evaluation of seismic performance of SPSW systems is mainly limited in nonlinear dynamic analysis. Due to its complexity and time-consuming manner, nonlinear dynamic analysis is not very convenient for design offices as well as for PBSD application. Therefore, simple and effective performance evaluation method needs to be developed for SPSW systems to apply performance based seismic design.

Various nonlinear static procedures are suggested by different guidelines (FEMA-273, FEMA-356) for performance evaluation. Capacity-spectrum method and modal pushover analysis are two nonlinear static procedures and tools for performance based seismic design, which are simple and effective methods for performance assessment of any structure. Effectiveness of these methods has been proved for various framed structures. No research work has been conducted to assess the applicability of these methods for seismic performance

evaluation of SPSW system. Applicability and accuracy of these two procedures for seismic performance assessment of SPSW should be investigated. Due to the expenses involved in the experimental study, an analytical tool that can accurately predict the monotonic, cyclic and dynamic behaviour of thin unstiffened SPSWs is also essential. Applicability of capacity-spectrum method and modal pushover analysis for seismic performance evaluation should be examined by comparing their results with nonlinear dynamic analysis of the SPSWs.

## 1.2. Objectives and Scope

Major objectives of this research are listed below:

1. To develop an effective finite element model to study the behavior of unstiffened steel plate shear wall. A finite element model is developed by considering material and geometrical nonlinearities. This finite element model is verified with two experimental studies.
2. To assess seismic performance of steel plate shear walls. Nonlinear seismic analyses are performed and important performance parameters of steel plate shear wall are investigated.
3. One of the major objectives of this study is to verify seismic performance of steel plate shear walls by applying capacity-spectrum method. Inelastic roof displacement demand and Structural actual ductility demand are estimated as the performance parameter for this analysis method.
4. Another main objective of this research is to assess seismic parameters of SPSW using modal pushover analysis method. Different major seismic performance parameters are estimated for all significant vibration modes. Three steel shear walls (4-, 8-, and 15-

storey) are considered to investigate the applicability of modal pushover analysis technique and capacity-spectrum method for SPSW systems. The applicability of capacity-spectrum method and modal pushover analysis method to assess seismic performance of SPSW is investigated by comparing their results with results from detailed nonlinear seismic analysis.

## 1.3. Thesis Outline

This thesis has primarily been divided in six chapters. In this chapter, a brief discussion of existing problems related to performance evaluation of SPSW systems has been discussed. At last, objectives and scope of the thesis have also been presented.

Chapter 2 presents review of some previous research works. A brief review of some relevant analytical and experimental research works on unstiffened thin SPSW systems and current design standards of SPSW are discussed in the beginning of the chapter. Some previous studies on Capacity-Spectrum method and Modal-Pushover analysis are also discussed in this chapter.

Chapter 3 describes the selection of finite element modeling technique. It also describes the finite element model that was developed to study the performance of unstiffened thin SPSW system. The finite element model has been validated with two experimental programs of quasi-static cyclic analysis. Chapte-3 also provides the description of the design and modeling of one 4-storey and one 8-storey SPSW systems, which designed based on capacity design approach of CSA\CAN S16-09. Finally, nonlinear time history analysis and response of SPSWs have been presented.

Chapter 4 and 5 present the application of Capacity Spectrum method and Modal pushover method respectively to estimate seismic performance as well as seismic demand of SPSW. At the end of each chapter, result and discussion are also discussed. Estimated performances of SPSWs by capacity-spectrum method and modal pushover analysis have further been compared with nonlinear dynamic analysis to evaluate the applicability of these methods for seismic performance evaluation of SPSW systems.

Finally, all of the major findings of this study are presented in chapter 6. Future scope and recommendations are also presented in this chapter.

Chapter-Two

# Literature Review on Steel Plate Shear Walls

## 2.1 Introduction

Several experimental and analytical research programs have been conducted since 1970s to investigate the behavior of Steel Plate Shear Walls (SPSWs) as well as its design procedure. In 1960s, SPSW was first introduced in Japan as a lateral load resisting system in the building. In that time, SPSWs were designed to resist lateral load by preventing shear buckling in infill plates under design seismic loads. Therefore, heavily stiffened thin-plates and moderately stiffened thick-plates were used in the SPSW design. Over time, analytical and experimental studies have shown that post-buckling strength of thin infill plate is significant and thus, the use of thin unstiffened infill plates in SPSW has been accepted by researchers and designers. In an unstiffened SPSW system, thin infill panels are the main energy dissipation element, which is allowed to buckle out-of-plane. The inclined tension field action of the plates develops the shear resistance. The primary objective of this chapter is to review some experimental and analytical research works on unstiffened SPSWs as well as the design guidelines in current US and Canadian provisions. The present condition of the seismic performance evaluation of SPSW system and some research works on simplified analysis procedures such as, modal pushover analysis and capacity spectrum method will be addressed in this chapter.

## 2.2 Selected Research on SPSW system

### 2.2.1 Experimental Research on SPSW

A number of experimental studies have been conducted in past 3 decades to analyse the behavior of unstiffened thin SPSW systems. Some of the major representative researches are discussed in this section.

Elgaaly (1998), Elgaaly et al. (1993), Caccese et al. (1993) carried out a number of cyclic tests on small-scale SPSW systems to observe post-buckling behavior of unstiffened thin SPSWs. This whole study was performed in two different phases; such as eight quarter-scale specimens in phase-I and seven one-third scale specimens in phase-II. The Major findings of this study were: (a) SPSW specimens with welded plate showed higher stiffness than the specimens with bolted plate; (b) mode of failure was not affected by the bolt spacing and failure of the SPSWs with bigger bolt spacing were occurred due to the plate rupture and shearing of the bolts; (c) column axial compression up to 50% of column nominal axial force, had negligible effect on the SPSW capacity.

Caccese et al. (1993) conducted another experimental study for quasi-static cyclic loading on small scale, single bay SPSW specimens to evaluate seismic effectiveness of the system. Effects of beam-to-column connections and the plate thickness on the overall SPSW behavior were evaluated on these experimental programs. The main outcomes of the program were: (a) beam-to-column connections had minor effect on the SPSW behavior but greater energy dissipation was achieved by moment connection; (b) plate has an optimum thickness, thicker plate could not increase system strength but in that case plate failed by buckling or yielding in the boundary columns.

Driver et al. (1997, 1998) performed an experimental test on a large-scale four storeys single bay SPSW specimen for quasi-static cyclic loading. Moment resisting beam-to-column connections were used for the boundary members of SPSW specimen. Infill plates were welded to fishplates and at the same time, those plates were welded to the boundary elements. Schematic figure of Driver et al. (1997, 1998) test specimen with all geometrical details is presented in Figure 2.1. Cyclic lateral loads were applied as per the requirements of ATC-24 (Applied Technology Council 1992) and gravity load was applied prior to cyclic load application. A total 30 load cycles were applied to the test specimen including 20 cycles in inelastic range. The test specimen showed very high initial stiffness and significant energy dissipation with very high ductility. The deterioration of the load-carrying capacity was found very stable and gradual beyond the ultimate strength. It was concluded that a properly designed SPSW system is an excellent lateral load-resisting system for seismic loading.

Behbahanifard et al. (2003) performed a quasi-static cyclic testing on a large scale, three-storey, single bay SPSW specimen which was the top three stories of Driver et al. (1997) test specimen. Significant yielding was observed only in the bottom storey of Driver et al. (1997) test specimen and top three stories infill plates buckled elastically during the previous test. During the test by Behbahanifard et al. (2003), it was observed that ultimate capacity of the first storey of three-storey specimen was seven times of its yield displacement. After that, degradation started gradually due to the tears in the bottom-storey infill plate. This test again proved the high initial stiffness, excellent ductility and high-energy absorption capacity of the SPSW system.

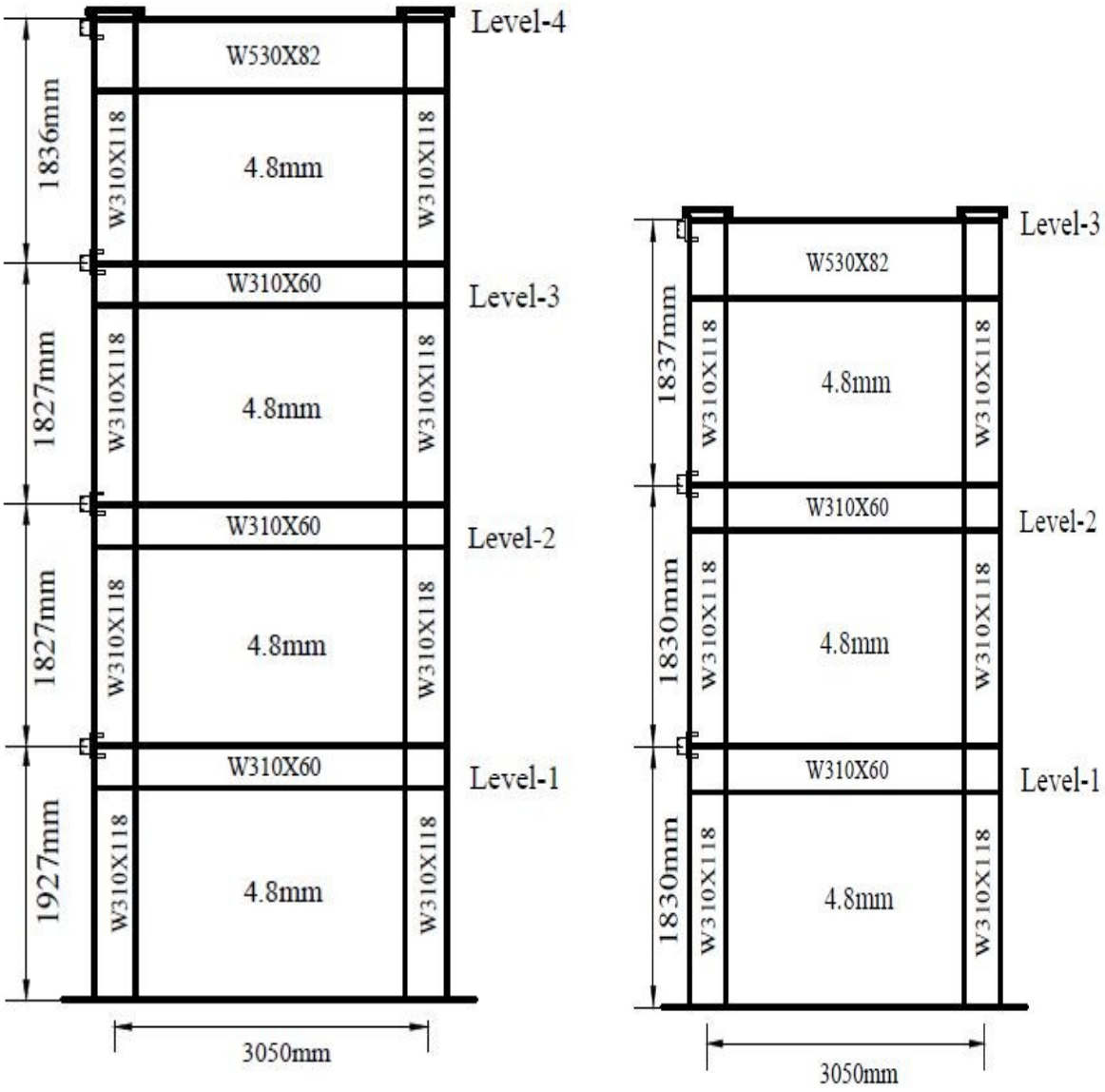


Figure 2.1: Schematic figure of Driver et al. (1997) test specimen (left) and Behbahanifard et al. (2003) test specimen (right)

Lubell et al. (2000) conducted experimental studies on two single-storey steel plate shear wall (SPSW1 and SPSW2) and one 4-storey steel plate shear wall (SPSW4) specimen. Quasi-static cyclic analysis was conducted on those specimens where ATC-24 (Applied Technology Council 1992) guidelines were followed for the loading history. The entire specimen showed very high initial strength, well-defined load-deformation envelopes as well as stable hysteresis behavior. Major findings of this study were: (1) stiffness and capacity of SPSW significantly increased when top beam can offer better anchorage for the tension field developed in the infill plate (2) Insufficient column flexural stiffness can produce significant "pull-in" in the column and undesirable yielding sequence which can create global instability of the system (3) due to the high axial forces and moments in the columns the yielding sequence can be altered. It also indicated that the behavior of a single isolated SPSW is different from a multistory SPSW.

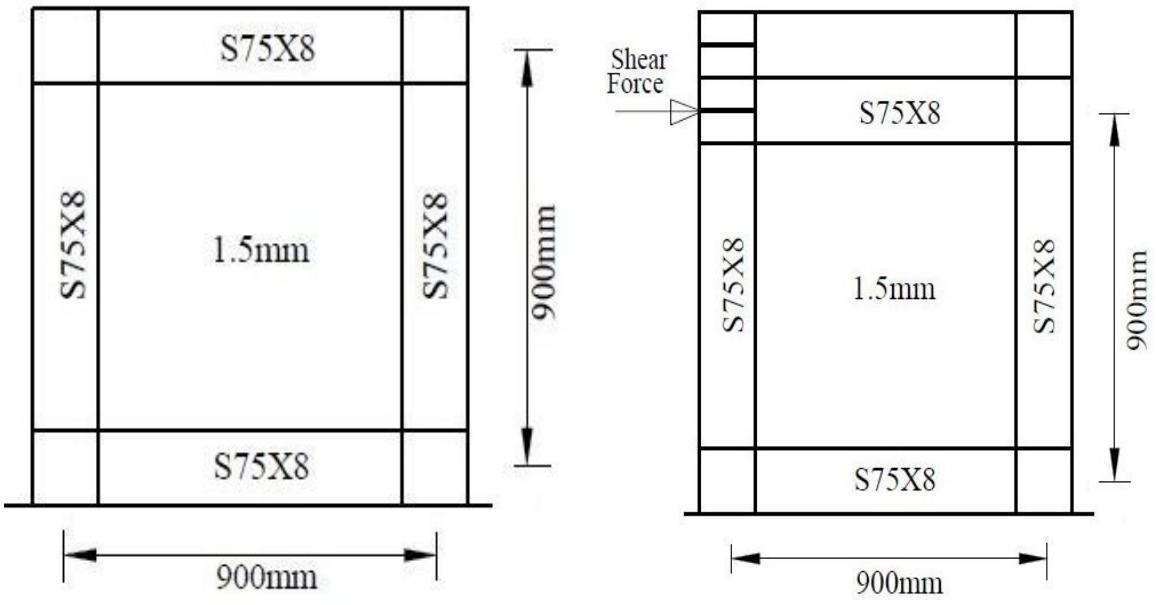


Figure 2.2: Two single-storey test specimens, SPSW1(left) and SPSW2(right) of Lubell et al. (2000)

### 2.2.2 Analytical Research on SPSWs

Analytical research studies were mainly based on non-laboratory theoretical works. Main purpose of these studies is to investigate the behavior of the SPSW and to develop the design method of SPSW systems through the modeling and analysis in order to represent the pre- and post-buckling behavior of SPSW.

#### 2.2.2.1 Development of "Strip-model"

Thorburn et al. (1983) introduced an analytical model to study shear resistance of a thin unstiffened SPSW based on the theory of pure diagonal tension proposed by Wagner (1931). Post-buckling shear resistance by tension field action was considered as the force resisting mechanism. SPSW was modeled as a series of pin-ended strips oriented in the similar direction as the main tensile stress in the infill plate. Each strip was modeled with an area equal to the width of the strip multiplied by the plate thickness. Beams were assumed as infinitely stiff and simply connected with columns. The angle of tension field was obtained by using the principle of least work. This model is known as "strip-model" which has later been acknowledged by Canadian Steel Design Standards (CSA 2009) later on. The angle of inclination of the tension field, α, was developed as___

$$\tan^4 \alpha = \left[ \frac{1 + \frac{L t_w}{2 A_c}}{1 + \frac{h_s t_w}{A_b}} \right] \qquad 2.1$$

where, $h_s$ is the storey height, $t_w$ is the infill plate thickness, $L$ is the frame width, and $A_b$ and $A_c$ are the cross-sectional areas of the beam and column respectively. In addition to the strip-model, Thorburn et al. (1983) proposed a Pratt truss-model for analysis of unstiffened thin SPSW that is

known as "equivalent brace model". A diagonal brace was used to represent the infill plate and its equivalent stiffness was calculated from the original strip-model. It can reduce a significant amount of computational complexity than original strip-model. The area of the brace ($A$) is calculated as follows:

$$A = \frac{t_w L \sin^2 2\alpha}{2 \sin \varphi_b \sin 2\varphi_b} \qquad 2.2$$

Where, $\varphi_b$ is the inclination of the brace and all other parameters are as defined earlier. CAN/CSA-S16-09 (CSA 2009) recommended the equivalent brace model as a preliminary tool for SPSW analysis and design. However, this model is not able to represent the distributed forces that are applied on the boundary element from the plate. Analytical model of Thorburn et al. (1983) for strip-model is presented in Figure 2.3

Timler and Kulak (1983) verified strip-model by an experimental study of a single storey- single bay large scale SPSW specimen with service and ultimate level of loading. It was observed that the angle of inclination of the tension field was affected by the bending stiffness of the columns. Equation 2.1 was modified as follows by considering the bending strain energy of the boundary columns:

$$\tan^4 \alpha = \left[ \frac{1 + \frac{L t_w}{2 A_c}}{1 + h t_w \left( \frac{1}{A_b} + \frac{h^3}{360 I_c L} \right)} \right] \qquad 2.3$$

Where, $I_c$ is the moment of inertia of the adjacent columns. The "strip-model" developed by Thorburn et al. (1983) and the angle of inclination modified by Timler and Kulak (1983) have been approved by CAN/CSA S16-09 (CSA 2009) and (ANSI/AISC 2010).

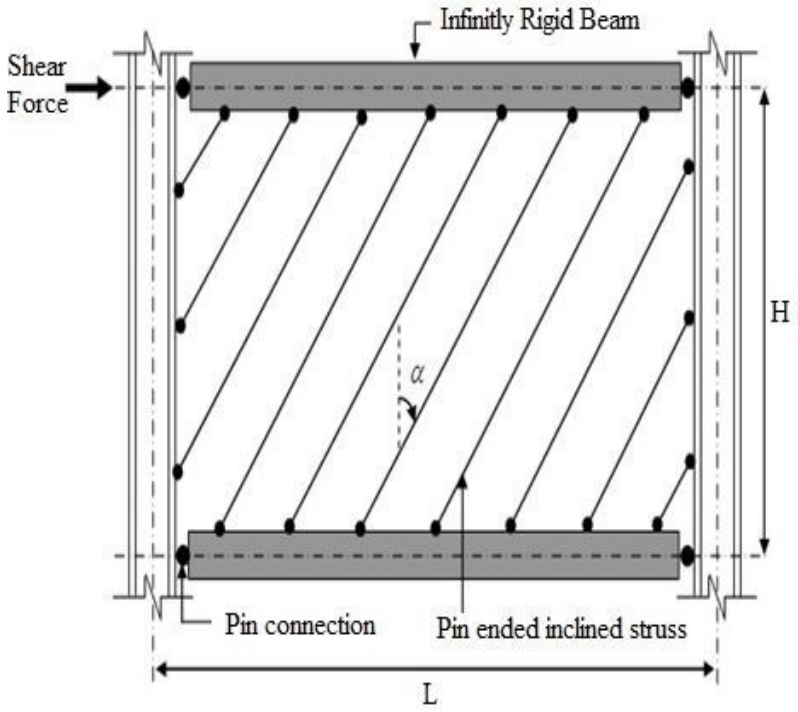


Figure 2.3: Analytical model (Strip-model)of Thorburn et al. (1983)

#### 2.2.2.2 Detailed Finite Element Model of SPSW

Various researchers have utilized the detailed finite element analysis (FEA) approach to study post-buckling behavior of unstiffened SPSWs through the simulation. In this section, selected research works on FEA of SPSW are briefly discussed.

Driver et al. (1997) developed a finite element model of their test specimen in a commercial general purpose nonlinear FE package ABAQUS (Hibbitt et al. 2011). In this study, the strip-model was extended to include inelastic behavior. Inelastic behavior in both the inclined strips and the boundary members were modeled. Even though strip-model analysis result showed a little underestimation in the initial stiffness of the test specimen, excellent agreement was obtained for the ultimate strength. Eight-node quadratic shell elements

(ABAQUS element S8R5) and three-node quadratic beam elements (ABAQUS element B32) were used to model infill plates and boundary elements respectively. Materials stress-strain curve were taken from the actual coupon tests for FE modeling while actual connection between infill plate and boundary elements were not modeled. FEM predicted the ultimate strength very well but initial strength was little overestimated.

Behbahanifard et al. (2003) developed a nonlinear finite element model in ABAQUS (Hibbitt et al. 2011) using explicit formulation to simulate the behavior of both test specimens of Behbahanifard et al. (2003) and Driver et al. (1997) under monotonic and quasi-static cyclic loading. In the development of the FEM, a four-node shell element with reduced integration (ABAQUS element S4R) was used for all of the elements of SPSW. A kinematic hardening material model was used to simulate the Bauschinger effect and residual stress was not included for simplicity. Validation of these FEMs showed that the analytical model has good agreement with experimental specimen with 12% and 7.8% underestimation for three-storey and for four-storey test specimen respectively. A parametric study was conducted with this validated model where researchers reported a set of ten independent parameters, which can be used to characterize the behavior of SPSW systems. Major findings of this parametric study were: (1) aspect ratio from 1 to 2 has very little effect on the SPSW capacity. When aspect ratio is less than 1, normalized shear capacity of SPSW increases; (2) Increment in the ratio of axial stiffness of infill to column axial stiffness would increase the stiffness of the SPSW; (3) the influence of initial imperfection on the stiffness of SPSW is significant, reduction of stiffness is evident when out-of-plane imperfection is more than 1% of $\sqrt{(Lh)}$; (4) increase in gravity load and overturning moments on SPSW would reduce the elastic stiffness and the strength of the SPSW panel.

Bhowmick (2009) conducted an analytical study by detailed finite element modeling. Implicit dynamic integration algorithms of ABAQUS (Hibbitt et al. 2011) were used in this study. Beams, columns and plates were modeled with general purpose four-node doubly curved shell elements with reduced integration (ABAQUS element S4R). Rayleigh proportional damping of 5% was used for this entire study. Available capacity design approaches of that time were evaluated and a new SPSW design approach was proposed based on indirect capacity design approach. It was found that, other capacity design approaches generally underestimate the maximum design forces in the column and thus overall design was overly conservative. Effect of loading rate on the dynamic behavior of the steel plate was also investigated. Studies showed that, high strain rate can reduce the SPSW ductility and increase the average flexural demand at the base of the wall. It also showed that the stability approach in NBCC was overly conservative. A simple and improved formula for estimating the fundamental period of steel plate shear wall was developed in the analytical program. Proposed equation for fundamental equation was $T = 0.03h_n$, where $h_n$ is the total height of SPSW.

### 2.2.3 Design and Analysis Method of SPSWs System

Early design process of unstiffened SPSW system was equivalent to the design of a vertical cantilever plate girder. Later, Berman and Bruneau (2004) showed that stiffness of SPSW is more influenced by its boundary members and thus designing SPSW considering it as a plate girder can lead to unconservative and uneconomical design of SPSW.

Berman and Bruneau (2003) derived formulations to calculate the ultimate strength of SPSW by applying the concept of plastic analysis and strip-model for single-storey and multi-storey system with pin or rigid beam-to-column connections. Assumed collapse mechanism for single-storey SPSW system with simple beam-to-column connections are presented in Figure 2.4 and the storey shear strength $V_{yp}$, of Berman and Bruneau (2003) is identical to the CAN/CSA S16-01 probable storey strength equation.

$$V_{yp} = 0.5 F_{yp} t_w L \sin 2\alpha \qquad 2.4$$

where, $F_{yp}$ is the yield strength of the infill plate, rest of the parameters is as defined earlier. For rigid beam-to-column connection equation-2.4 was modified by including internal work done by plastic moment in the column and (or) beams. Berman and Bruneau (2003) assumed two failure mechanisms (Figure 2.4) to calculate the ultimate capacity of multi-storey SPSWs, named soft-storey mechanism and uniform collapse mechanism. In the second mechanism, it was assumed that, all of the infill plates, beam-ends and column-bases would produce plastic hinge simultaneously. The researchers also used the design provision of CAN/CSA S16-01 (CSA 2001) and used the equivalent lateral force method to get storey shear, $V_s$, for calculation of infill plate thickness.

$$t_p = \frac{2 V_s \Omega_s}{F_y L \sin 2\alpha} \qquad 2.5$$

Where, $F_y$ is the nominal strength of the infill plates. $\Omega_s$ is the system over strength factor with values between 1.1-1.5. As per the minimum stiffness requirements, boundary elements were selected and the strip-model was developed for analysis. Proposed SPSW design was an iterative method, which starts with an assumed angle of inclination. This angle needs to be recalculated

when beams and columns were designed according to capacity design approach. Preliminary design of SPSW is used to develop the strip-model for analysis and the design may revise as per the analysis requirement.

A reasonably accurate and relatively efficient capacity design method was proposed by Berman and Bruneau (2008) to design boundary columns of unstiffened SPSW system with fully yielded infill plate under applied lateral loads. This proposed method combines a linear elastic model of SPSW and plastic analysis concepts. At first, the axial forces in the beams were calculated from a linear model of the column with elastic support. In this design approach, uniform collapse mechanism (Figure 2.4) was assumed to calculate the seismic loads from the plate yielding and plastic hinge formation of the beam-ends. Berman and Bruneau (2008) presented a column free body diagram for estimating design column axial forces and moments (shown in Figure 2.5). The free body diagram shows distributed force ($\omega_{xci}$ and $\omega_{yci}$) generated due to the infill plate yielding at storey $i$; reduced moment ($M_{prli}$ and $M_{prri}$) from plastic hinge formation in the beam ends; axial force ($P_{bli}$ and $P_{bri}$) from the beams; applied lateral forces ($F_i$) which can cause plastic collapse mechanism and base reaction ($R_{yl}$, $R_{xl}$, $R_{yr}$ and $R_{xr}$) for those lateral loads.

Berman and Bruneau (2008) also demonstrated the usefulness of the proposed capacity design approach with Indirect Capacity Design (ICD) approach and the combined linear elastic computer programs and capacity design concept (LE+CD) according to (ANSI/AISC 2005). It was also shown that the proposed design approach could predict axial loads and moments better than the two existing approaches. It was concluded that the proposed capacity design approach is

an effective way to design column especially for short SPSW, but it would be conservative for tall SPSW where uniform yielding in SPSWs are not very common.

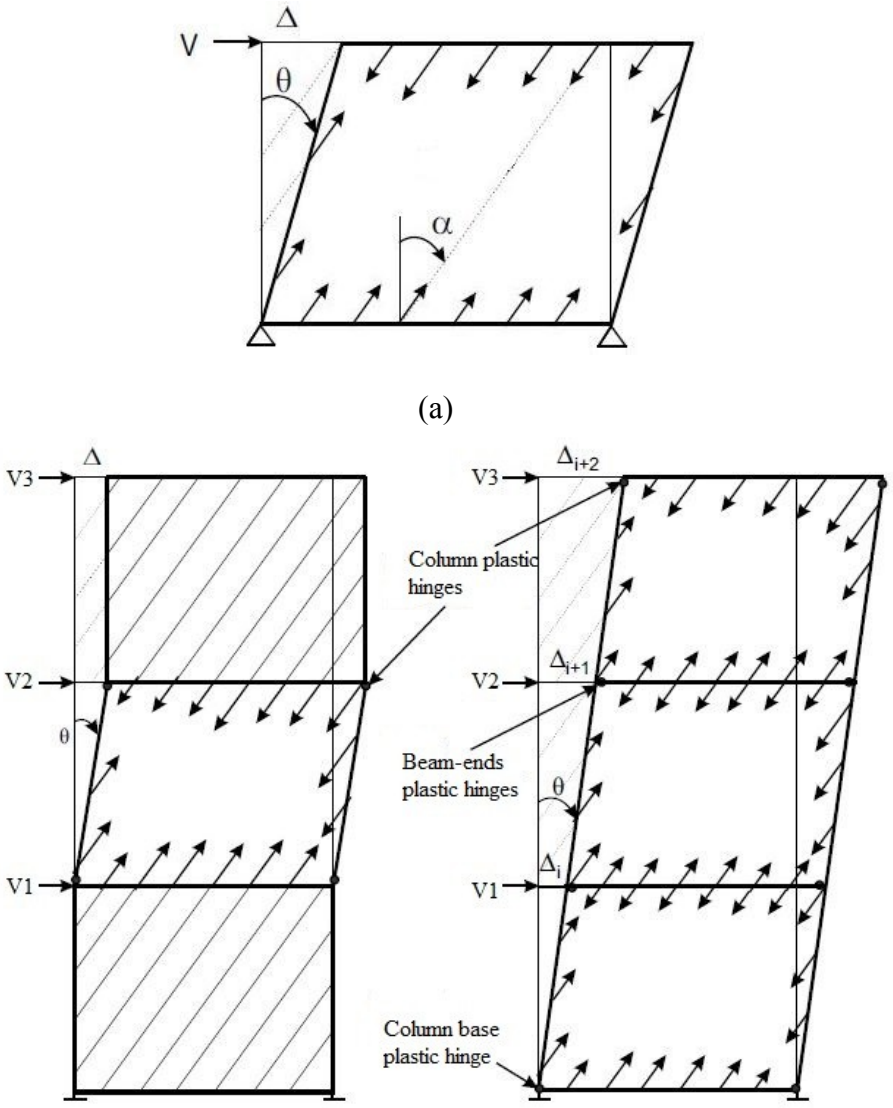


(a)

(b) (c)

Figure 2.4: SPSW collapse mechanisms: (a) Single-storey; (b) soft-storey mechanism for multi-storey SPSW; (c) uniform-storey mechanism for multi-storey SPSW (Berman and Bruneau 2003)

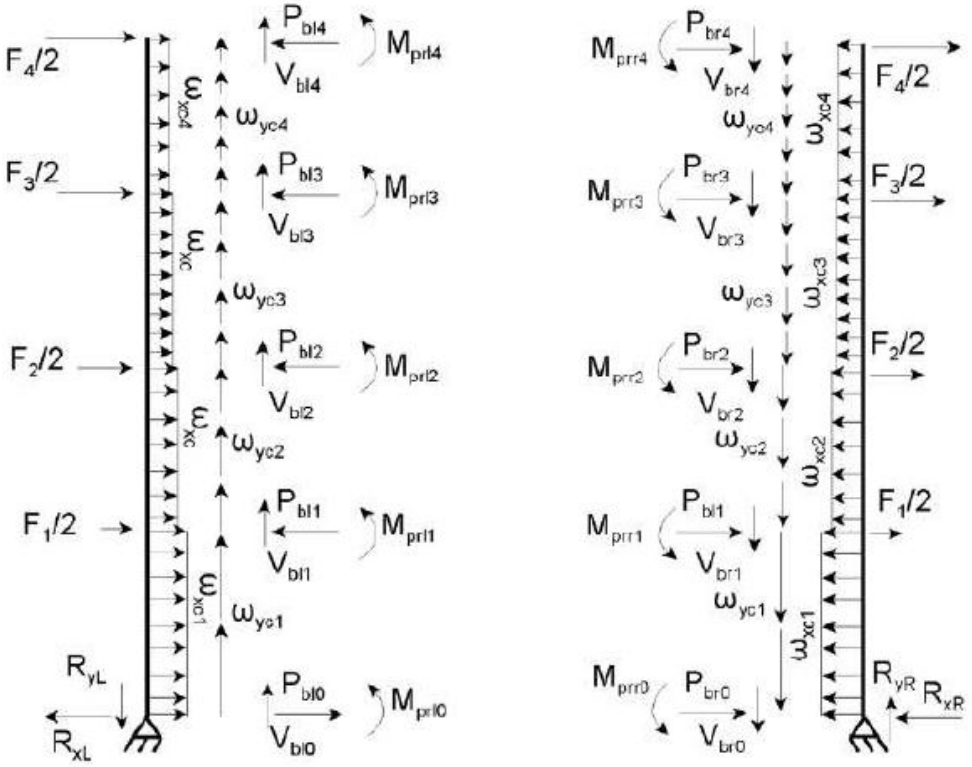


Figure 2.5: Free body diagram of SPSW boundary columns (Berman and Bruneau 2008)

### 2.2.4 Current Design Standards of SPSW

Design provision for SPSW was first incorporated in Canadian Standard (CSA 1994) in 1994 and in the AISC Seismic Provision (ANSI/AISC 2005) in 2005. With time, design guidelines have been updated and developed. In this section, current Canadian and American design provisions of SPSW are briefly discussed.

#### 2.2.4.1 CAN/CSA S16-09 (CSA 2009)

CSA design provision of SPSW is according to capacity design approach, where infill plates are designed to resist 100% of the storey shear. For preliminary design, SPSW can be

analyzed using equivalent brace model proposed by Thorburn et al. (1983) where, the equivalent area can be calculated by Equation 2.2. Once preliminary sections are calculated, forces and moments can be estimated by strip-model. Buckling strength of infill plate is negligible and post-buckling tension field is developed to the direction of the principal tension stress. Factored shear resistance of the plate is,

$$V_r = 0.4\varphi F_y L t_w \sin 2\alpha \qquad 2.6$$

In the ductile SPSW system, beam-to-column connection has to be rigid. Beams may develop plastic hinges at their ends. Beams should have sufficient flexural resistance such that it can resist at least 25% of applied storey shear by framing action. Boundary elements must be designed to resist axial forces, moments and shear due to gravity loads, infill plate yielding and development of plastic hinges. In the ductile SPSW, only column base may develop plastic hinges and all columns should be of Class1 sections. To allow full development of tension field in the infill plate, columns have to satisfy the flexibility parameter indicated in CSA S16 09.

#### 2.2.4.2 ANSI/AISC-341-10 (ANSI/AISC 2010)

US provision for SPSW design consists of both direct and indirect capacity approach. The beams and columns are designed to remain elastic under maximum tension forces generated from the infill plates. For the boundary elements, beams may develop plastic hinges and the nominal shear strength of an infill plate is:

$$V_n = 0.42 F_y t_w L_{cf} \sin 2\alpha \qquad 2.7$$

where, $L_{cf}$ is the clear distance between column flanges and rest of the terms are as defined earlier. In ANSI/AISC-341-10, three different capacity design approaches for the design of SPSWs have been enlisted. They are nonlinear pushover analysis; indirect capacity design approach; and combined linear elastic computer programs and capacity design concepts. Capacity design concept of SPSW in ANSI/AISC-341-10 and CAN/CSA S16-09 is identical. Other parameters, such as flexibility parameter of boundary elements and angle of inclination are also similar to the CAN/CSA S16-09. In the indirect capacity design approach, loads in the column can be estimated from the gravity loads combined with the seismic loads by using amplification factor $B$, which is the ratio of the expected shear strength ($V_e$) of the SPSW to the factored lateral seismic force ($V_b$).

$$B = V_e / V_b \qquad V_e = 0.5 R_y F_y t_w L \sin 2\alpha \tag{2.8}$$

For calculating the axial loads and moments in the boundary columns, the amplification factor $B$, should not be greater than the ductility related force reduction factor ($R_d$) that is specified in the code for SPSW.

## 2.3 Performance Evaluation of SPSW

Structural performance in recent seismic events pointed to the limitation of the performance evaluation in current seismic design procedure. It shows the needs of new methodologies and concepts for the seismic performance evaluation of structures, which should be simple and computationally inexpensive. Traditional strength based design procedure in current building code has very little scope to evaluate the seismic performance of the structures. Therefore, Performance-Based-Seismic-Design (PBSD) has been developed to ensure structure's

actual performance in the design phases through the evaluation of whether the building is performing up to the desired level or not. In FEMA-273 (FEMA 1997) specified four levels of structural performances; they are, collapse prevention, life safety, immediate occupancy and fully operational. FEMA-273 (FEMA 1997) also specified four analytical procedures to evaluate structural performances; they are linear-elastic, linear-dynamic, nonlinear-static and nonlinear-dynamic. Nonlinear dynamic analysis is the most appropriate and complex analysis procedure. Nonlinear static analysis is an approximate, reasonably accurate and relatively simple procedure for performance evaluation. Here, development of two nonlinear static procedures, capacity spectrum method and modal pushover method are described.

### 2.3.1 Research on Capacity Spectrum Method

Structural design or performance evaluation based on the graphical intersection of seismic demand and capacity curve to account structure's inelastic behavior, is called Capacity Spectrum Method (CSM). CSM compares the seismic demand with the capacity of a structure, which gives a visual representation of the seismic performance of the structure. A nonlinear base shear forces-top displacement curve (pushover curve) represents the capacity of the structure. Pushover curve is converted to equivalent spectral accelerations and spectral displacement by using effective modal mass and modal participation factors. Response spectrum is used as the seismic demands of the structure. When both curves are plotted in the same coordinate, demand-capacity relationship readily comes out. The intersection of the two curves is called performance point that represents the probable performance of the structure to the particular seismic demands. CSM can be used to (Freeman 1998):

a) Evaluate performance level without performing nonlinear time history analysis

b) Rapid evaluation of a large group of existing building

c) Detailed structural evaluation

d) Verify the code designed structural system to ensure the performance goals

Seismic design guidelines in National Building Code of Canada are based on linear elastic design spectra. Application of these types of elastic spectra to analysis inelastic structure is approximate. An inelastic design spectrum can be used for design of structure, which behaves inelastically during an earthquake. A direct approach to obtain inelastic spectra is nonlinear dynamic analysis of a series on inelastic Single-Degree-of-Freedom (SDOF) systems. Another approach is indirect procedure, where a reduction factor is applied to reduce elastic curve and to obtain inelastic spectrum. These types of spectra not only depend on ground motion's characteristics and damping, they depend on structure's inelastic behavior (Fajfar 1996) as well. Several researchers have proposed different approximate expression of force reduction factors (Krawinkler and Nassar 1992), (Newmark and Hall 1982), (Vidic et al. 1994).

Since, direct approach is a time consuming method, indirect approach has been used for in this study to obtain inelastic spectra. Force reduction factors in national building code are generally based on experience and engineering judgement. It is defined as the ratio of the elastic strength demand to the inelastic strength demand of the structure. Reduction factor depends on some structural properties such as; natural period, ductility, hysteretic behavior and damping (Vidic et al. 1994). It is also influenced by ground motion characteristics. This reduction factor is often called ductility based reduction factor because of its direct relation with structural ductility.

Another reduction factor is over strength related reduction factor. It is the ratio of structure's actual strength to design strength. Over strength can be determined through the nonlinear pushover analysis.

Several methods have been proposed by researchers to estimate Seismic demand of an inelastic structure. Inelastic response of the structure can be estimated by analyzing equivalent linear SDOF system with equivalent damping and equivalent period (Applied Technology Council 1996) (Freeman et al. 1975). Equivalent damping is the function of ductility and period of the structure. On the other hand, elastic-plastic system of SDOF model can be used for analysis with inelastic response spectrum. Some selected researches on CSM are discussed in this section.

Freeman et al. (1975) first introduced CSM in 1970s as a rapid evaluation procedure in a pilot project of seismic assessment of building at the Puget Sound Naval Shipyard. In that project, structure's capacities were determined based on visual inspection, review of available drawings, determination of approximate force-top displacement relationships, and some engineering judgement. The capacity was defined by three essential points on a graph: origin, yield point, and ultimate point (Freeman et al. 1975). This approximate capacity graph is now referred to as a pushover curve.

Fundamental concept of CSM came from Reserve Energy Technique (RET) (Blume et al. 1960), where energy balance concept was implemented by equating elastic energy with inelastic energy to estimate inelastic displacement as shown in Figure 2.6. The area within ADEF

trapezoid is equated to the area in the ABC triangle. The AD line plateau is equal to the peak of the triangle divided by reduction factor R. The ratio of D to E is the ductility $\mu$ of this inelastic system and force reduction factor $R = (2\mu - 1)^{1/2}$. In Figure 2.6 the elastic period is 0.7sec, the inelastic secant period is 1.4sec, the $\mu$ is 4.0 and $R$ is 2.65.

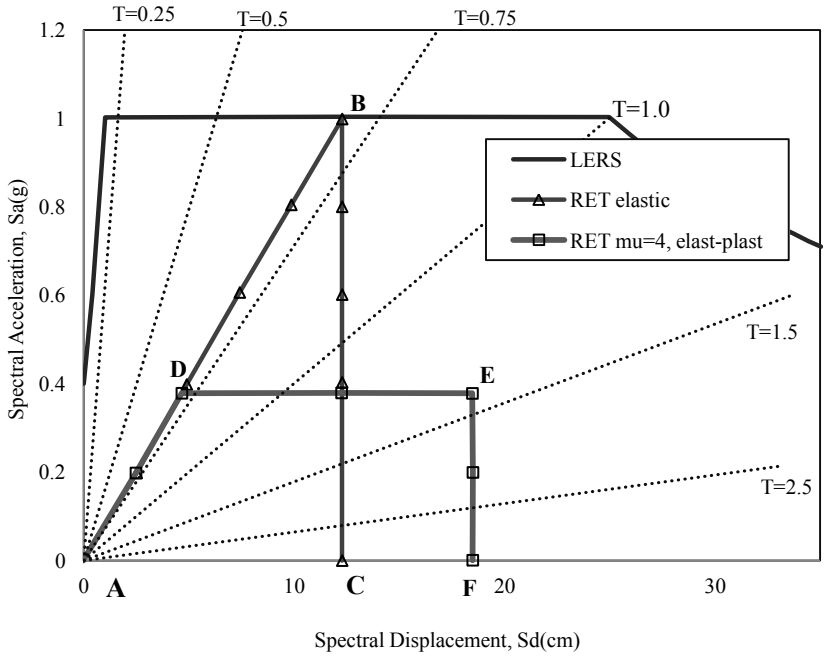


Figure 2.6: Reserve energy technique (RET) (Blume et al. 1960)

CSM was primarily developed in “Seismic Design Guidelines for Essential Buildings Manual." It was the design verification procedure for the Tri-services (Army, Navy, and Air Force) in 1986 (Freeman et al. 1984) (Army 1986). To obtain the nonlinear inelastic behavior of the structural system, effective viscous damping values were applied to the linear-elastic response spectrum and system was considered as equivalent linear system. The seismic demand curve (response spectra) was plotted with different levels of “effective” viscous damping. The

intersection point, where this capacity spectrum intersect the seismic demand, can give an estimation of the force, displacement, and damage that may occur in the structure to a given level of earthquake (Freeman 2004). Difference modifications have been proposed in the CSM to find the "exact" intersection point for accurate level of damping.

ATC-40 (Applied Technology Council 1996) utilized equivalent linear systems with equivalent damping to develop " Nonlinear Static Procedure". This simplified approximate analysis procedure has been proposed to predict the earthquake-induced deformation of an inelastic system without performing nonlinear dynamic analysis. A series of equivalent linear systems with successively updated value of equivalent period and damping offer an approximate estimation of the deformation of an inelastic system. ATC-40 presented three different procedures of nonlinear static procedure; all of them are based on the same concepts and principles with different application process.

Procedure A is an iterative method, where demand curves are updated corresponding to the equivalent damping of the system. This iterative procedure converges to a deformation much smaller than "exact value" (nonlinear dynamic analysis result) (Chopra and Goel 1999). In some cases, procedure A does not converge as well. Procedure B gives a unique result of deformation, which is equal to the result of Procedure A, if it converged. Therefore, discrepancy between approximate and exact result is same as Procedure A that is very high. Both of the procedures (A and B) require analyses of series of equivalent linear systems and still produce very poor estimation of deformation demand (Chopra and Goel 2000).

Fajfar (1999) proposed a simple and easy to use Capacity Spectrum Method (CSM) by using inelastic seismic demand spectrum based on constant ductility. Like other proposed CSM, structural capacity and seismic demand is presented in the same graph. In this proposed method, highly damped elastic spectra were used to determine seismic demand. Relationship between the hysteretic energy dissipation with equivalent viscous damping for highly inelastic structure is one of the controversial points for capacity spectrum method, which was ignored in this proposed method. Inelastic demand spectra are determined from a typical smooth elastic design spectrum with constant ductility of the structure. A simple transformation is used to obtain equivalent single degree of freedom (ESDOF) system from multi degree of freedom (MDOF) system. In this proposed method, assumed displacement shape is the first mode shape of the structure, so higher mode effect is not considered. An inelastic demand spectrum has been determined by using constant ductility and ductility related reduction factor. This relationship originally come from a statistical study of a stiffness-degrading system with 10% strain hardening and 5% damped system by Vidic et al. (1994). In that study ductility, hysteretic behavior, and damping were considered to get the bi-linear relationship between reduction factor and ductility. Two different types of model with 10% strain hardening and 0.5% unloading stiffness degradation was considered where two mathematical model of damping was utilized. Vidic et al. (1994) found out that $R$ factor depends on period and ductility where hysteretic behavior and damping has moderate influence on it. This study also showed that reduction factor increases with decrease of damping. Influence of damping on acceleration and displacement spectra is higher for "Q model" with "mass proportional damping" (Vidic et al. 1994). Reduction factor and ductility are related to the characteristic period of the elastic spectra, which is the point where constant acceleration phase and constant velocity phase intersect in the spectrum.

Several Studies has been performed to judge $R_\mu$-$\mu$ bi-linear relation of Vidic et al. (1994) and it was accepted by several researchers (Cuesta et al. 2003) (Chopra and Goel 1999). In this proposed CSM, reduction factors for "Q-model" with "mass proportional damping" was used. This method is applicable for performance evaluation of the existing building and as a tool for the direct-displacement based method by using a pre-selected target displacement.

Chopra and Goel (2000) developed two improved capacity-demand-diagram method by using constant-ductility design spectrum as the demand spectrum. One of the improved methods is graphically similar to ATC-40 Procedure A and another one is similar to Procedure B. The main and important difference between these improved methods and ATC-40 are the demand curve. ATC-40 used equivalent linear system to determine the demand; on the other hand, improved method used inelastic system. The improved method can be implemented numerically as well (Chopra and Goel 2000). Three different $R_y$-$T_n$-$\mu$ relations have been used for same examples and compared with ATC-40 result. The primary purpose of this study is to introduce an improved and simplified analysis method, based on capacity and demand diagrams using the inelastic response (or design) spectrum (Chopra 2007). A series of demand spectrum have been plotted for different ductility demand. The yielding branch of the capacity curve can intersect in several demand curves for different ductility. One of the intersection points provides the equal ductility factor for the capacity diagram and for the demand curve (Chopra and Goel 2000).

FEMA-440 (FEMA 2005) was developed to assess current nonlinear static procedures (NSP) including capacity-spectrum method (CSM) of ATC-40. Based on the assessed results, some suggestions of possible improvement have been given to improve the results. One of the

major objectives of this document is to find out the reasons for the difference between CSM and nonlinear time history. A series of nonlinear single-degree-of-freedom systems for varying period, strength, and hysteretic behavior were subjected to ground motion for different soil conditions. The output database was utilized as a standard to judge the accuracy of CSM of ATC-40.

- For longer period response, different hysteresis model shows different discrepancies. Hysteretic behavior type A and B shows underestimation of the results. On the other hand, type C gives over estimation which also increases with increase of R
- In short-period response, ATC-40 gives a significant overestimation of the displacement which at the same time increases with decreasing strength and it was up to two times of the exact displacement.
- ATC-40 does not show any potential dynamic instability for strength degradation or P-delta effect.

FEMA-440 (FEMA 1999) offers a modified acceleration-displacement response spectrum (MADRS), which will intersect with capacity spectrum at the performance point. This document gave some suggestions for amelioration those were the improved estimation of equivalent period and damping. Usually, the optimal effective period is less than the secant period, which is less than that period specified in ATC-40 (Applied Technology Council 1996). Improved methods were further investigated and compared with original ATC-40 results. These improved methods produced more accurate approximations of displacements.

### 2.3.2 Research on Modal Pushover Analysis

Nonlinear dynamic analysis is one of the most rigorous and reasonable analysis procedure to evaluate nonlinear behavior of the structure. Its time-consuming and complex procedure makes it incompatible choice for regular use. Therefore, a simplified method for seismic performance evaluation and seismic demand estimation is essential. This simplified procedure needs to be accurate enough so that it can predict very close result to nonlinear dynamic analysis. Inelastic behavior of the structure needs to be accounted while estimating seismic demand especially when buildings are assumed to be in lower performance level. Nonlinear pushover analysis is one of the common and simple method to assess seismic performance of any structure when structural vibration is dominated by its fundamental mode of vibration and the mode shape is constant during the earthquake. According to its basic assumptions, pushover analysis is not developed to estimate higher mode effect on the structure. On the other hand, response spectrum analysis considers higher mode contribution in the structural response by elastic analysis.

To overcome the limitation of pushover analysis and response spectrum analysis, a Modal Pushover Analysis (MPA) has been proposed which reformulate the response spectrum analysis method to determine inelastic behavior of the structure by utilizing pushover analysis with inertia force distribution for each mode (Chopra and Goel 2001). The main purpose of MPA is to improve pushover analysis that is computationally more accurate without increasing complexity in the design.

**The static pushover analysis** is a simple and effective technique to estimate structural properties, such as strength, stiffness, deformation capacity as well as seismic performance evaluation. In terms of seismic performance evaluation, purpose of the static pushover analysis is to determine the effect of individual member deterioration on the structural system, identify the critical region and the strength discontinuities, evaluation of inter-storey drift and P-delta effect (Krawinkler and Seneviratna 1998). In the static pushover analysis, structures are pushed monotonically up to a target displacement with a reasonable load pattern. Basic assumptions of static pushover analysis are; (1) structural response can relate with an equivalent single degree-of -freedom (SDOF) system, which means that the response is controlled by only one mode. (2) The mode shape remains constant throughout the seismic event. Target displacement and lateral load pattern are very important parameters for the pushover analysis to represent the accurate estimation of structural response (Wang and Yang 2000). Different load patterns have been proposed by researchers for this purpose, but none of the lateral force distribution can include the higher mode effect and also it cannot redistribute the inertial force due to the structural yielding (Goel and Chopra 2003). Both the assumptions become approximate when structures start yielding.

**The modal response spectrum analysis** is a linear analysis method to compute maximum structural response of a single-degree-of-freedom system. Each mode of vibration of the structure is presented by particular single-degree-of-freedom systems with their respective modal properties, which estimates each mode contribution in the vibration of that structure. Number of significant modes should be such that their total modal participating mass is not less than 90% of the total effective mass of the structure. Total response of the structure is computed

by superposition of responses of all the significant modes. This analysis procedure is often called as modal analysis. Modal analysis generally provides conservative estimation of the response by linear analysis (Saatcioglu and Humar 2003), (Chopra 2007).

Chopra and Goel (2001) developed modal pushover analysis (MPA) for seismic performance evaluation by reformulating standard response spectrum analysis by nonlinear pushover analysis. MPA was first introduced for linearly elastic buildings, which is equivalent to the response spectrum analysis. Then, MPA was extended to inelastic structure to estimate inelastic behavior of the structure. In MPA procedure, pushover analysis is performed to determine maximum response of the structure due to its $n^{th}$-vibration mode. Lateral force distribution pattern in the modal pushover analysis is associated with its inertia force for different mode of vibration. Base shear-roof displacement curve of the MDOF system is idealized as a bilinear force-deformation relation of the $n^{th}$-mode inelastic SDOF system. Structure is pushed up to the peak deformation of the $n^{th}$-mode inelastic SDOF system that is determined by nonlinear dynamic analysis of that SDOF system. Any appropriate modal combination rule may apply to combine all peak modal responses. This approximate analysis procedure provides good estimation of seismic behavior (roof displacement, storey drift, plastic hinge location, etc.) when it is compared with nonlinear dynamic analysis. Moreover, MPA procedure can make better prediction in seismic demand estimation than the all the FEMA-356 and FEMA-273 force distribution method (Goel and Chopra 2003). It has been found that, MPA with 2D frame shows good prediction of hinge rotation and storey drift. It also accurately accounts higher mode effect in both 2D and 3D model and reliably predicts the nonlinear dynamic analysis response (Yu et al. 2004). The method has also been applied for asymmetric building with in-plane irregularities.

Chopra et al. (2004) have proposed anther modified MPA (MMPA) procedure by assuming the linear elastic behavior of the structure during the higher mode vibration. By using MMPA, a significant computational effort may be reduced but it cannot assure better accuracy than MPA. In some cases, MMPA produces large estimation of seismic demands that may improve the accuracy of MPA, as well as it increases conservatism. This conservative estimation increases with the decrease of damping, especially for such system that has significantly lower damping. Effectiveness of MMPA for seismic performance evaluation has been investigated for several SAC Buildings (Chopra et al. 2004).

Higher mode pushover analysis and associated plastic mechanism are very important part of MPA, where "reversal" in pushover curve may occur. However, "reversal" in pushover and in nonlinear dynamic analysis is not very common for regular buildings; still it can appear during MPA. When in pushover analysis, a plastic mechanism moves the roof opposite to its original mechanism formation, is referred to as a "reversal" in pushover. Three different procedures may apply to stay away from such "reversal" (Goel and Chopra 2005). Firstly, if the structure does not deform beyond its elastic limit in its "reversal" mode, this reversal is very unlikely to occur. Secondly, Seismic demand of a structure associated with higher mode can estimate within its elastic limit (Chopra et al. 2004). Finally, Base shear-floor displacement curve for the storey that is above the yielded stories can also eliminate the reversal in pushover curve.

## 2.4 Summary

Several experimental and analytical research studies have proved the effectiveness and performance of the SPSW system by conducting nonlinear dynamic analysis. Nonlinear dynamic analysis is the most accurate, but time consuming, complex and computationally expensive technique. Seismic performance evaluation of a SPSW is mainly confined in nonlinear dynamic analysis. Performance based seismic design requires assess actual performance of the structures. Therefore, relatively simple and effective methods need to be used for seismic performance evaluation and seismic demand estimation.

CSM and MPA are two simple and approximate procedures to estimate seismic demand, which have been proved by previous researches. Application of CSM and MPA on the framed structures has been shown very impressive prediction of seismic force and displacement demand. However, no research programs have been found that use CSM and MPA to investigate seismic performance and force demand for SPSW. Applicability and accuracy of these approximate analysis procedures to assess seismic performance of SPSWs needs to be investigated.

## Chapter- Three

# Seismic Design and Analysis of Steel Plate Shear Walls

### 3.1 Introduction

Several numerical studies have been conducted on nonlinear seismic analysis of steel plate shear walls. Many researchers have used Finite Element (FE) analysis technique to study SPSWs behavior by considering materials and geometrical nonlinearities. ABAQUS (Hibbitt et al. 2011) has been utilized here to develop Finite Element Model of SPSW to examine its detail nonlinear behavior under quasi-static loading as well as dynamic loading.

The equivalent static force procedure in NBCC-2010 can be utilized for SPSW design when building is located in low seismic regions or regular building below a certain height limits. Dynamic analysis is obligatory for regular structures that are higher than 60m or having fundamental period more than 2.0 seconds and are located in high seismic region. Prior to dynamic analysis, a mathematical model of the structure needs to be developed by which strength, stiffness, mass and inelastic member properties can be assigned.

This chapter illustrates the development of FE model of SPSW. Selection of analysis technique, element type and material properties are discussed. Initial considerations and boundary conditions are explained here as well. The model has been validated with two experimental program of quasi-static loading analysis of SPSWs. The validation of the model by comparing the result of FE model with experimental programs is explained here. Geometrical

and material properties as well as loading technique are selected in such a way that is close to the experimental set up.

In this chapter, seismic design of a 4-storey and an 8-storey SPSWs system according to seismic design provision of NBCC 2010 has been presented. Seismic performance of SPSWs under seismic records compatible with the NBCC 2010 uniform hazard spectrum of Vancouver has been evaluated. Previously validated finite element model has been utilized for this dynamic analysis of SPSWs. Important structural performance parameters like, inter-storey drift, storey displacement, maximum base reaction and storey-shear is presented in this chapter. In addition, selection of ground motion records and the method of scaling were also described.

## 3.2 Selection of Finite Element Analysis Technique

ABAQUS is a general-purpose finite element-modeling tool, which is designed for the simulation of both linear and nonlinear analysis. ABAQUS has a good number of pre-defined materials model, large elements library and various solver techniques. In this study, thin steel infill plates are expected to have initial imperfection; it may buckle under very small lateral loads. So, severe geometric and materials nonlinearity are expected. Therefore, the modeling and analysis technique should be selected carefully to minimize convergence problem and analytically less expensive.

Severe convergence problems were experienced in implicit analysis scheme in past studies (Behbahanifard et al. 2003). In order to avoid extreme convergence problems Behbahanifard et al. (2003) used explicit analysis technique (ABAQUS/EXPLICIT) for quasi-

static loading. An explicit finite element modeling analysis uses incremental analysis procedure. At the end of each increment, stiffness matrix is updated based on its change in geometric and material properties. Before application of next load increment to the system, a new stiffness matrix is constructed in that procedure. This is a non-iteration based process. Quasi-static analysis could be performed by proper control of the kinetic energy. This analysis accuracy is directly related to the time step of the analysis. The increment steps have to be small enough to get accurate results, which often consumes a lot of analysis time.

On the other hand, ABAQUS/Standard analysis is an implicit analysis scheme, which uses Newton-Raphson iteration process at the end of each increment. In the analysis scheme, calculation of current time step is based on the results of the previous time step. This solution technique remains stable, even if large time steps are taken; therefore, this analysis scheme is also called an unconditionally stable scheme. This process implements equilibrium of the internal structural force to the externally applied loads and often requires specific tolerance to get the equilibrium. Implicit is generally accurate than explicit scheme. Therefore, the implicit time integration method ABAQUS/STANDARD (Hibbitt et al. 2011) with Hilber-Hughes-Taylor (HHT) operator was used for the analysis. HHT integration method allows energy dissipation and it solves the Second Order linear problem. This method is an extension of the trapezoidal method that is unconditionally stable (Bhowmick 2009). HHT includes numerical damping without disturbing the system stability as well.

For any nonlinear system, it is tough to obtain a solution for static analysis by using implicit time integration method. However, nonlinearities can easily be accounted for in dynamic

analysis than in static analysis because the inertia provides mathematical stability to the system, making the method more strong. As a result, an automatic time incrimination scheme is used within the implicit dynamic integration method. To determine whether a dynamic simulation is producing an appropriate quasi-static response, the work done by the external forces should be nearly equal to the internal energy of the system, while the kinetic energy remains bounded and small.

## 3.3 Characteristics of the Finite Element Model

### 3.3.1 Geometry and Initial Conditions

Finite Element Model (FEM) was used for evaluation of seismic performance of SPSW. At first, FEM was used to validate with two experimental programs of SPSW. In the validation process physical configuration, material properties, loading techniques, support conditions and overall environment was maintained as close as possible to the laboratory environment and test set up. All geometrical dimensions of FEM were same as the experimental specimen. In the test specimens, fishplates were used to connect steel plates with boundary elements, which have very little effect on the overall performance. In FEM, steel plates were directly connected with its boundary elements, and thus fishplates were ignored.

A perfectly flat steel plate has a very high in-plane shear, but its stiffness significantly reduces when it has a small amount of initial imperfection. For steel infill plate, it is normal to have a little amount of initial imperfection. Fabrication error, welding distortion and deformation of boundary beam due to gravity load cause initial out of plane deformation in infill plate. To get real strength and stiffness of the SPSW, initial imperfection should be considered. In this study,

initial imperfection pattern was considered corresponding to the first buckling mode shape as loaded in the physical test. The out of plane deformation was considered as two times of the corresponding plate thickness (Bhowmick et al. 2011).

Accuracy of a finite element analysis is significantly influenced by the mesh size and aspect ratio. Course mesh size may produce inaccurate estimation; however, using finer mesh is computationally expensive. Therefore, optimal mesh size is required to get precise analysis result with minimum analysis time. To model a multi-storey SPSW and especially for time-history analysis, optimal mesh is necessary. Optimum mesh size was selected for SPSW modeling by performing convergence study with different mesh size.

### 3.3.2 Element Selection

ABAQUS element library offers flexibility in modeling with various types of elements for different analysis purposes. A steel plate shear wall consists of beams and columns connected with thin infill plates. Shell element was used to model infill plates and all boundary elements in order to account local buckling in infill plates, its boundary beams and columns. When one dimension (the thickness) is significantly smaller than the other dimension of any structure, shell elements are generally used in such modeling. The webs and flanges of boundary members (beams and columns), and infill plates were modelled using S4R element from ABAQUS/Standard element library. This element is a general purpose four-node doubly curved shell element with reduced integration. The element S4R uses for finite membrane strains and large rotations. This element is a general purpose quadrilateral element that is suitable for a wide range of applications. It uses thick shell theories when it is modeled as thick shell otherwise it

uses classical (Kirchhoff) shell theory. S4R element has six degrees of freedom in each node: three translations ($u_x$ ,$u_y$ ,$u_z$) and three rotations ($\theta_x$, $\theta_y$, $\theta z$ ) defined in a global coordinate system.

This element follows an isoperimetric formulation, which shows that the identical shape function is used for interpolation of displacement fields and for the geometry of the elements. It applies one integration point on its mid surface to form the element internal force vector. The default number of integration point along the thickness is five, which is also used in this modeling. Reduced integration elements give accurate results and significantly reduce running time if the elements are not distorted locally.

### 3.3.3 Materials Properties

ABAQUS offers various options to select material properties so that material can behave close to its real behaviors. For finite element model validation, material properties were chosen based on stress strain curve obtained from tension coupon test performed by the original researchers where tension coupon test was performed for different parts of the SPSW system. The Von Mises yield surface has been introduced to account multi axial stress corresponding to the plastic flow. An isotropic hardening model was used to specify the plastic flow. In this model, yield surface changes (increase and decrease) with the plastic strain occurrence. Isotropic hardening model is useful for monotonic pushover analysis where high rate of deformation is expected. Therefore, isotropic hardening model was used for all pushover analysis. For seismic analysis, elasto-plastic stress-strain curve was adopted. Rayleigh proportional damping with 5% of critical damping was assumed in all seismic analysis procedure that includes damping from

partition walls as well as unclad steel frames.

### 3.3.4 Displacement Control Analysis

ABAQUS/Standard has two control schemes, named force control scheme and displacement control scheme. Response at the limit point and cross the limit point during the loading period is very important to obtain the accurate capacity of the structure. The load response near the limit point is very flat which results a large amount of displacement due to a small increment of load. After this limit point, a small increment of force can make the system unstable. Therefore, displacement control analysis is more preferable for pushover analysis. In displacement control scheme, one can apply history of displacement, velocity or acceleration to one or more nodes separately. These nodes are referred to as boundary nodes and required force to reach the specific displacement is obtained through the equilibrium. The top storey displacement has been considered as the control parameter and the analysis has been stopped after the target displacement is reached.

## 3.4 Validation of Finite Element Model

Finite element models for SPSWs have been developed according to above-mentioned method and validated with two experimental test results. A single-storey and a three-storey SPSW specimen were modeled and validated with a single-storey test specimen of Lubell et al. (2000) and a three-storey test specimen of Behbahanifard et al. (2003) respectively. Pushover analyses were performed and the resulting curves were compared to the corresponding envelope of hysteresis curves taken from the experimental analyses.

### 3.4.1 Validation for Lubell et al. (2000) Specimen

Lubell et al. (2000) conducted quasi-static analysis on two single-storey SPSW specimens (SPSW1 and SPSW2). All the beams-to-columns connections were moment resisting connections. All the boundary elements were S75X 8 structural steel section and plate thickness was 1.5mm. The only difference between these two specimens was that SPSW2 consisted two S75X8 sections as its top beam. Those two S75X8 sections were fully welded together to provide better anchor to the tension field that developed in the infill plate. Out-of-plane distortion in SPSW2 was less than 5mm. All the beams and columns yield strength was 380Mpa and yield strength of infill plate was 320Mpa. Schematic figure of two single-storey SPSW specimen are presented in (Figure 2.2).

SPSW2 specimen was modeled and used for finite element model validation. All the geometric and material properties reported by Lubell et al. (2000) were used to develop finite element model. Monotonic pushover analysis was performed by applying a lateral load along the centerline of the top beam and deformation was monitored from the same level of the beam. Load application was carried out until top deformation was reached at 50mm. Base reaction-top displacement curve of this analysis has been compared with the envelope of the hysteresis curve of the physical test of SPSW2 specimen (Figure 3.2). Initial stiffness of FEM was very close to the experimental results where post yielding maximum capacity of FEM was 3% lower than the maximum capacity of the test specimen.

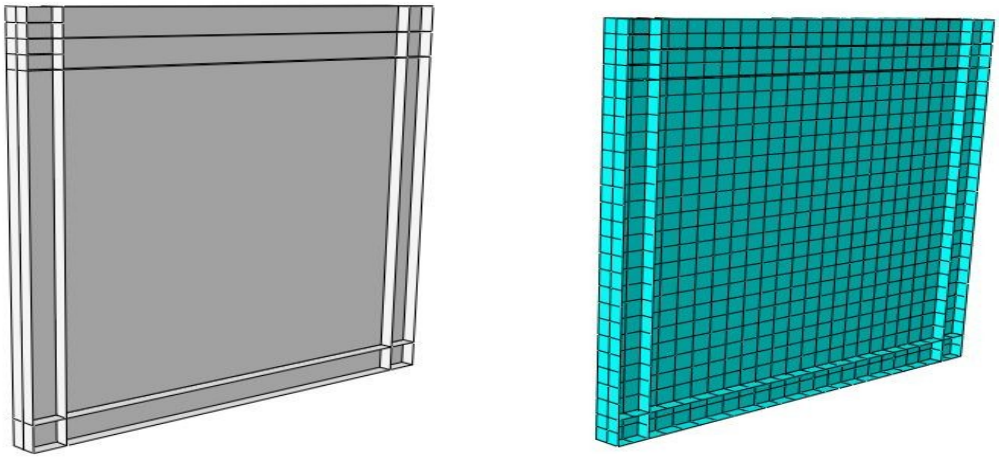

Figure 3.1: Schematic Figure of the model (left) and meshed geometry of the FEM (right) of Lubell et al. (2000) test specimen

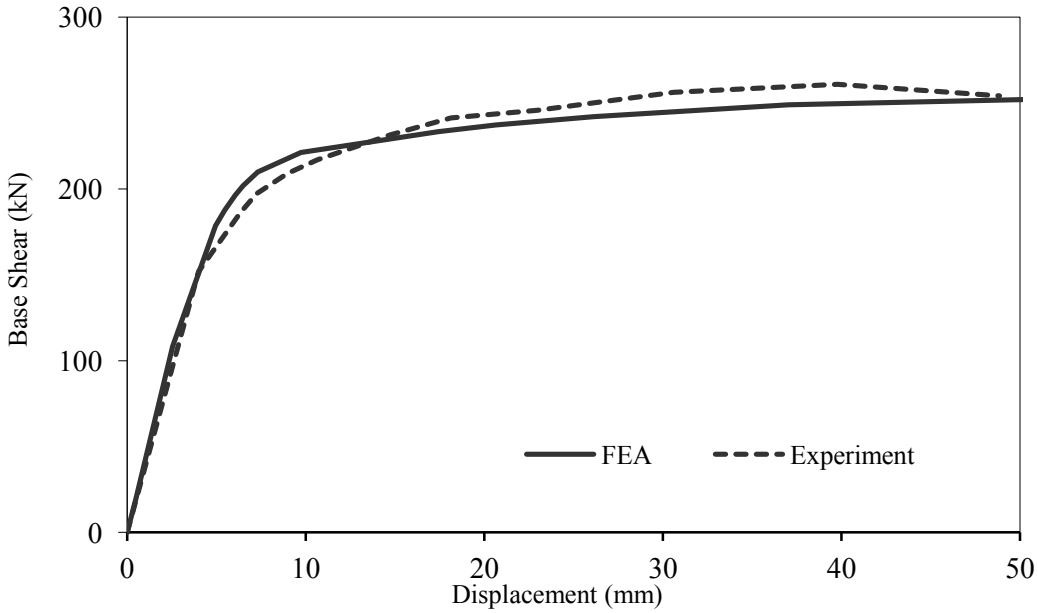


Figure 3.2: Pushover curve from FEA and experimental result of Lubell et al. (2000) test specimen

### 3.4.2 Validation for Behbahanifard et al. (2003) Specimen

Behbahanifard et al. (2003) performed a physical test on a large-scale 3-storey SPSW specimen, which was taken from Driver et al. (1997) test specimen. Driver et al. (1997) conducted quasi-static cyclic analysis of a large-scale 4-storey SPSW specimen. Bottom storey of that specimen was significantly damaged, rest of the parts were in good condition. Behbahanifard et al. (2003) retested the top three storey of the 4-storey test specimen of Driver et al. (1997) after removing the damaged bottom storey. Though specimen has already faced a large deformation during the previous test, the material may change its property. However, it was not possible to evaluate materials property for 3-storey SPSW specimen after its first cyclic test. Therefore, the materials property for 3-storey specimen was taken from the materials test report provided by Driver et al. (1997). The initial imperfections were measured in the bottom panel of the three-storey specimen, which was the permanent deformation of the panel due to the previous test. The peak out of plane deformation was 39mm. The bottom part of the test specimen was welded with a 90mm thick rigid steel plate to ensure the fixed support condition. Several bracings were used to prevent out of plate movement of the specimen.

3-storey SPSW test specimen of Behbahanifard et al. (2003) was modeled and pushover test was carried out. Geometrical dimension was used same as the test specimen. Materials property was taken from original materials test report of Driver et al. (1997). The measured initial imperfection data was not available for modeling, for which first buckling shape was considered as imperfection pattern.

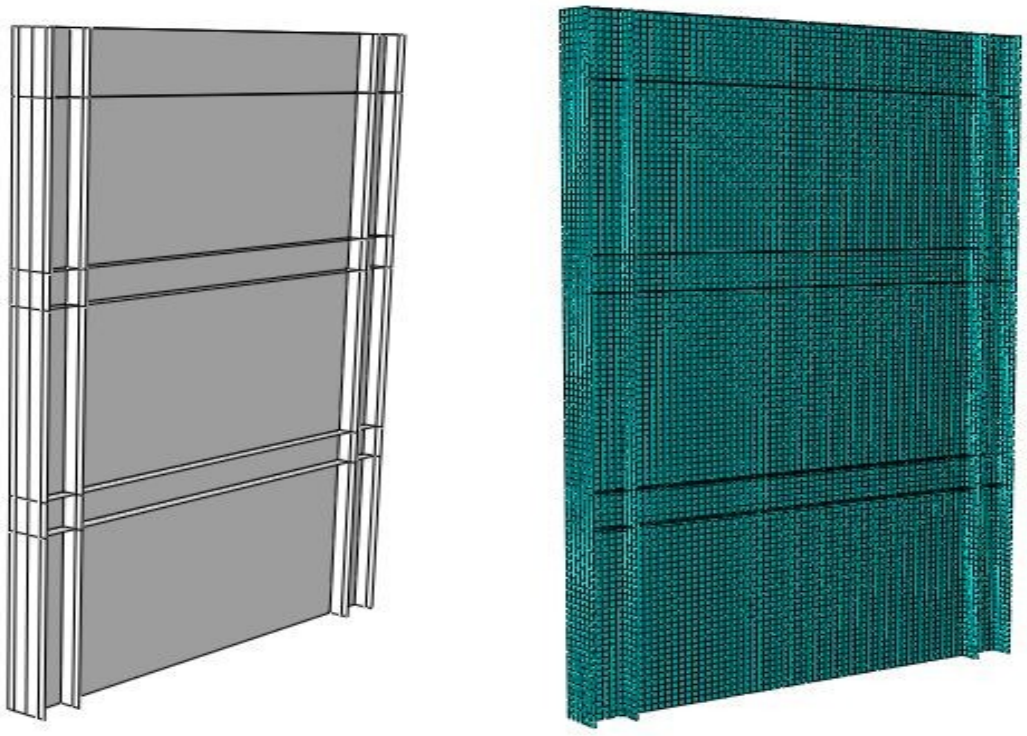

Figure 3.3:Schematic Figure of the model (left) and meshed geometry of the FEM (right) of Behbahanifard et al. (2003) test specimen

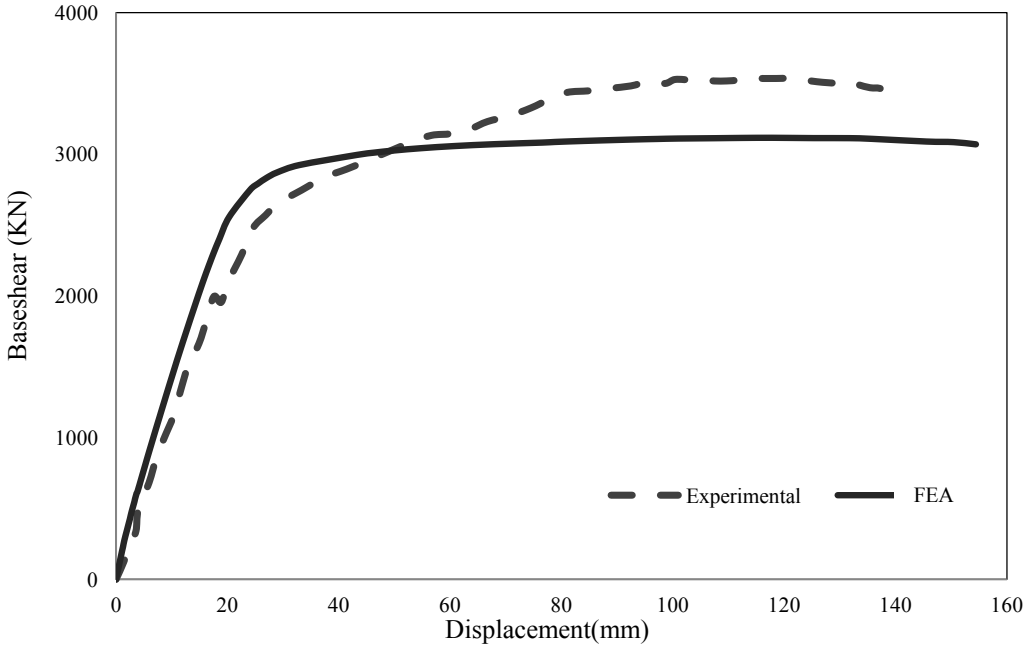


Figure 3.4: Pushover curve from FEA and experimental result of Behbahanifard et al. (2003) test speciman

The peak imperfection was considered 39mm for bottom storey. For rest of the structure, 10mm was considered as maximum out of plane deflection. All bottom nodes were fixed and several nodes in each floor were restrained for out-of-plane movement. Therefore, the boundary condition was applied in such a way that can represent the original test set up. External reference points were used to apply force at specific points for pushover analysis. The finite element model mesh and base shear versus displacement curve is presented in Figure 3.3 and Figure 3.4 respectively. Finite element analysis (FEA) showed an excellent agreement in initial stiffness while peak capacity of the test specimen was underestimated by about 8%.

## 3.5 Selected Steel Plate Shear Walls

### 3.5.1 Description of the selected Building

A four-storey and an eight-storey building with SPSWs are designed and modeled to evaluate seismic performance. Both of the buildings are identical in plane, which represents a hypothetical office building located in Vancouver. Total floor area of the buildings is 2631.7$m^2$. A simplified plan view of the building with gravity columns, beams and SPSWs are shown in Figure 3.5. SPSWs are placed in such ways that maintain structural symmetry in horizontal and vertical direction. In each direction, building has two identical SPSWs to resist lateral forces; therefore, each shear wall will resist one-half of the design seismic loads. Though the structure is symmetric, only accidental torsion was considered in seismic load calculation. Building was assumed to be on very dense soil and soft rock (according to NBCC 2010, site class is C). Each shear wall panel is 5.7m wide and storey height is 3.8m, so the aspect ratio of SPSW is 1.5. For each floor, dead load of 4.26kpa and live load of 2.4kpa were considered. For the roof, dead load of 1.12kpa and snow load was considered instead of live load. Live load reduction factors have

been utilized in the gravity load calculation for columns design.

### 3.5.2 Design of Selected Steel Plate Shear Walls

The nominal yield strength for the beams, columns and infill plates of SPSWs is 350MPa and modulus of elasticity of all steel members is 200000 MPa. The design load combination of $D+0.5L_L+E$ (where, $D$=dead load, $L_L$=live load and $E$= earthquake load) has been considered for floors and $D+0.25S_{nL}+E$ ($S_{nL}$= snow load) has been considered for roof. In the design process of SPSW, beam-to-column connections are considered as a moment-resisting frame; in addition, SPSWs are rigidly connected with its boundary beams and columns.

The equivalent static lateral loads due to design earthquake were calculated using the seismic provision of NBCC 2010. Fundamental periods of the buildings have been calculated using empirical formula, as specified in NBCC, which is a function of the building height. The design seismic base shear is estimated by (NBCC 2010):

$$V_b = \frac{S(T_a) M_V I_E W}{R_d R_o} \tag{3.1}$$

$$\frac{S(2.0) M_V I_E W}{R_d R_o} \le V_b \le \frac{2}{3} \frac{S(0.2) I_E W}{R_d R_o} \tag{3.2}$$

where, $S(T_a)$ is the design spectral acceleration for fundamental period $T_a$ of the building, expressed as a ratio of gravitational acceleration ; $M_V$ is an amplification factor to account for higher mode effects on the base shear; $I_E$ is an earthquake importance factor for the structure; $W$ is the total dead load plus 25% of the design snow load, 60% of the storage load, and the full

contents of any tanks. According to NBCC-2010, a ductility related reduction factor, $R_d$ of 5.0 and an over strength related reduction factor, $R_o$ of 1.6 were used in the calculation of seismic demand for SPSWs. Estimated base-shear was finally distributed based on following equation;

$$F_x = (V_b - F_t)\frac{W_x h_x}{\sum_{i=1}^{n} W_i h_i} \qquad 3.3$$

Where, $F_t$ is the portion of $V_b$ placed at the top of the building; $W_x$, $W_i$ are the portion of $W$ which are located at the level $x$ or $i$ respectively and $h_x$, $h_i$ are the height above the base to level $x$, $i$ respectively. Estimated equivalent lateral forces for 4-storey and 8-storey SPSW are presented in Table 3-1.

SPSWs are designed according to capacity design concepts, where the boundary members are designed to allow the development of full capacity of infill plates, the factored shear resistance of the infill plate $V_{re}$ is given by:

$$V_{re} = 0.4\phi F_{py} t_w L Sin\, 2\alpha \qquad 3.4$$

All the parameters are defined earlier. All the boundary elements are designed according to CSA S16-09 to develop the full capacity of the infill plates. As such, design philosophy for boundary elements were taken from Berman and Bruneau (2008). This design process is the implementation of capacity design approach in SPSW system, where infill plate is assumed as the energy dissipation fuse. SPSW was designed to resist 100% of lateral force by inclined tension field and the capacity of the boundary beam must be enough to carry the maximum force coming from the adjacent infill plates. Similarly, columns must have the capacity to stay elastic

when beam-ends start yielding. Uniformly distributed tension forces from infill plate were considered for beam and column load calculation as follows:

$$\omega_{yci} = 0.5F_{yp}t_{wi}Sin(2\alpha) \tag{3.5}$$

$$\omega_{xci} = F_{yp}t_{wi}(Sin\alpha)^2 \tag{3.6}$$

$$\omega_{ybi} = F_{yp}t_{wi}(Cos\alpha)^2 \tag{3.7}$$

$$\omega_{xbi} = 0.5F_{yp}t_{wi}Sin(2\alpha) \tag{3.8}$$

Where, $\omega_{yci}$ and $\omega_{xci}$ are the vertical and horizontal distributed force to the column respectively; $\omega_{ybi}$ and $\omega_{xbi}$ are the vertical and horizontal distributed force to the beam respectively. Boundary member were designed based on free body force analysis for these distributed force due to the infill plate yielding (Figure 2.5). Stiffness of the columns, top and bottom beam cross-sections to allow uniform tension field development in the adjacent infill plates are specified in CAN/CSA S16-09 in some stiffness checks.

$$I_c \geq \frac{0.0031t_w h_s^4}{L} \tag{3.9}$$

$$I_{tb} \geq \frac{t_w L^4}{650L - \left(\frac{t_w h_s^4}{I_{tb}}\right)} \tag{3.10}$$

$$I_{bb} \geq \frac{t_w L^4}{267L - \left(\frac{t_w h_s^4}{I_{bb}}\right)} \tag{3.11}$$

where, $h_s$ is the storey height, and $I_c$, $I_{tb}$, $I_{bb}$ are the moment of inertia of the cross-sections of boundary columns, top beam and bottom beam. All the Boundary members were class1 sections, which satisfied these above mentioned stiffness checks.

### 3.5.3 Selection of Steel Plate Shear Walls

For 4-storey SPSW, a 3 mm infill plate was selected as thinnest infill plate to meet the minimum practical availability of steel plates as well as welding and handling requirements. Even though smaller plate thickness would theoretically be sufficient for this structure, 4-storey SPSW was designed with same plate thickness to meet the practical availability. For 8-storey SPSW, 4.8 mm plate thickness was used at the base to resist lateral force. W690X350 has been selected as bottom and top beams for both of the multi-storey SPSWs to fasten the forces developed from the bottom and top storey infill plates respectively. In the 8-storey building, infill plate thickness was changed at 5th-floor so that the forces due to plate yielding have additional effect in that level. Therefore, W690X192 section was used at 4th-level beam. For intermediate beams, yield forces from the infill plate of two adjacent storey may cancel out each other, so only the axial load from the columns were considered, W530X109 was adequate for those stories. All the columns were designed to take the reduced plastic moment under axial force of the connected beams. So all the beams and columns were design as a beam-column elements. Elevation view of selected 4-storey and 8-storey SPSWs with all beams and columns sections are presented in Figure 3.6.

## 3.6 Finite Element Model of selected Steel Plate Shear Walls

The selected SPSWs are modeled in ABAQUS (Hibbitt et al. 2011) according to previously validated modeling techniques and analysis procedure as described in section-3.3. Yield strength of 350 MPa have selected for all infill plates, beams and columns of multi-storey SPSW systems. In the seismic analysis, a pin supported dummy gravity column is added to the

finite element model of the SPSW. This dummy column is connected to the plate wall at every floor level with pin ended rigid links, which maintain the constant horizontal displacement between SPSW and gravity column. This gravity column is made of 2-node linear 3-D truss (ABAQUS T2D3). It has been designed to carry half of the total remaining mass at each floor level with zero lateral stiffness. The gravity loads of each storey are added as lumped masses on the column at corresponding floor. 5% Rayleigh proportional damping ratio is used in all the seismic analysis. Frequency analysis has performed with gravity load of the building to find out natural frequency and the fundamental period of the structure before proceeding to seismic analysis.

Fundamental periods of the 4-storey and 8-storey SPSWs are 0.73 sec and 1.78 sec respectively, which were longer than the calculated periods according to NBCC 2010. Empirical equation to obtaining fundamental period of the structure in NBCC 2010 is as follows:

$$T_a = 0.05(h_n)^{3/4} \qquad 3.12$$

where, $T_a$ is the fundamental period of the building. $h_n$ is the total building height in meter. Estimated fundamental frequencies were used to calculate the damping factors for the materials in the finite element model according to Raleigh proportional damping of 5%.

Table 3-1: Estimated equivalent lateral forces for 4-storey and 8-storey SPSWs

| 4-Storey SPSW | | 8-Storey SPSW | | | |
|---|---|---|---|---|---|
| Storey Level | Lateral Force (KN) | Storey Level | Lateral Force (KN) | Storey Level | Lateral Force (KN) |
| 1 | 416 | 1 | 192 | 5 | 962 |
| 2 | 833 | 2 | 385 | 6 | 1154 |
| 3 | 1249 | 3 | 577 | 7 | 1347 |
| 4 | 598 | 4 | 770 | 8 | 553 |

Table 3-2: Summary of 4-storey and 8-storey SPSWs section properties

| Storey | 4-storey SPSW | | | 8-Storey SPSW | | |
|---|---|---|---|---|---|---|
| | Plate thickness (mm) | Column | Beam | Plate thickness (mm) | Column | Beam |
| 0 | | | W690X350 | | | W690X350 |
| 1 | 3 | W360X634 | W530X109 | 4.8 | W360X634 | W530X109 |
| 2 | 3 | W360X634 | W530X109 | 4.8 | W360X634 | W530X109 |
| 3 | 3 | W360X634 | W530X109 | 4.8 | W360X382 | W530X109 |
| 4 | 3 | W360X634 | W690X350 | 4.8 | W360X382 | W690X192 |
| 5 | | | | 3.0 | W360X216 | W530X109 |
| 6 | | | | 3.0 | W360X216 | W530X109 |
| 7 | | | | 3.0 | W360X216 | W530X109 |
| 8 | | | | 3.0 | W360X216 | W690X350 |

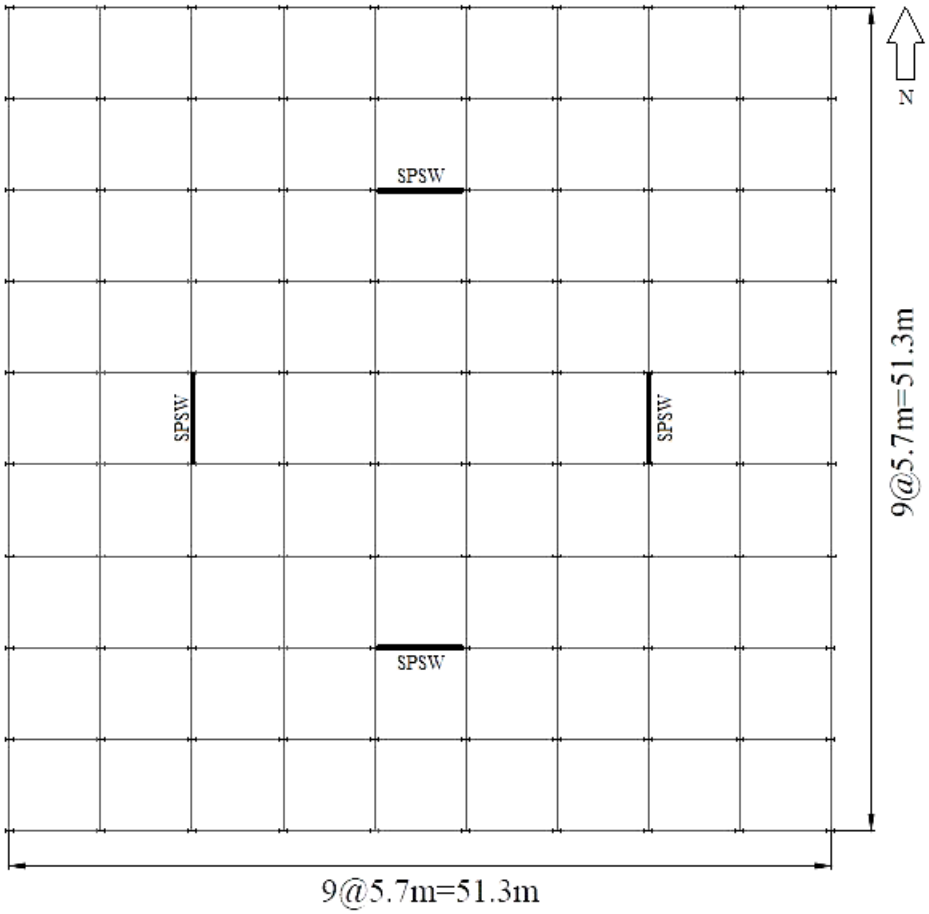


Figure 3.5**:** Building plan with gravity system and two identical SPSWs in each direction

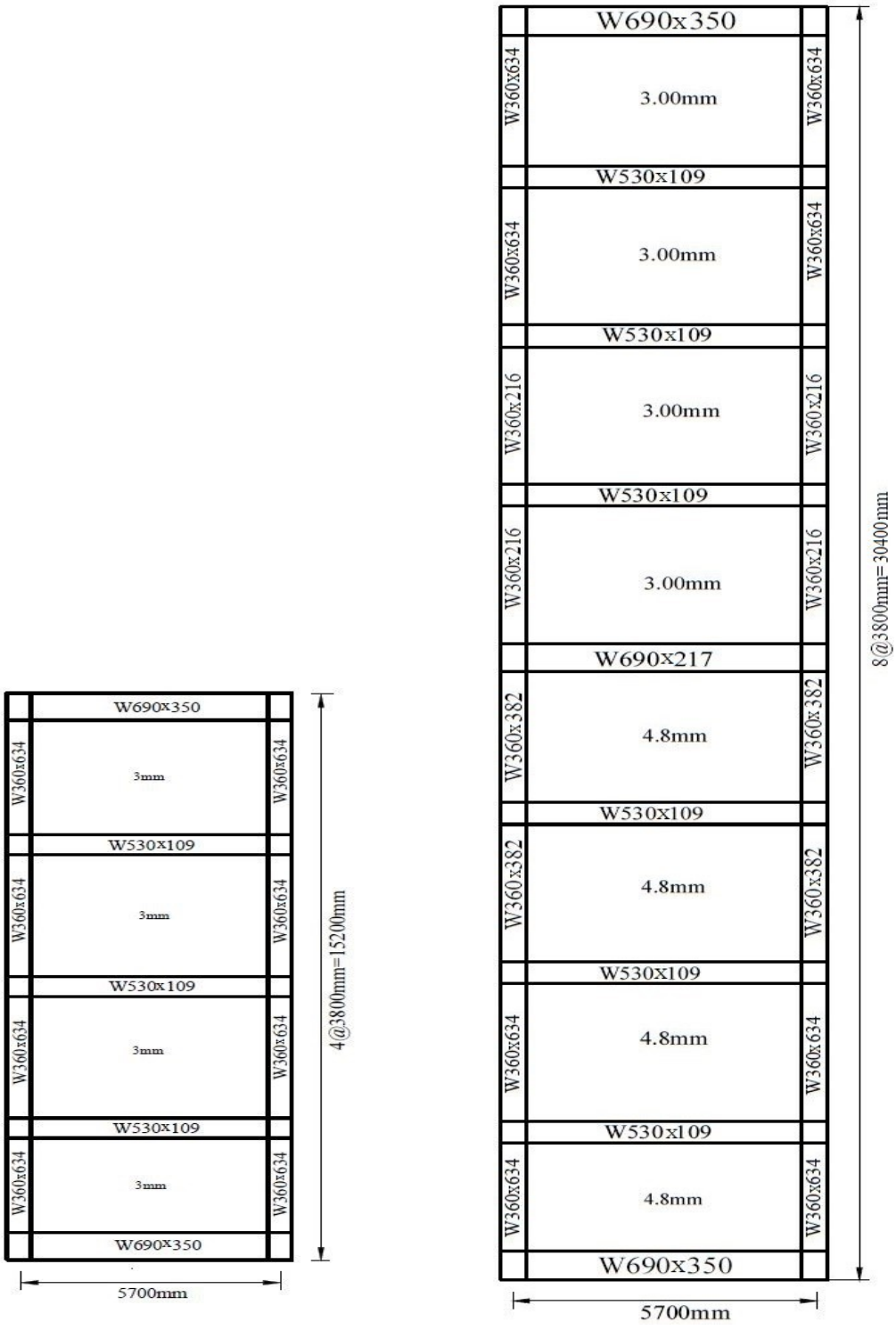


Figure 3.6: Schematic figure of 4-storey SPSW (left) and 8-storey SPSWs (right)

## 3.7 Earthquake Ground Motion Records

A set of ground motion records are required for nonlinear time history analysis, those have to be compatible with the earthquake hazard spectrum of Vancouver region provided by NBCC 2010 (John and Halchuk 2003). According to ASCE 7-10, minimum three ground motion records are recommended for response history analysis, when peak responses are considered as component checking. Moreover, minimum seven ground motion records are suggested for the same purpose when average of maximum response can be used for component checking.

Eight ground motion records have been selected and scaled for nonlinear time history analysis. Four real ground motion records are collected from strong ground motion database of Pacific Earthquake Engineering Research center, California (PEER 2010). Real Ground Motion Records (GMR) are selected based on the ratio of peak ground acceleration ($A$) to peak ground velocity ($V$) of ground motion records (where acceleration is in unit of g; velocity is in *m/s* and gravitational acceleration $g$, is in unit of $m/s^2$). It has been found that spectral shape of any GMR is significantly controlled by its peak ground acceleration and peak ground velocity. Real GMR were selected as such that they have $A/V$ ratio close to 1.0, which is the recommended value for Vancouver region (Naumoski et al. 2004). Therefore, real GMRs have been selected from 0.8 to 1.2 of $A/V$ ratio. Only horizontal component of the ground motion records were selected for this study. Canadian earthquake records between the years 1600 to 2006 show that more than 60% seismic events have occurred in Vancouver and the offshore region of British Colombia. Most of these earthquake magnitudes are in the range of 6.0 to 7.0 in Richter scale (Lamontagne et al. 2008). Therefore, 6 to 7 magnitude earthquake GMRs having $A/V$ ratio of 0.8 to 1.2 have been selected for dynamic analysis. Four simulated GMRs are collected from engineering

seismotoolbox (Atkinson 2009). Two different set of records are selected having magnitude of 6.5 and 7.5 for soil class C. Each of the magnitude set has one near fault and one far fault earthquake records.

Partial Area method of ground motion scaling has been conducted to scale the selected GMR with the design response spectrum of Vancouver. In this approach, area under the acceleration-response spectrum curve of selected GMR and design response spectrum of Vancouver were compared to get appropriate scaling factor. Area under the acceleration response spectrum of selected GMRs ($A_2$) between $0.2T_1$ to $1.5T_1$ ($T_1$ is the first period of vibration of the building) has been compared with the area under the design response spectrum of Vancouver ($A_1$) for the same period range. Scaling factor for selected GMR is the ratio of $A_1/A_2$ where both of the response spectrums is prepared for 5% of critically damped single degree of freedom system and for soil class C. The period range for the scaling was assumed as the most probable range of the vibration during the earthquake event. When structure goes through the plastic deformation, period of the building may lengthened; for that reason, scaling factor was increased up to 1.5 times of fundamental period ($1.5T_1$). Lower limit of the range has been selected to account the higher mode effect of the structure in the seismic event (Naumoski et al. 2004). Scaling factor for each earthquake was from 0.5 to 2.0, which represents that the selected GMRs are close to the Vancouver hazard spectrum. Summary of real GMR and simulated GMR are presented in Table 3-3 and Table 3-4 respectively. Real and simulated ground motion acceleration time-history is presented in Figure 3.7 and Figure 3.8 respectively. In addition, 5% damped scaled ground motion response spectrum with Vancouver design response spectrum are illustrated in Figure 3.9and Figure 3.10 for 4- and 8-storey SPSW respectively.

Table 3-3: Summary of real ground motion records and scaling factors

| Event name | Mag[n] | Station | PGA (g) | PGV (m/s) | A/V | Scaling factor | |
|---|---|---|---|---|---|---|---|
| | | | | | | 4-Storey | 8-Storey |
| Kobe, Japan,1995 | 6.6 | HIK | 0.143 | 0.148 | 0.97 | 1.757 | 1.56 |
| San Fernando, California, 1972 | 6.61 | LA-Hollywood Stor FF | 0.188 | 0.18 | 1.04 | 1.637 | 1.58 |
| Kern County, California, 1952 | 6.53 | Taft Lincoln School | 0.156 | 0.153 | 1.02 | 1.880 | 1.810 |
| Imperial Valley, California, 1979 | 6.53 | El Centro | 0.525 | 0.502 | 1.04 | 1.000 | 1.03 |

Table 3-4: Summary of simulated ground motion records and scaling factors

| Event name | Magnitude | Distance (Km) | Peak acceleration ($cm/s^2$) | Scaling factor (4 Storey) | Scaling factor (8 Storey) |
|---|---|---|---|---|---|
| 6C1 | 6.5 | 8.8 | 487 | .69 | 0.78 |
| 6C2 | 6.5 | 14.6 | 265 | 1.3 | 1.48 |
| 7C1 | 7.5 | 15.2 | 509 | 0.85 | 0.91 |
| 7C2 | 7.5 | 45 | 248 | 1.69 | 1.83 |

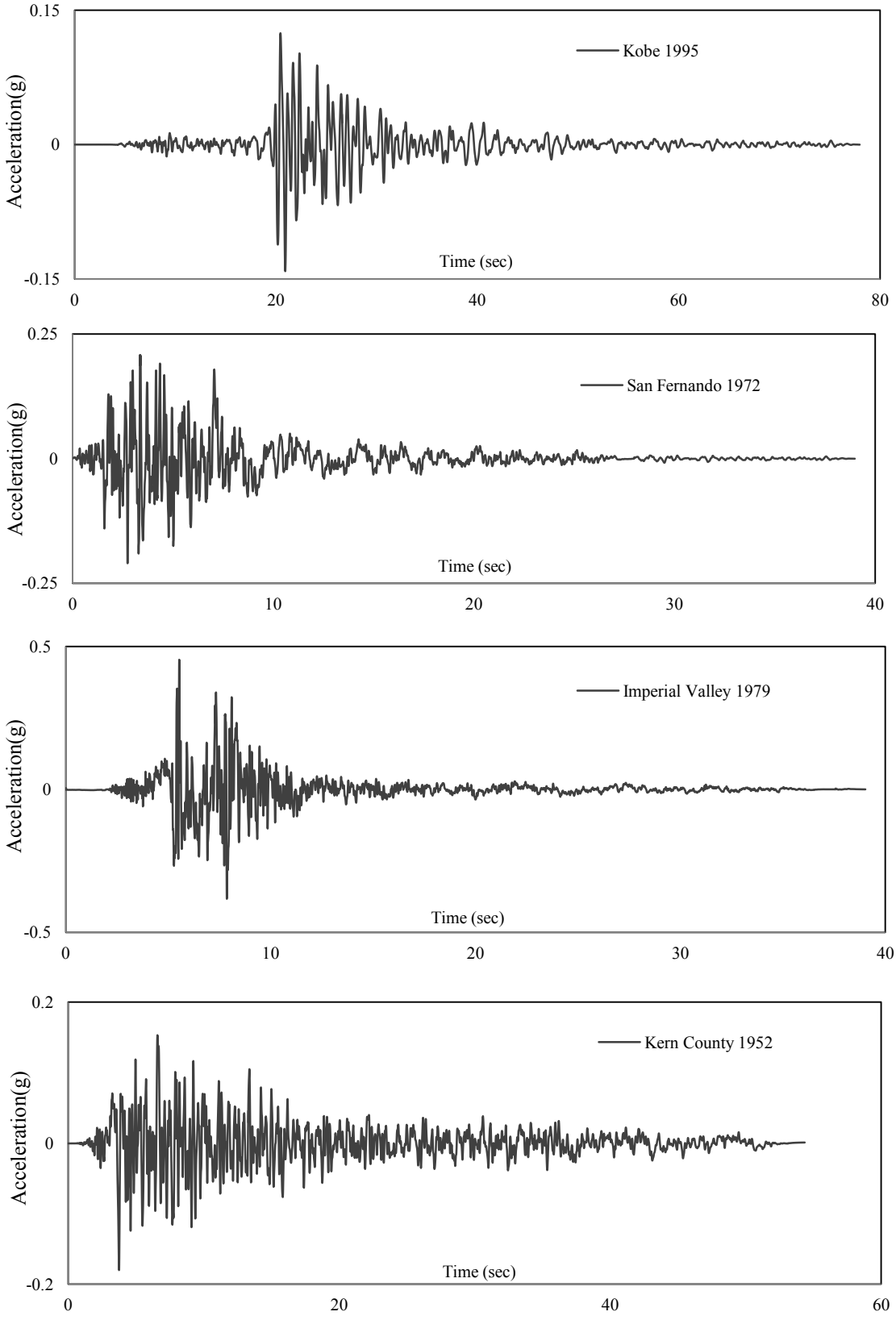


Figure 3.7: Selected real unscaled GMRs collected from PEER (2010)

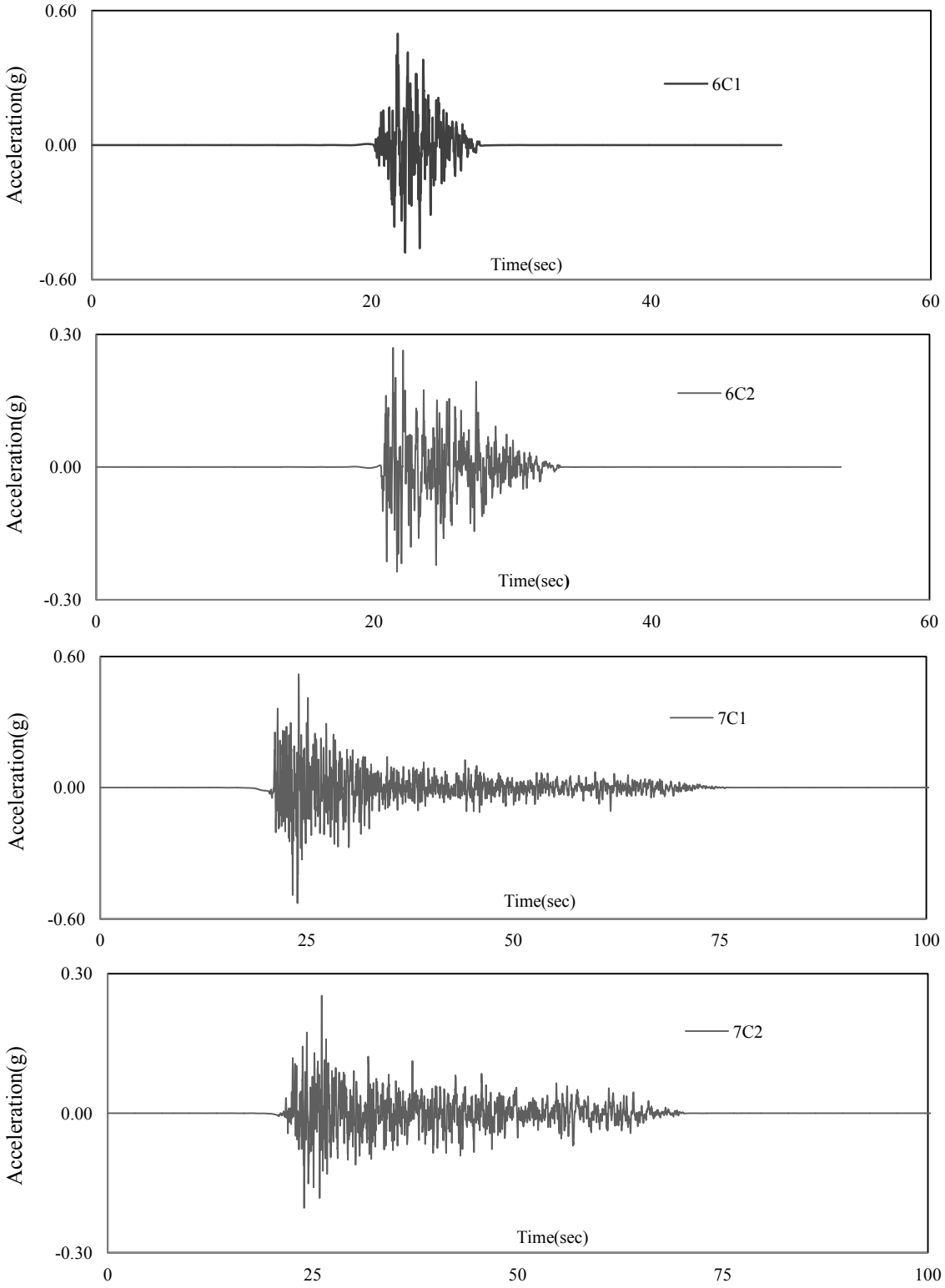


Figure 3.8: Selected simulated unscaled GMRs collected from engineering seismotoolbox.

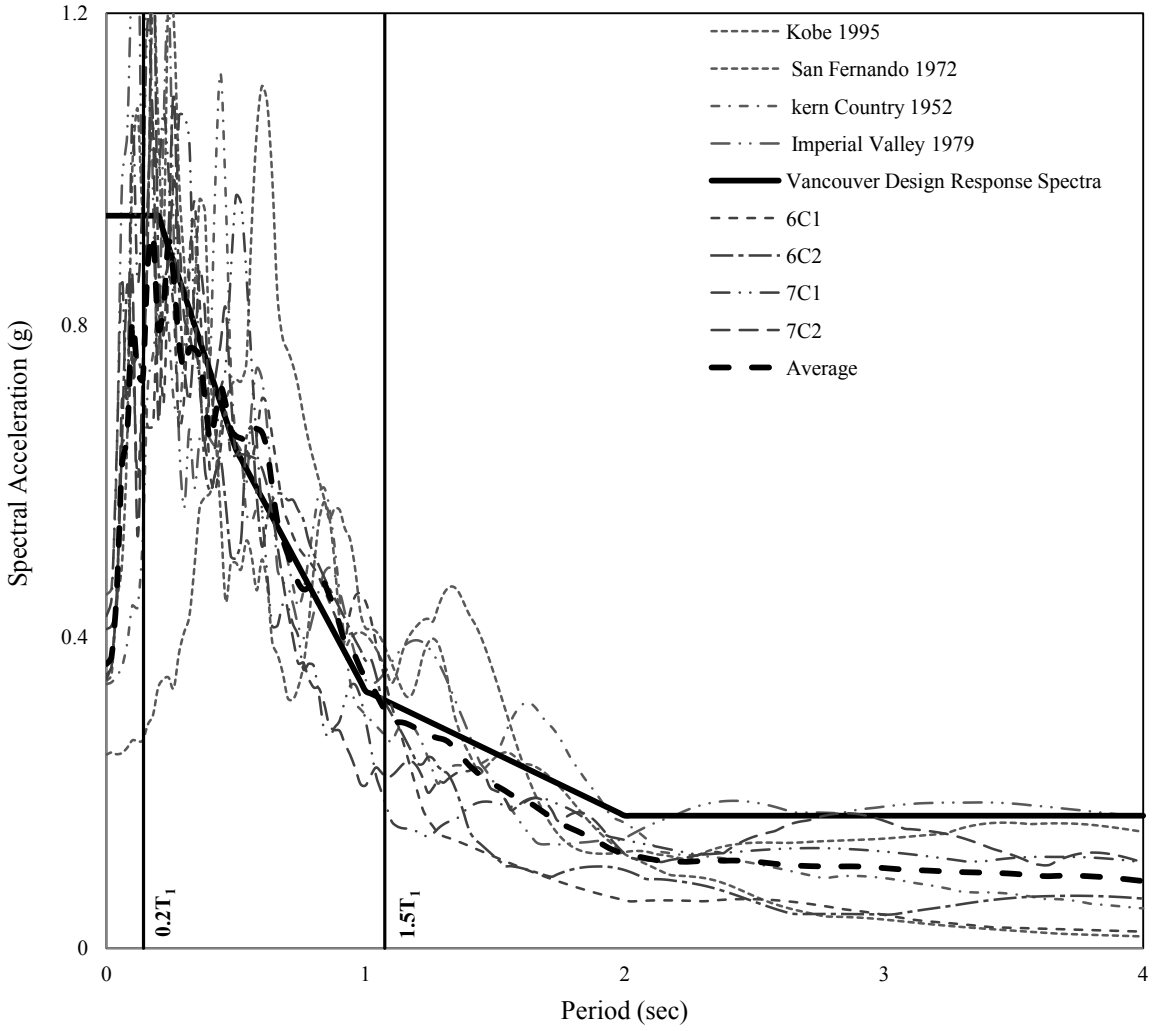


Figure 3.9: Acceleration Response spectrum of scaled GMRs for 4-storey SPSW and Vancouver design response spectrum

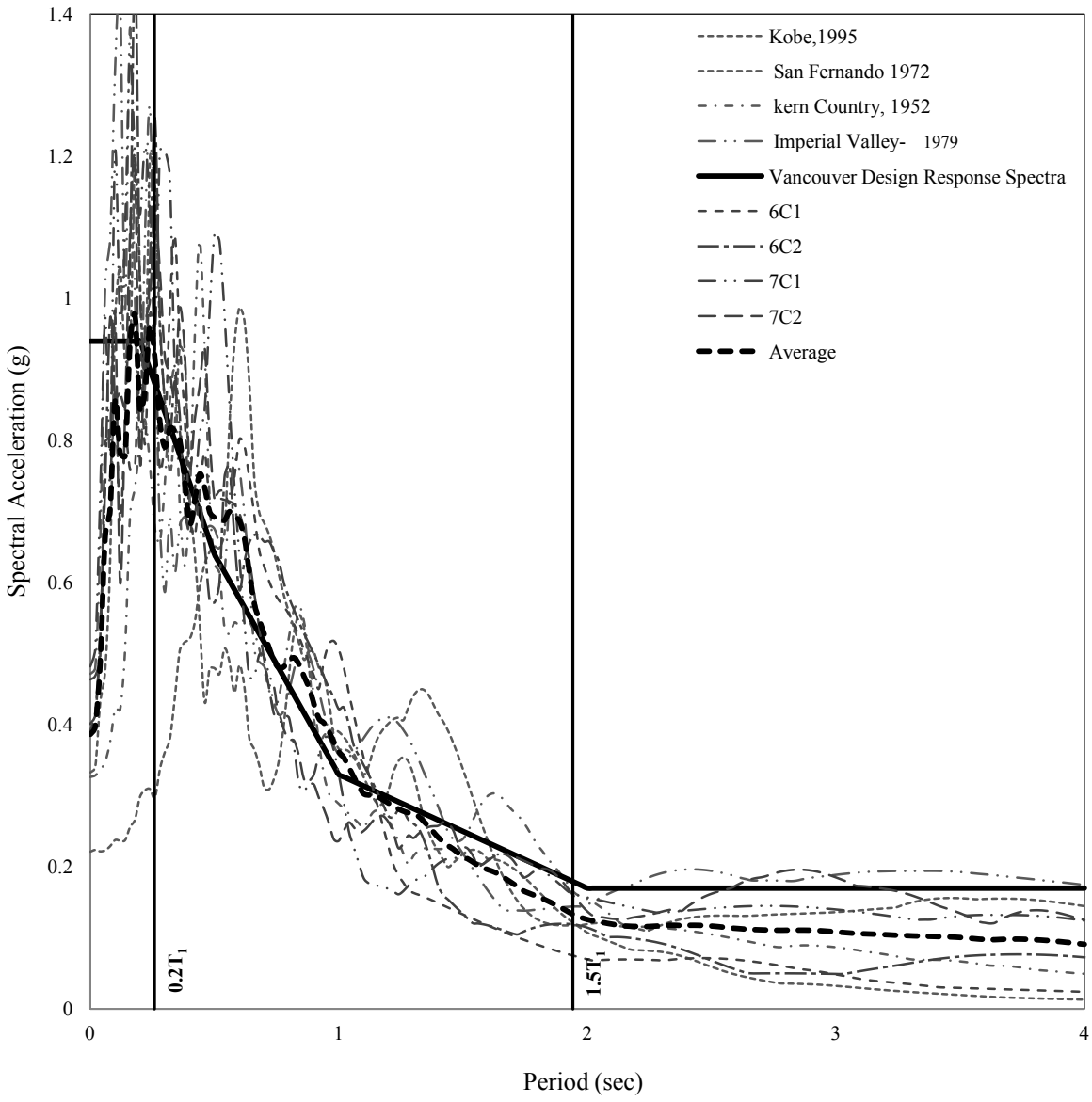


Figure 3.10: Acceleration Response spectrum of scaled GMRs for 8-storey SPSW and Vancouver design response spectrum

### 3.8 Seismic Response of Steel Plate Shear Walls

Nonlinear time history analysis has been conducted for 8-storey and 4-storey SPSW with selected and scaled ground motion records. Peak responses of SPSWs under those selected earthquake GMR were estimated and presented in this section. Maximum base reaction and storey shear for 4-storey and 8-storey SPSW have been presented in Figure 3.11 and Figure 3.12. Where for both of the cases, maximum base shear reaction for nonlinear seismic analysis were much higher than the static equivalent force of NBCC 2010. Dynamic storey shear distributions for SPSWs were higher than NBCC 2010 storey shear force as well. Average maximum base reaction of selected GMR is 5036 KN for 4-SPSW, which is 42% higher than the probable storey shear resistance. Similarly, average maximum base reaction for 8-storey SPSW is 6606 KN and it is 34% higher than the probable shear resistance. This increase in shear at the base is because of the over strength of the SPSW. Steel infill plate was selected based on practical availability, so the plate thickness was much higher than the design requirement. Therefore, total strength of the SPSW system was increased. Moreover, a good amount of shear contribution was found from boundary steel columns, which has been ignored in probable shear resistance calculation. Base reaction time histories for 4-storey and 8-storey SPSWs are presented in Figure 3.11 and Figure 3.12. Besides that, extents of yielding in 4-storey and 8-storey SPSW system under 6C1 earthquake record are presented in Figure 3.19. During the seismic analysis of 4-storey SPSW, plates yielding are found in bottom 3-storeys in all of the cases, where two bottom beams were also yielded in those cases. Only in simulated earthquake 7C1, top storey plate and 3rd-storey beam reached in the yielding point, in the same time column base also showed partial yielding. Boundary columns were essentially elastic for most of the seismic events, so steel plates and lower level beams were the main location for energy dissipation. In 8-storey SPSW system, four

bottoms steel plates were yielded in all the cases; in addition, bottom two storey beams showed some yielding. Partial yielding in the column base was also found in some cases. Therefore, capacity design concept in the design of boundary members worked well where columns remained elastic during the full yielding of the steel plates and adjacent beams.

Finally, peak relative storey displacement and maximum inter-storey drift have estimated from seismic analysis under selected GMRs and presented in Figure 3.15 to Figure 3.18. Inter-storey drift for all of the seismic events were much lower than the NBCC 2010 drift limit. Floor displacement pattern for both SPSW systems were taken at the instant of maximum roof displacement and floor displacement pattern for all the results are similar to each other. Inter-storey drift pattern for most of the result are close to each other, where different ground motion characteristics may cause the variation in the results.

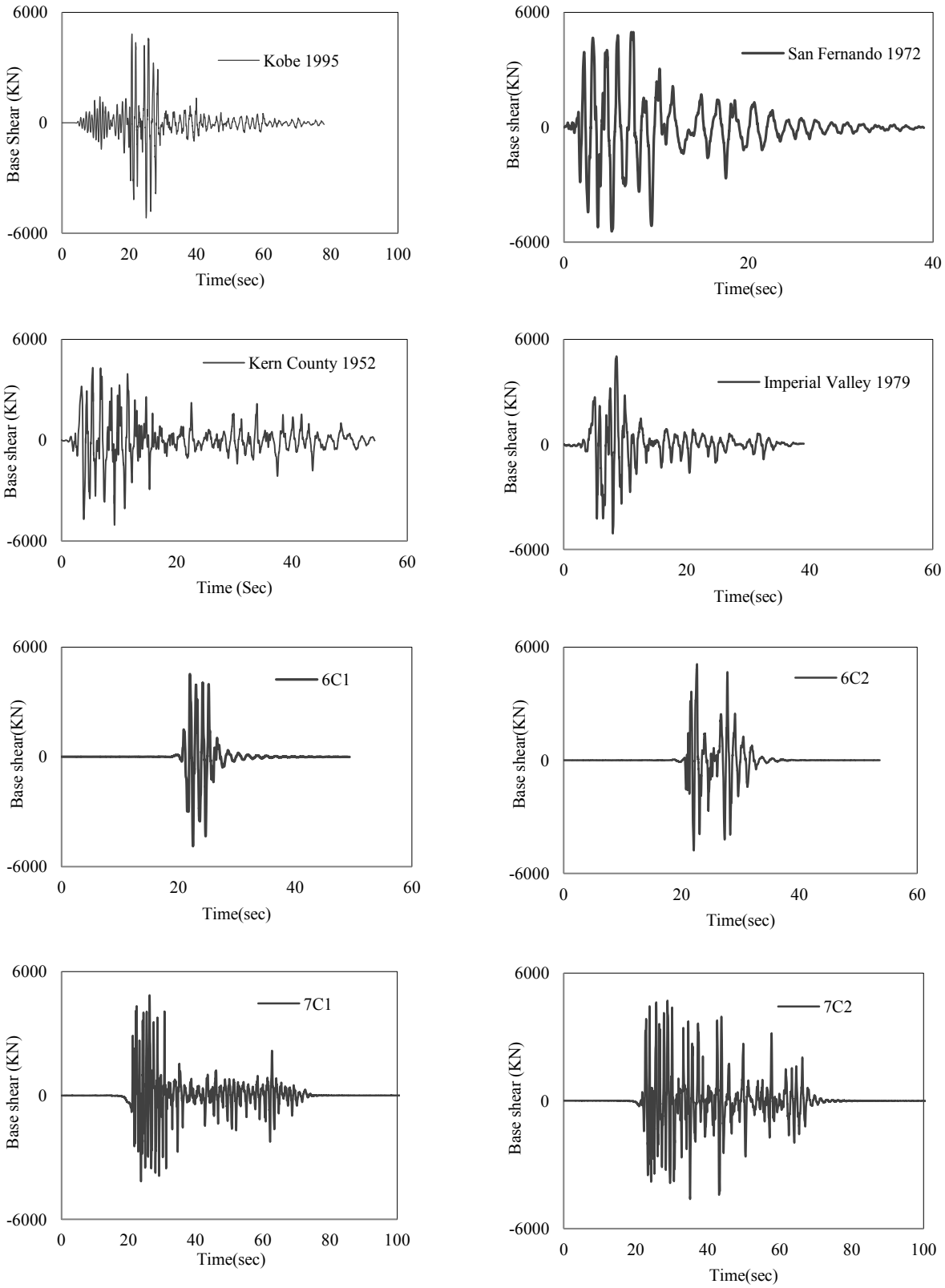


Figure 3.11: Base shear history of 4-storey SPSW

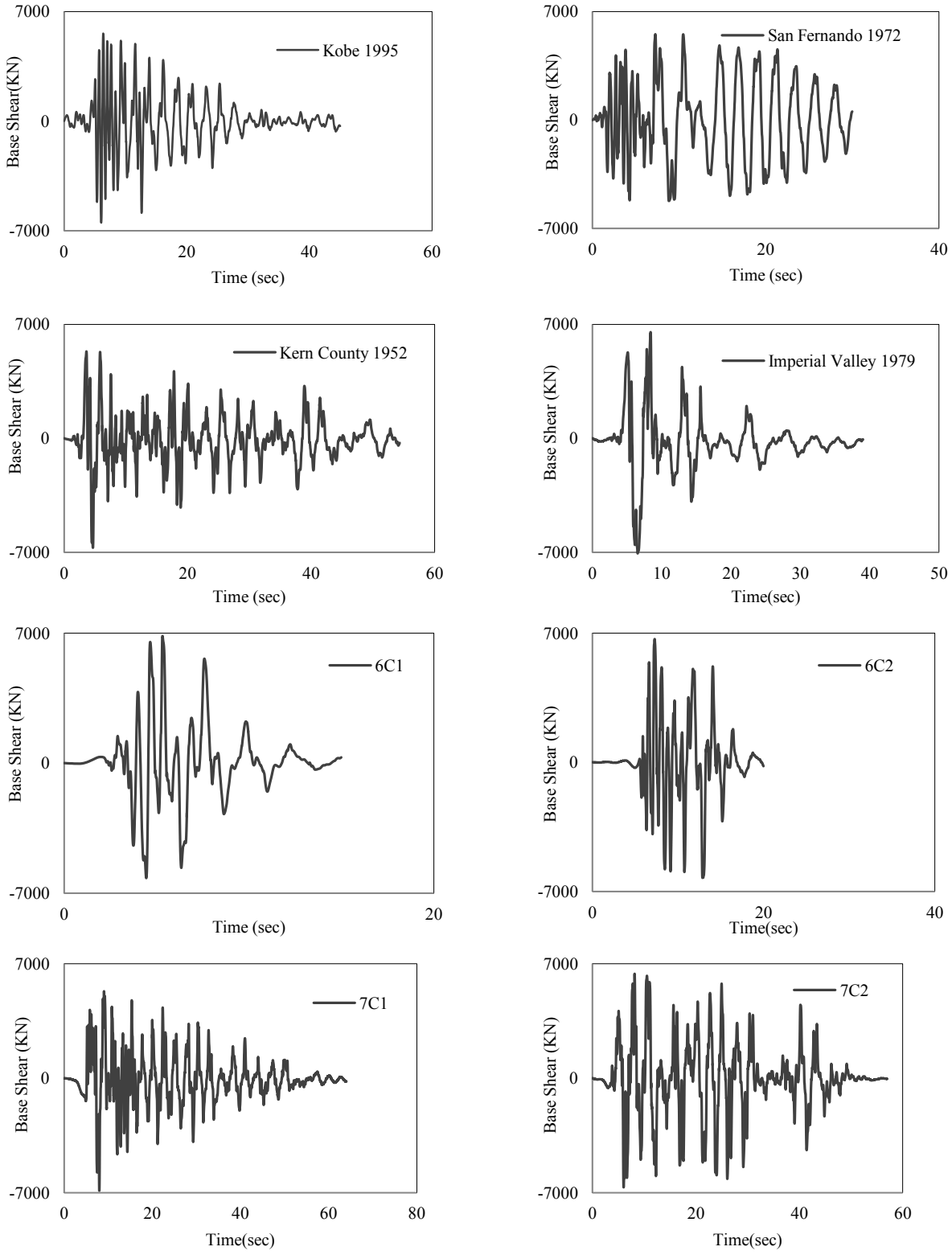


Figure 3.12: Base shear history of 8-storey SPSW

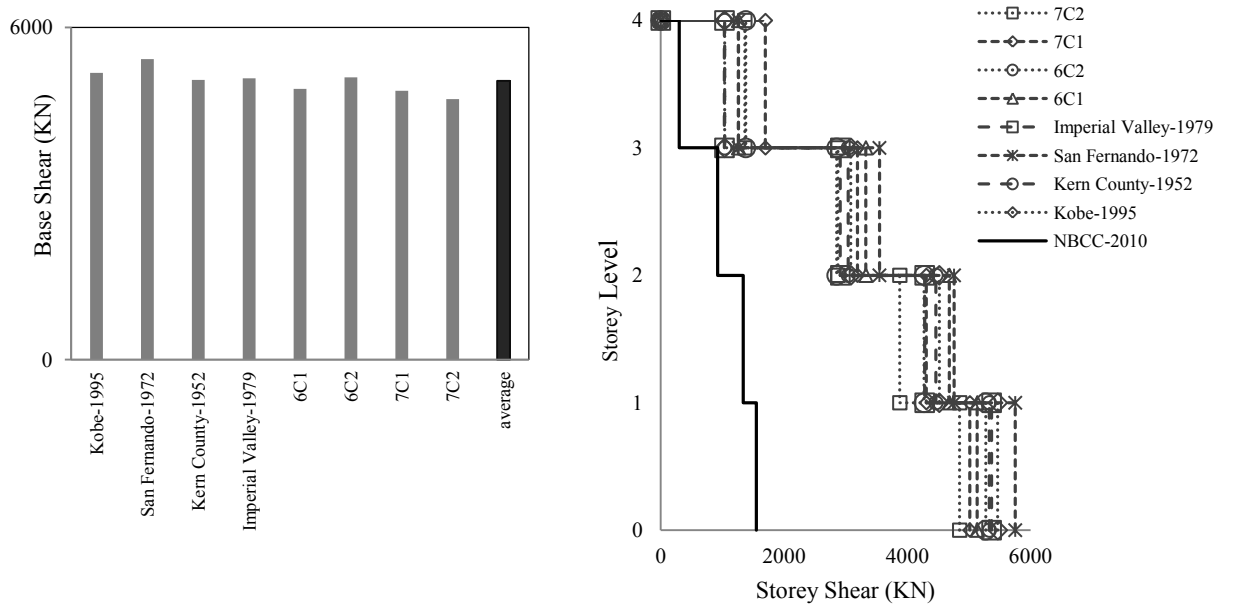


Figure 3.13: Maximum base shear for 4-storey SPSW system: base shear (left) and storey shear distribution (right) under selected GMRs

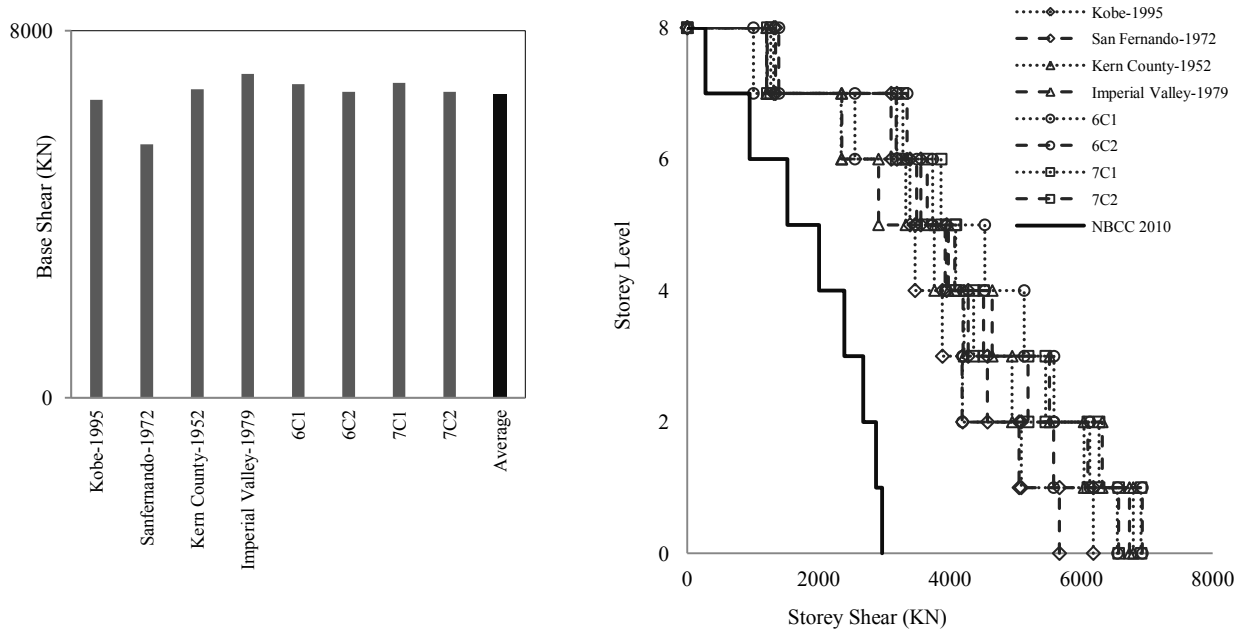


Figure 3.14: Maximum base shear for 8-storey SPSW system: base shear (left) and storey shear distribution (right) under selected GMRs

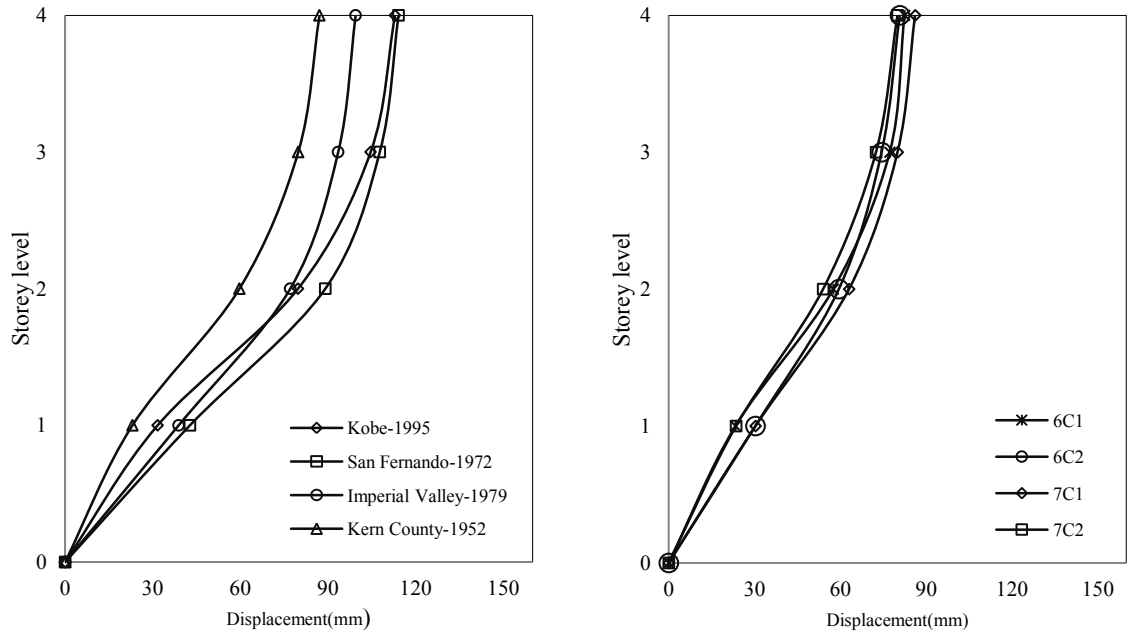


Figure 3.15: Maximum storey displacements for 4-storey SPSW system: under real GMRs (left) and under simulated GMRs (right)

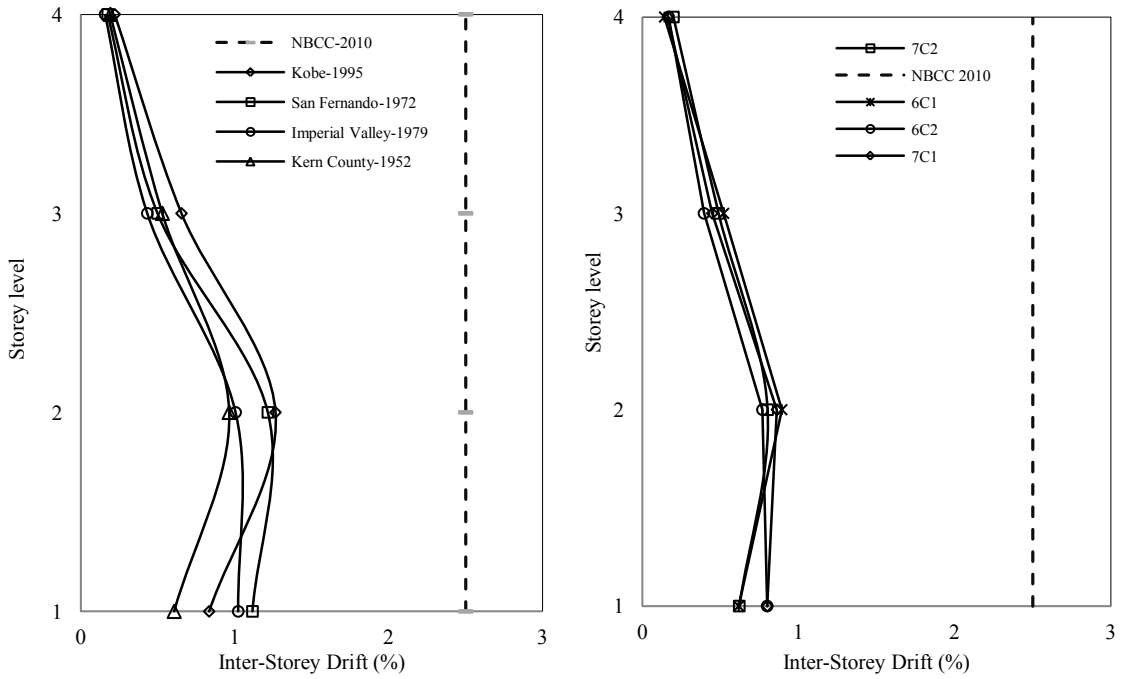


Figure 3.16: Maximum inter-storey drifts for 4-storey SPSW system: under real GMRs (left) and under simulated GMRs (right)

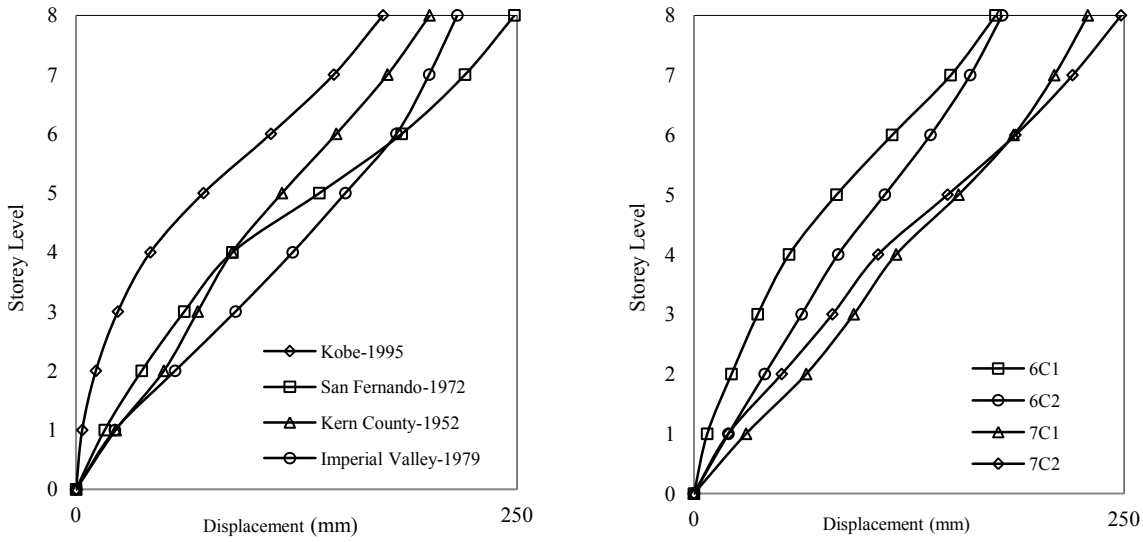


Figure 3.17: Maximum storey displacements for 8-storey SPSW system: under real GMRs (left) and under simulated GMRs (right)

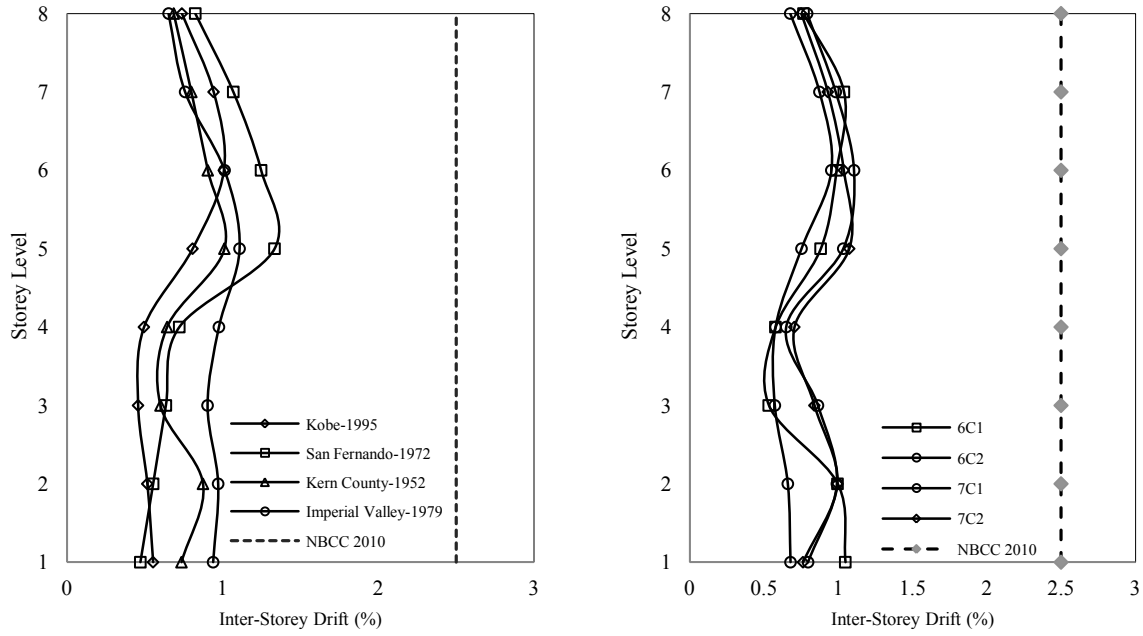


Figure 3.18: Maximum inter-storey drifts for 8-storey SPSW system: under real GMRs (left) and under simulated GMRs (right)

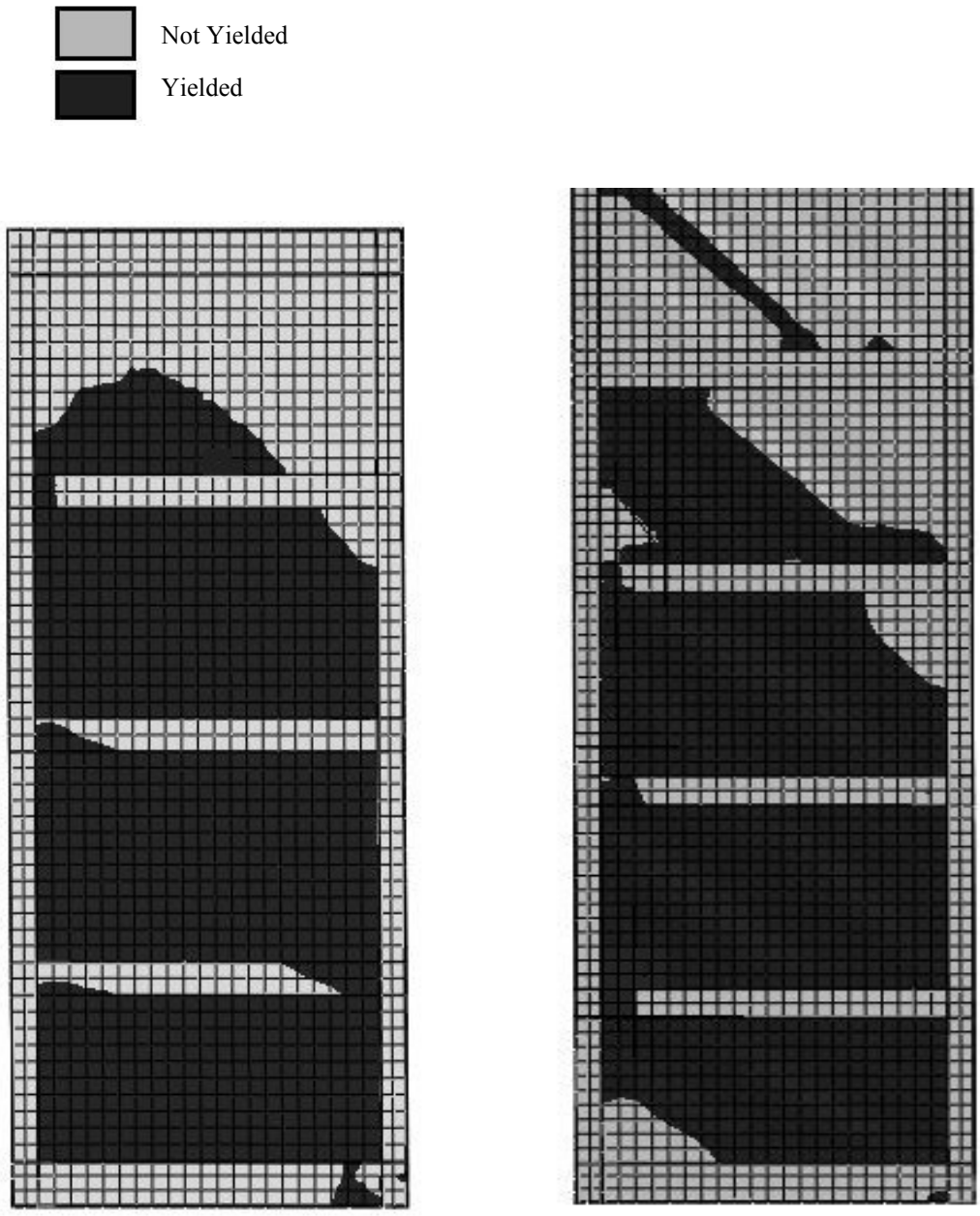


Figure 3.19: Yield pattern of 4-storey SPSW (right) and bottom 4 storey of 8-storey SPSW (left) at peak base shear instant under 6C1 ground motion

## 3.9 Conclusion

A finite element model of SPSW system has been validated with experimental result, which shows the essential properties of the model was very close to the experimental model. Initial stiffness of the FEM was very close to experimental one, where post-yielding strength was around 3% under the experimental result of single-storey test specimen of Lubell et al. (2000). On the other hand, around 8% underestimation was observed in the ultimate strength of 3-storey test specimen of Behbahanifard et al. (2003) due to its excessive initial imperfection, which was unknown for this study. Therefore, the selected modeling technique was served well under quasi-static loading condition. This specified modeling technique has been utilized for modeling and nonlinear dynamic of SPSW to estimate seismic performance of SPSW.

One 4-storey and one 8-storey SPSW systems have been designed according to Capacity method by using Berman and Bruneau (2008) proposed design method. Infill plate thickness was selected based on practical availability, so that SPSWs capacity was increased. To evaluate seismic behavior and performance of SPSW, nonlinear time history analysis was performed with a previously validated finite element model. A set of ground motion records for Vancouver were selected and scaled prior to seismic analysis. Some essential parameters were evaluated and estimated from seismic analysis.

- SPSW system with moment resisting frame perform well under real and simulated GMRs. In most of the cases, only steel infill plates and beam-ends were yielded in the bottom storeys. In some cases, column base also partially yielded. The capacity design method for both of SPSW was performed according to its design principle.

- Maximum estimated inter-storey drift for all of the seismic events were below the NBCC-2010 drift limit of 2.5%. Some permanent deformations were observed in the steel plate after completion of the seismic analysis. Displacement patterns and inter-storey drift patterns were similar to each other.
- Maximum base reactions of dynamic analysis for both SPSW systems were higher than the equivalent static base shear and probable storey shear of the SPSWs. Other strength of the SPSW due to its design considerations and shear participation by the boundary column were the main reason for this higher base reaction during the dynamic analysis.

**Chapter- Four**

# Seismic Performance Evaluation of Steel Plate Shear Walls Using the Capacity Spectrum Method

## 4.1 Introduction

The Capacity Spectrum Method (CSM) is a nonlinear static analysis procedure as well as a performance-based seismic design tool, which is applicable for performance evaluation and design verification of new and existing buildings. Inelastic behaviors of the buildings are considered in CSM by using inelastic response spectra or equivalent damped spectra. Appropriateness of both response spectra have been evaluated in previous studies (Chopra and Goel 1999). Fajfar (1999) introduced a relatively simple and easy to use CSM procedure with a constant ductility demand spectra developed by Vidic et al. (1994).

The aim of this chapter is to evaluate seismic performance of SPSW systems using CSM. CSM proposed by Fajfar (1999) are applied in this study, where inelastic demand spectra have been estimated by using approximate bilinear expression of force reduction factor of Vidic et al. (1994). The seismic performance of 8-storey and 4-storey buildings with SPSW (designed and modeled in chapter 3) is evaluated by CSM. Seismic performance of a high-rise (15-storey) building with SPSW has also been evaluated by CSM. Design acceleration response spectrum of Vancouver has been transformed into the constant ductility demand spectra. The pushover (base shear versus roof displacement) curves of the SPSWs are converted into the capacity spectrum of the equivalent single-degree-of-freedom (ESDOF) systems. Finally, applicability of the CSM for

performance evaluation of low-rise, medium-rise and high-rise SPSW has been justified through the comparison to the response obtained from extensive nonlinear dynamic analyses for a number of site-specific ground motion records.

## 4.2 Capacity-Spectrum Method

Capacity-Spectrum method proposed by Fajfar (1999) is originally a nonlinear seismic design and performance evaluation method, which has been used in this chapter. It compares capacity of the structures and the demand of seismic ground motion for the structure. Major steps of capacity-spectrum methods are presented below:

**Development of capacity curve of Equivalent-Single Degree of Freedom (ESDOF) system:**

Step-1: Pushover curve of MDOF system: Estimate the first natural frequency of vibration $\omega_n$, and associated normalized elastic vibration mode shape, $\varphi$ of a multi-storey building (multi-degree of freedom system). Here, φ is considered as an assumed displacement shape for this MDOF system. Base shear-roof displacement (pushover) relation for MDOF system needed to be developed, where lateral force in the $i^{th}$ storey is proportional to the assumed displacement shape weighted by the $i^{th}$ storey mass $m_i$ .

$$p_i = m_i \phi_i \tag{4.1}$$

Where, $P_i$, is the lateral force, physical basis of this force distribution is the inertia forces of the system that oppose any displacement in the system.

Step-2: Transformation of MDOF to ESDOF System: A transformation factor *Γ,* is calculated to convert from MDOF system to ESDOF system. *Γ* is called modal participation factor. All the properties such as base shear, top displacement, and hysteretic energy of MDOF can be transferred in to force, top displacement and hysteretic energy of ESDOF system respectively.

$$L_n = m^* = \sum m_i \phi_i \tag{4.2}$$

$$\Gamma = \frac{m^*}{\sum m_i \phi_i^2} \tag{4.3}$$

Where, $m^*$ is the mass of equivalent single degree of freedom system.

Step-3: Determination of Capacity Spectrum for ESDOF system: Top displacement *($D_t$)* and base shear *($V_b$)* curve of MDOF system are transformed into force *($F^*$)*-displacement *($D_t^*$)* relationship of ESDOF system by following relationship.

$$F^* = V_b / \Gamma \qquad\qquad D_t^* = D_t / \Gamma \tag{4.4}$$

After that, force ($F^*$)-displacement ($D_t^*$) relation of ESDOF system are idealized based on energy balance consideration of FEMA-273. Finally, bilinear idealized force ($F^*$)-displacement ($D_t^*$) curve are transferred into capacity curve by representing spectral acceleration to spectral displacement curve of ESDOF system. Spectral acceleration at the yielding point is, $S_{ay} = F_y^* / m^*$ . Elastic period of the idealised bilinear system $T^*$ can be determined by,

$$T^* = 2\pi \sqrt{m^* D_y^* / F_y^*} \tag{4.5}$$

where, $D_y^*$ and $F_y^*$ are the yield displacement and yield strength of the ESDOF system.

Schematic figure of the development of capacity curve from pushover curve of MDOF to force-displacement curve of ESDOF system is presented in Figure 4.1. Bilinear transformation of force-displacement curve is and capacity curve of ESDOF system are presented in this figure.

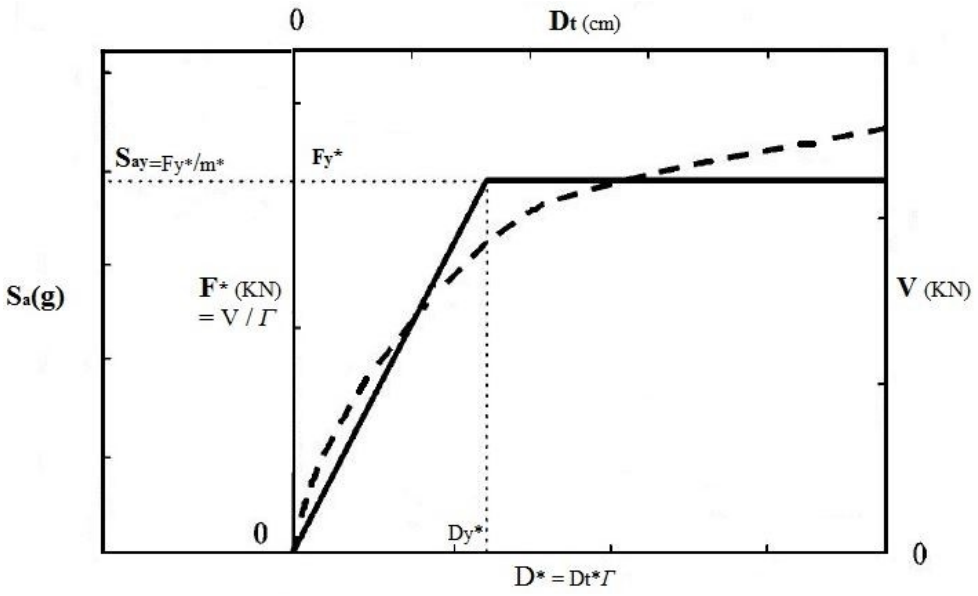


Figure 4.1: Development of the capacity spectrum of an ESDOF system by Fajfar (1999).

**Seismic Demand in Acceleration Displacement Response Spectrum Format (ADRS):**

Seismic demand spectra are developed from highly damped elastic spectra, which should be presented as spectral acceleration versus spectral displacement where period *T* are represented by redial lines. This type of representation is referred as acceleration-displacement response spectrum (ADRS). Acceleration response spectrum can be converted in to ADRS by utilizing following relation between Pseudo-acceleration and displacement for the Single-Degree-of-Freedom (SDOF) system,

$$S_{de} = \frac{T^2}{4\pi^2} S_{ae} \qquad 4.6$$

where, $S_{de}$ and $S_{ae}$ are the Spectral displacement and pseudo acceleration of elastic response spectrum respectively corresponding to the period $T$. Inelastic ADRS can be obtained directly from time-history analysis of a series of inelastic SDOF system, or indirectly from elastic ADRS. The acceleration spectra $S_a$ and displacement spectra $S_d$ has been determined for an inelastic SDOF system, by using strength reduction factor $R$ proposed by Vidic et al. (1994). This reduction factor is the ratio of elastic strength demand to inelastic strength demand of an ESDOF system for a specified ductility ratio. Reduction factor (R) mainly depends on the ductility and on the period of the system.

$$S_a = \frac{S_{ae}}{R_\mu} \tag{4.7}$$

$$S_d = \mu \frac{T^2}{4\pi^2} S_a \tag{4.8}$$

$$R_\mu = (\mu - 1)\frac{T}{T_o} + 1 \quad , T \le T_o \; ; \qquad R_\mu = \mu \quad , T \ge T_o \tag{4.9}$$

$$T_o = 0.65\mu^{0.3} T_s \le T_s \tag{4.10}$$

where, $T_s$ is the characteristics period which refers the transition period where constant acceleration region intersect the constant velocity region; and this is the period when largest force are applied to the structure; $\mu$ is the ductility demand structures, which is the ratio of maximum displacement to the yield displacement; $T_o$ is the transition period which depends on structural ductility and it should not be greated than $T_s$; $R_\mu$ is the reduction factor for corresponding ductility demand. In this procedure, 5% mass proportional damping for Q model was utilized. In addition to design response spectrum, "exact" response spectrum of expected ground motion can be used as seismic demand curve.

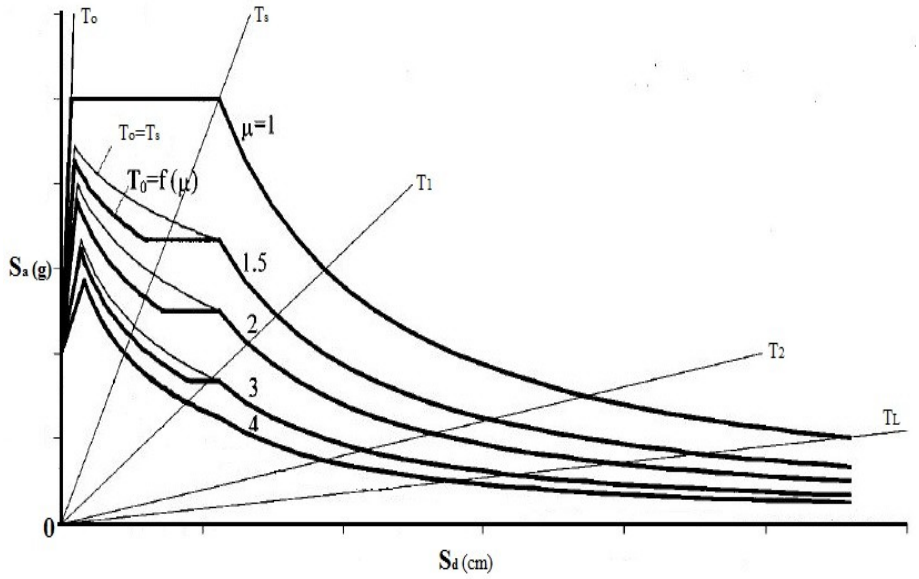


Figure 4.2: Schematic figure of an seismic demand spectrum (constant ductility response spectrum in ADRS format) by Fajfar (1999)

**Determination of Seismic Demand and performance of ESDOF system:** Demand spectra and capacity spectra for ESDOF system are established, now they needed to be drawn in the same plot. Intersection point of the redial line of the capacity curve corresponding to the elastic stiffness of the ESDOF system and the elastic demand spectrum, gives the strength requirement $(S_{ae})$ for elastic response of the structure. The yield acceleration $(S_{ay})$ for the ESDOF system refers the acceleration requirements for the inelastic behavior. Ratio of the elastic acceleration demand and inelastic acceleration capacity is the reduction factor $R_\mu$. After that, ductility demand can be calculated by the reverse calculation of equation 4.9. If the elastic period of the structures is larger than $T_s$, "Equal Displacement Rule" applies. It is assumed for medium-period and long-period range, inelastic displacement demand is equal to the elastic displacement demand. Displacement demand is determined from the intersection point of the capacity curve and the demand curve corresponding to the ductility demand.

## 4.3 Application of Capacity Spectrum Method (CSM)

### 4.3.1 SPSW systems for CSM application

One 4-storey and one 8-storey SPSW systems have been designed according to capacity design approach of CAN/CSA S16-09. Details of the preliminary design are described in chapter-3 and finite element model of SPSWs are developed in ABAQUS (Hibbitt et al. 2011) (Chapter-3). A 15-storey SPSW system for a hypothetical office building was taken from Bhowmick et al. (2011). 15-storey SPSWs was designed for Vancouver soil class B, where all the design loads (dead load, live load and snow load) and load combinations are same as 4-storey and 8-storey SPSW systems. Total height of this SPSW is 57m from the ground and aspect ratio is 2.0. 15-storey SPSW designed based on indirect capacity design approach in ANSI/AISC-341-10 and material yield strength was 385 MPa. Details of 15-storey SPSW design are described in Bhowmick et al. (2011). Schematic figure and boundary element section are presented in Table 4-1 and in Figure 4.3.

Seismic performance evaluation in chapter-3, four-real and four-simulated ground motion records have been selected and scaled. Due to the time consuming manner of nonlinear time history analysis in ABAQUS, two real (Kobe-1995, Kern County-1952) and two simulated (6C1 and 6C2) ground motion records have been used in this chapter for CSM application. Prior to CSM application, seismic performance of 15-storey SPSW has also been estimated under these ground motion records (two real and two simulated ground motion records). Maximum structural responses like, floor displacement and Inter-storey drift of 15-storey SPSW are presented in Figure 4.4. Average dynamic parameters will be used for investigating the applicability of CSM.

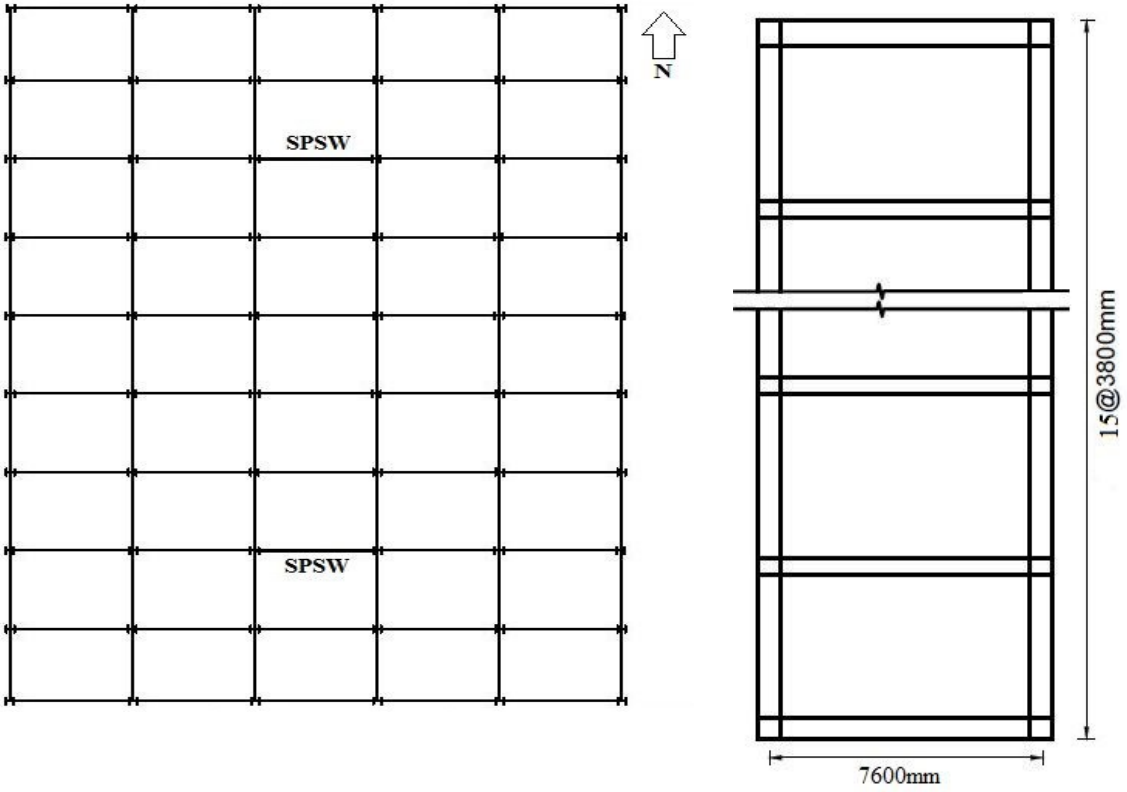


Figure 4.3 : Floor plan of 15-storey building with two identical SPSW (left) and elevation view of 15-storey SPSW system (right) of Bhowmick et al. (2010).

Table 4-1: Summary of 15-storey SPSW frame member properties and natural period of vibration

| Storey Level | Column Section | Beam Section | Plate thickness (mm) | Period | |
|---|---|---|---|---|---|
| 1-3 | W360X990 | W410X100 | 3 | Mode | Second |
| 4-6 | W360X900 | W410X100 | 3 | 1st | 3.01 |
| 7-9 | W360X744 | W410X100 | 3 | 2nd | 0.82 |
| 10-12 | W360X634 | W410X100 | 3 | 3rd | 0.42 |
| 13-14 | W360X592 | W410X100 | 3 | | |
| 15 | W360X592 | W760X582 | 3 | | |

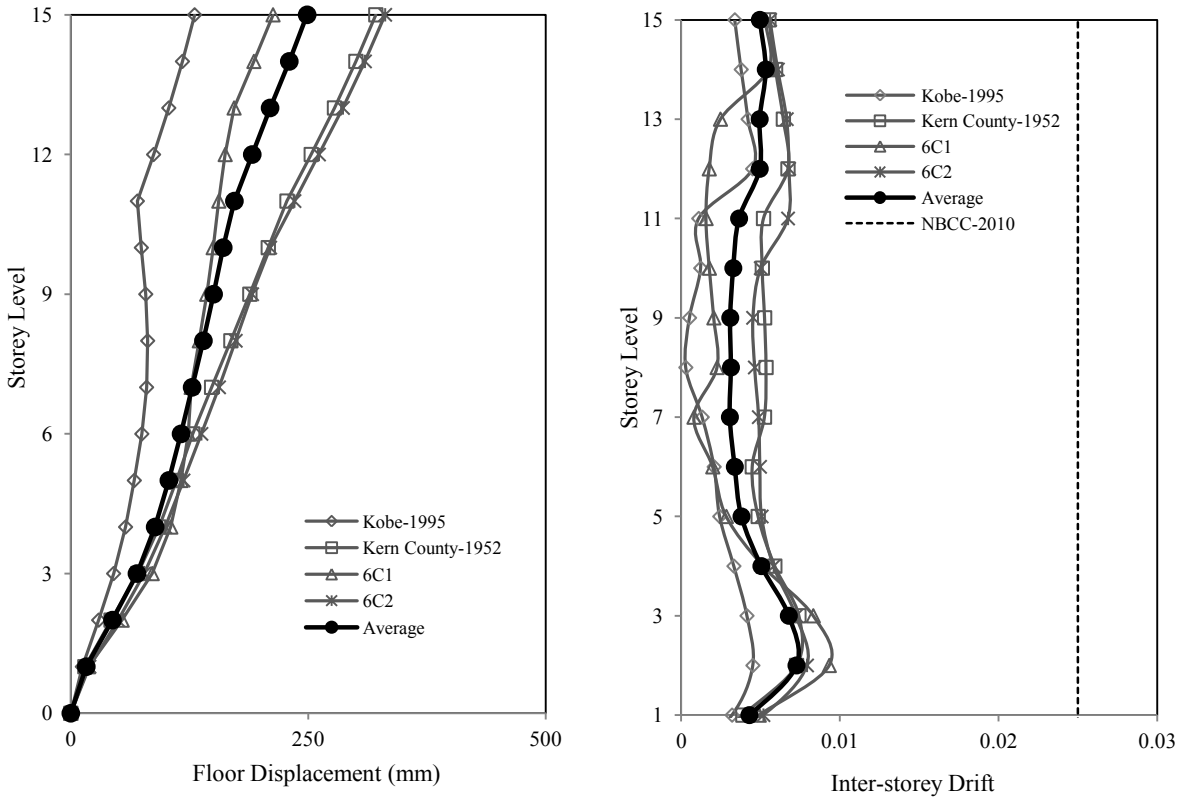


Figure 4.4 : Seismic response of 15-storey SPSW: maximum floor displacement (left) and inter-storey drift (right)

### 4.3.2 Capacity curve of SPSWs

Frequency analysis was performed for SPSWs to estimate fundamental frequency of the structure and associated elastic vibration mode shape of the structure. Base shear ($V_b$)-top displacement ($D_t$) relation were estimated from pushover analysis with a monotonically increased load pattern (equation-4.1). In this study, ABAQUS (Hibbitt et al. 2011) was used to perform nonlinear pushover analysis with calculated lateral load pattern. Pushover analysis was performed up to the failure mechanisms are appeared. Assumed failure mechanism of SPSW is a deformation pattern, when all the infill plates, all the beam-ends are yielded and column bases are started yielding. Nonlinear pushover curve are also presented in Figure 4.5. SPSW systems

(MDOF) were transferred in to ESDOF systems by introducing modal participation factor *(Γ)* by using equation 4.2 and 4.3. Mass of ESDOF systems are 1342 ton, 2052 ton and 3120ton for 4-storey, 8-storey and 15-storey building respectively. Modal participation factor of MDOF is 1.354 for 4-storey building, 1.566 for 8-storey building and 1.535 for 15-storey building. Top displacement *($D_t$)* and base shear *($V_b$)* relation of MDOF systems have been transferred into force *(F*)*-displacement *($D_t$*)* relationship of ESDOF system by using modal participation factor. After that, force *($F^*$)* to displacement *($D_t^*$)* relationship of ESDOF systems were idealized based on energy balance consideration where, the post-yielding stiffness of ESDOF system is zero and area under the original pushover curve and bilinear curve are same and two curves intersect at the 60% of the yield strength. Bilinear idealized force-displacement curve of ESDOF system were now converted in to Spectral acceleration versus spectral displacement curve, which is known as capacity curve of ESDOF system. Original force *($F^*$)*-displacement *($D_t^*$)* curve of ESDOF systems, bilinear idealized curves and spectral acceleration to spectral displacement curve for all SPSWs are presented in Figure 4.6. Properties of ESDOF system of all SPSW systems are presented below.

Table 4-2: Parameters of ESDOF systems

| Parameters | ESDOF system 1 (4-storey) | ESDOF system 2 (8-storey) | ESDOF system 3 (15-storey) |
|---|---|---|---|
| Effective mass, $m^*$ (ton) | 1342 | 2052 | 3120 |
| Modal participation factor, $\Gamma$ | 1.354 | 1.566 | 1.535 |
| Yield Strength, $F_y^*$ (KN) | 3650 | 3800 | 3018 |
| Yield displacement, $D_y^*$ (mm) | 40.5 | 128.9 | 248 |
| Elastic Period, $T^*$ (sec) | 0.767 | 1.66 | 3.18 |

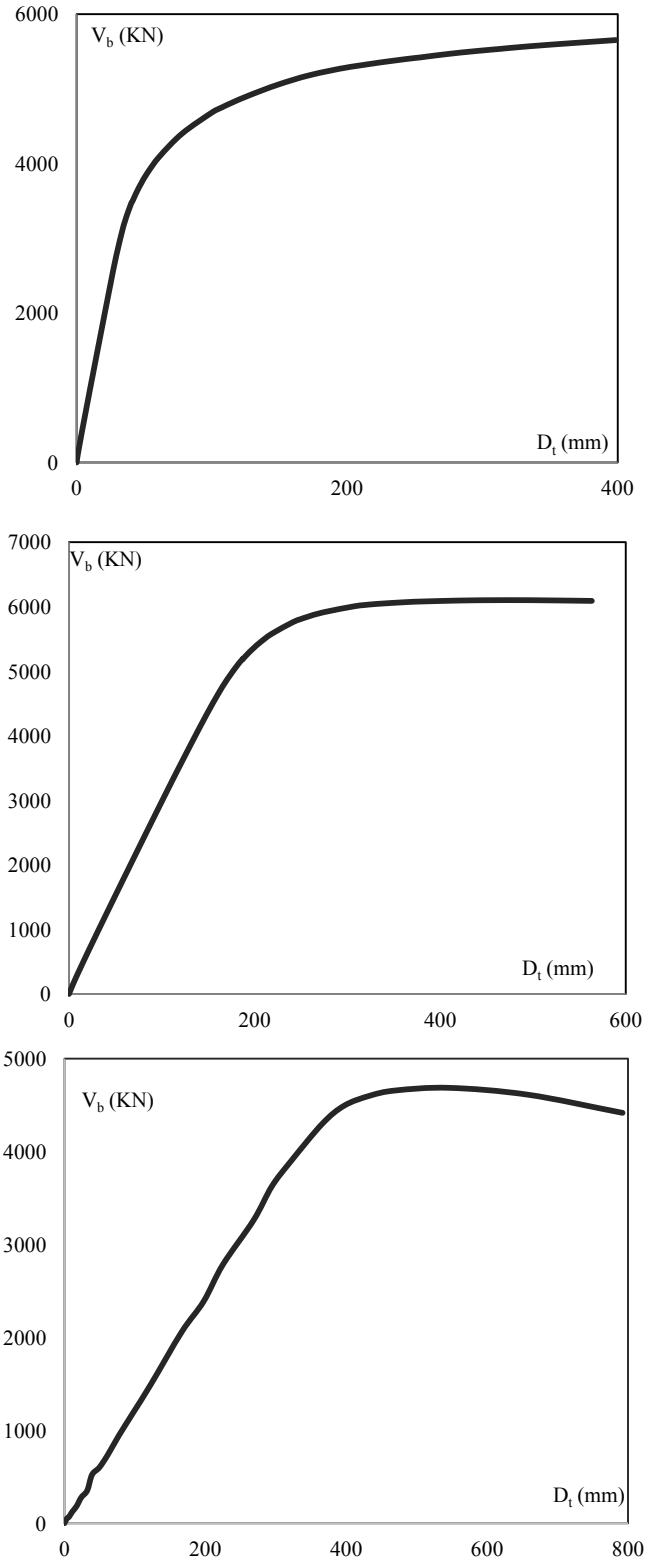


Figure 4.5: Base shear ($V_b$)-roof displacement ($D_t$) from nonlinear Pushover curve of 4-storey SPSW (top), 8-storey SPSW (middle) and 15-storey SPSW (bottom)

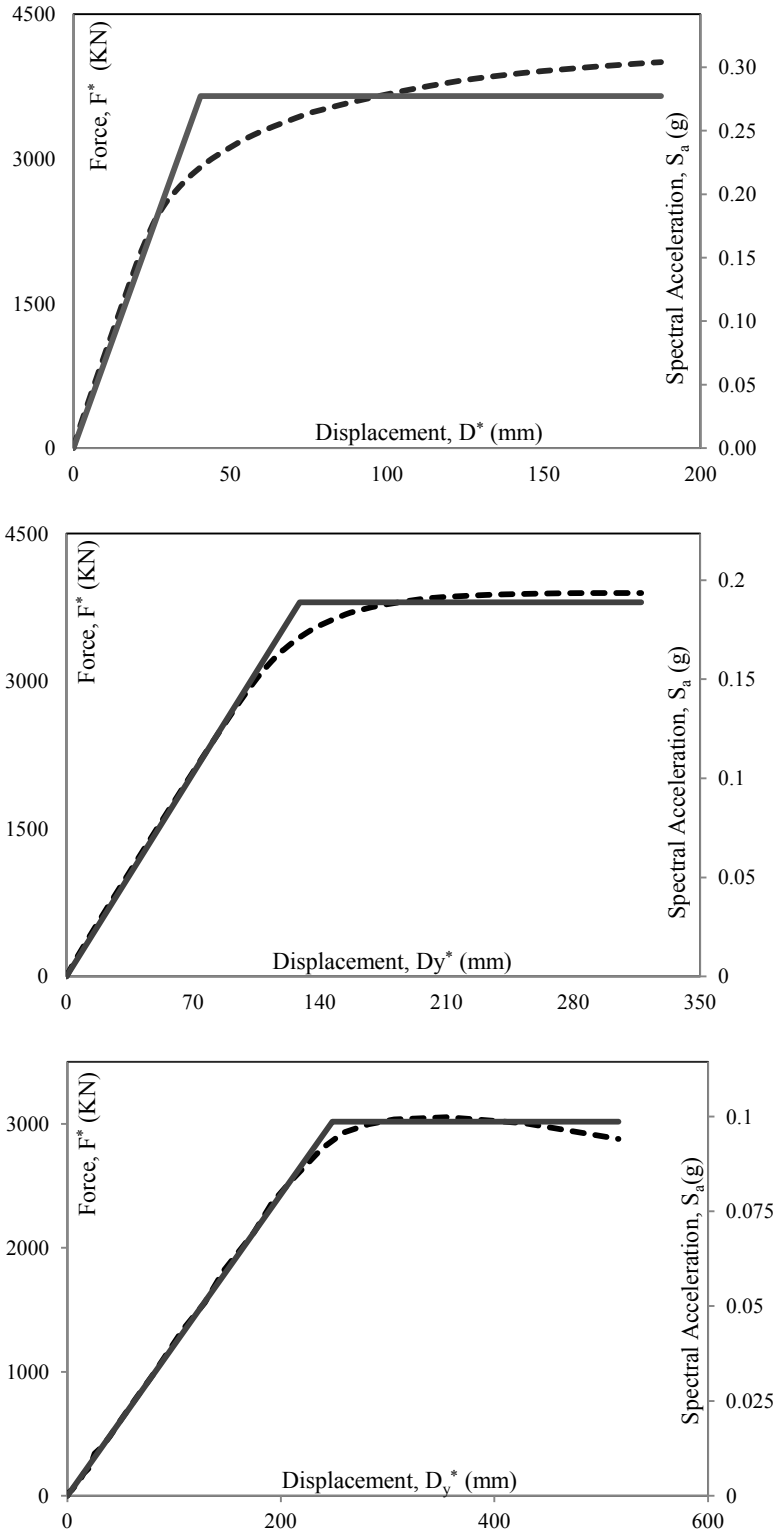


Figure 4.6: Force-displacement curve, bi-linear idealization and spectral acceleration versus spectral displacement curve of ESDOF system of 4-storey (top), 8-storey (middle) and 15-storey (bottom) SPSWs

### 4.3.3 Demand Spectrum for SPSWs

Vancouver design spectral acceleration parameters (5% damped structure and for reference soil class C) were used to obtain seismic demand curve (John and Halchuk 2003), which is presented in Figure 4.7. Displacement response spectrum is estimated from pseudo-acceleration to displacement relationship of SDOF system (equation-4.8).

For inelastic SDOF system, acceleration spectrum $S_a$ and displacement spectrum $S_d$ were determined from elastic ADRS by using linear expression of reduction factor by Vidic et al. (1994). The characteristics period ($T_s$) is 0.35sec. In the beginning of this procedure, demand curve has been constructed for elastic response of the structure (e.g., ductility is equal to one). In Figure 4.2, demand spectrums for constant ductility are presented for different ductility.

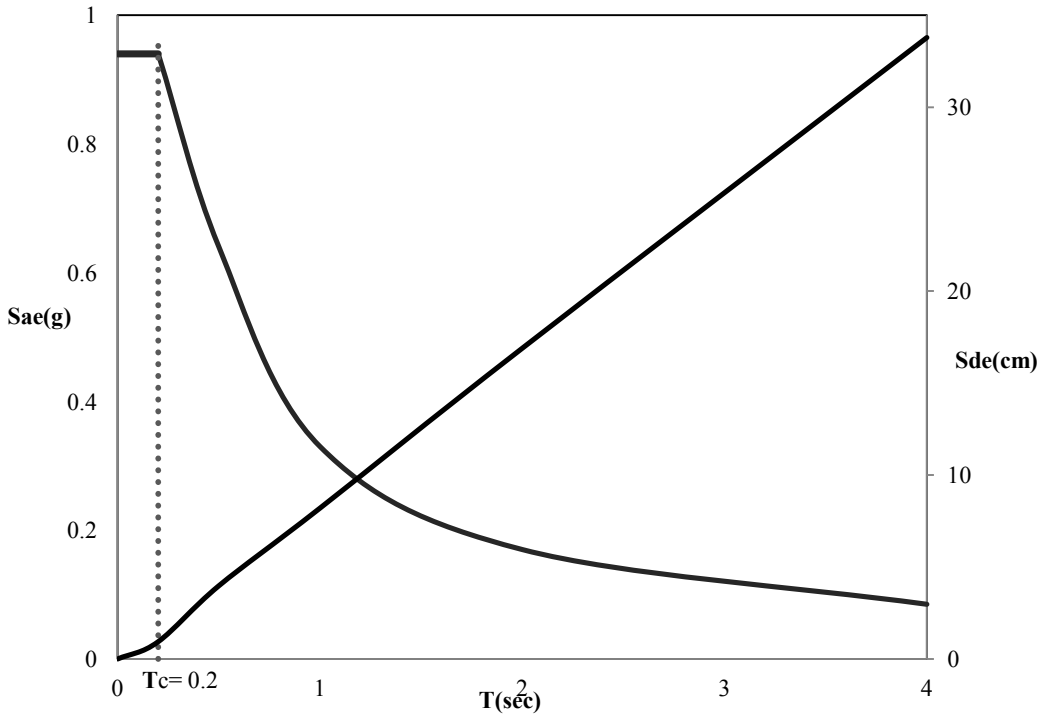


Figure 4.7**:** Elastic design acceleration response spectrum of Vancouver for 5% damped structure and corresponding displacement spectrum

### 4.3.4 Seismic Demand and Performance Evaluation of SPSW System

Demand spectra and capacity spectra for ESDOF system are now drawn in the same plot. Redial line of the capacity curve corresponding to the elastic period of the ESDOF system represents the elastic stiffness. Intersection of elastic demand spectrum and capacity spectra of ESDOF system gives the strength requirement $(S_{ae})$ for elastic response of the structure. This intersection point is generally referred as performance point. The yield acceleration $(S_{ay})$ for the ESDOF system refers the acceleration requirements for the inelastic behavior. Ratio of the elastic acceleration demand and inelastic acceleration capacity is the reduction factor $R_\mu$. After that, ductility demand can be calculated by the reverse calculation of equation 4.8 and 4.9. Displacement demand of ESDOF system is estimated from the same performance point. Figure 4.8, Figure 4.9 and Figure 4.10 are showing the graphical representation of the application of capacity-spectrum method for 4-storey, 8-storey and 15-storey SPSW respectively. For 4-storey and 8-storey SPSW systems, elastic demand spectrum is generated from Vancouver design response spectrum for soil class C (Figure 4.7). On the other hand, elastic demand spectrum for 15-storey SPSW was estimated from Vancouver design response spectrum for soil class B.

Capacity curves of 4-storey and 8-storey SPSW cannot intersect with elastic demand curve. Therefore, projected redial line of capacity curve intersects with demand curve. Thus, the elastic periods of both of the structures are larger than $T_s$, so "Equal Displacement Rule" applies here. Therefore, inelastic displacement demand is equal to the elastic displacement demand. Displacement demands are also determined from the intersection point of the capacity curve and the demand curve corresponding to the ductility demand. Next, this displacement demand of ESDOF system has been transferred in to displacement demand of MDOF by reverse

transformation from ESDOF to MDOF system. In this study, top displacement demand for 4-storey building is 85.33mm and for 8-storey building is 217.64mm, where both of them are very close to the nonlinear time history analysis of the structure. However, for 15-storey SPSW, the capacity curve intersected the demand curve of ductility one, meaning that the 15-storey SPSW remains elastic. The displacement demand of 15-storey SPSW was estimated from the intersection point, which was 305.53mm. Comparison between the maximum top displacements of the selected SPSWs by CSM and nonlinear time history analysis are given in Table-4-3.

According to current design standard of Canada, ductility based reduction factor for SPSW is 5 and over-strength related reduction factor is 1.6. In CSM, ductility demand of the structure for expected seismic demand was lower than the code suggested ductility; therefore, a seismic demand spectrum for ductility factor of 5.0 has been developed in Figure 4.8, Figure 4.9 and Figure 4.10 to show the design ductility. From these figures, it was evident that designed ductility and structural actual ductility demand is not same. According to nonlinear seismic analysis of SPSW (in Chapter-3), maximum dynamic base reaction was extremely higher than the design base shear. To maintain practical availability and handling requirements, minimum plate thickness in the SPSW design was higher than the theoretical requirement, which increases a significant amount of overall capacity. Moreover, framing action in beams and columns has good contribution to the storey shear resistance. Therefore, overall capacity of the structure was very high, which is one of the major reason for this lower ductility demand. On the other hand, elastic period may not be constants after yielding of the structure. In addition, all the analysis approximations also have some influence on this lower ductility demand. Performance parameters of SPSWs using CSM are presented in Table-4-3.

Table-4-3: Performance evaluation of the buildings using CSM and nonlinear time history analysis

| Parameters | 4-Storey building | 8-Storey building | 15-Storey building |
|---|---|---|---|
| Ductility (Pushover) | 4.6 | 2.6 | 2.3 |
| Ductility (CSM) | 1.55 | 1.11 | N/A |
| Maximum top displacement (mm)-CSM | 85.33 | 217.64 | 305.53 |
| Maximum Average top displacement(mm) - time history analysis | 90.81 | 182.224 | 249 |
| Maximum top displacement at plastic mechanism (pushover analysis) | 202.86 | 497.11 | 989 |
| Error in displacement demand | 6.03% | 19.4% | 22.7% |

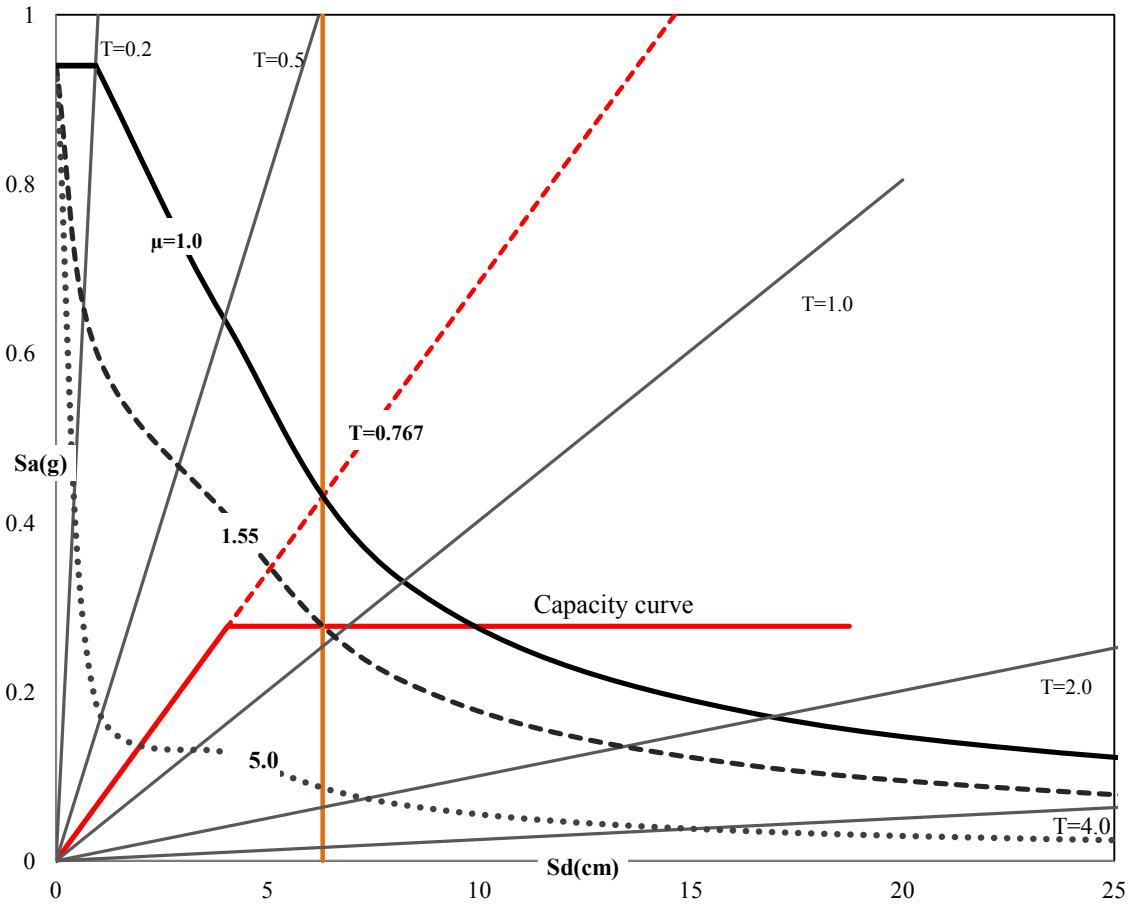


Figure 4.8: Graphical representation of the application of CSM on 4-storey SPSW

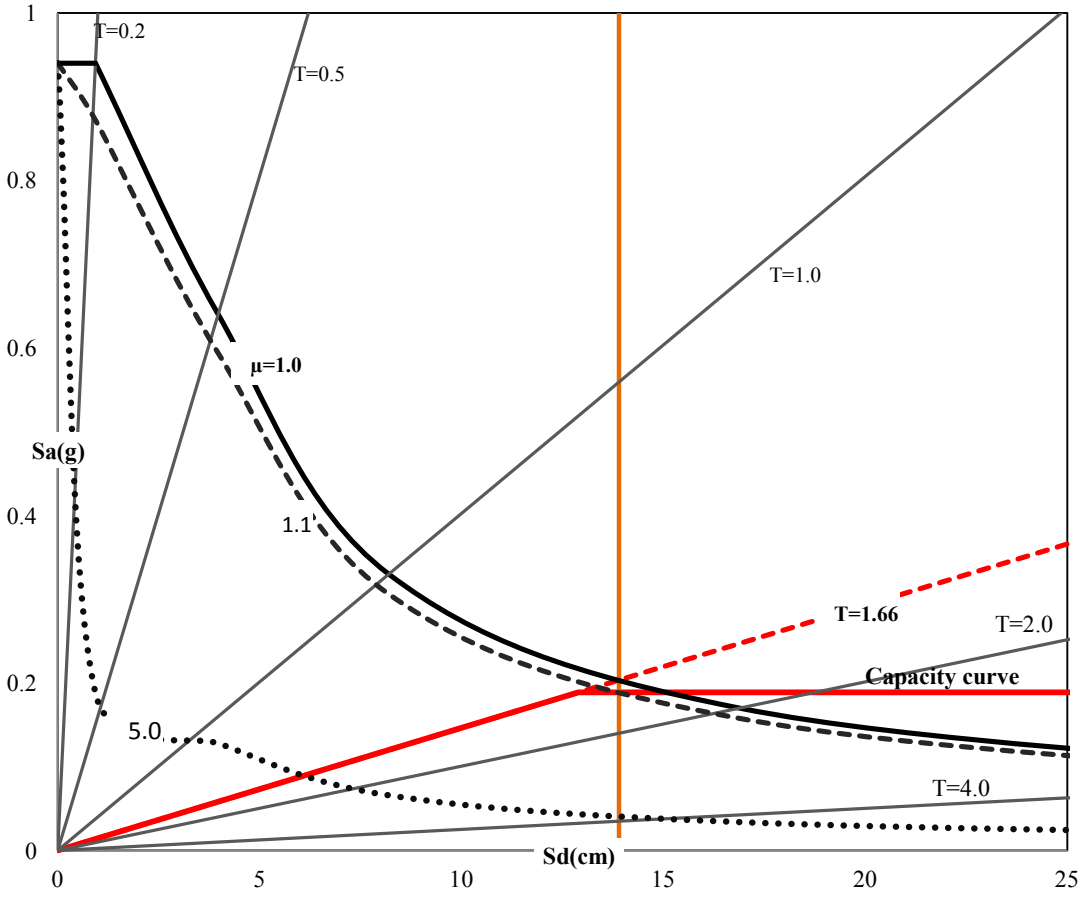


Figure 4.9: Graphical representation of the application of CSM on 8-storey SPSW

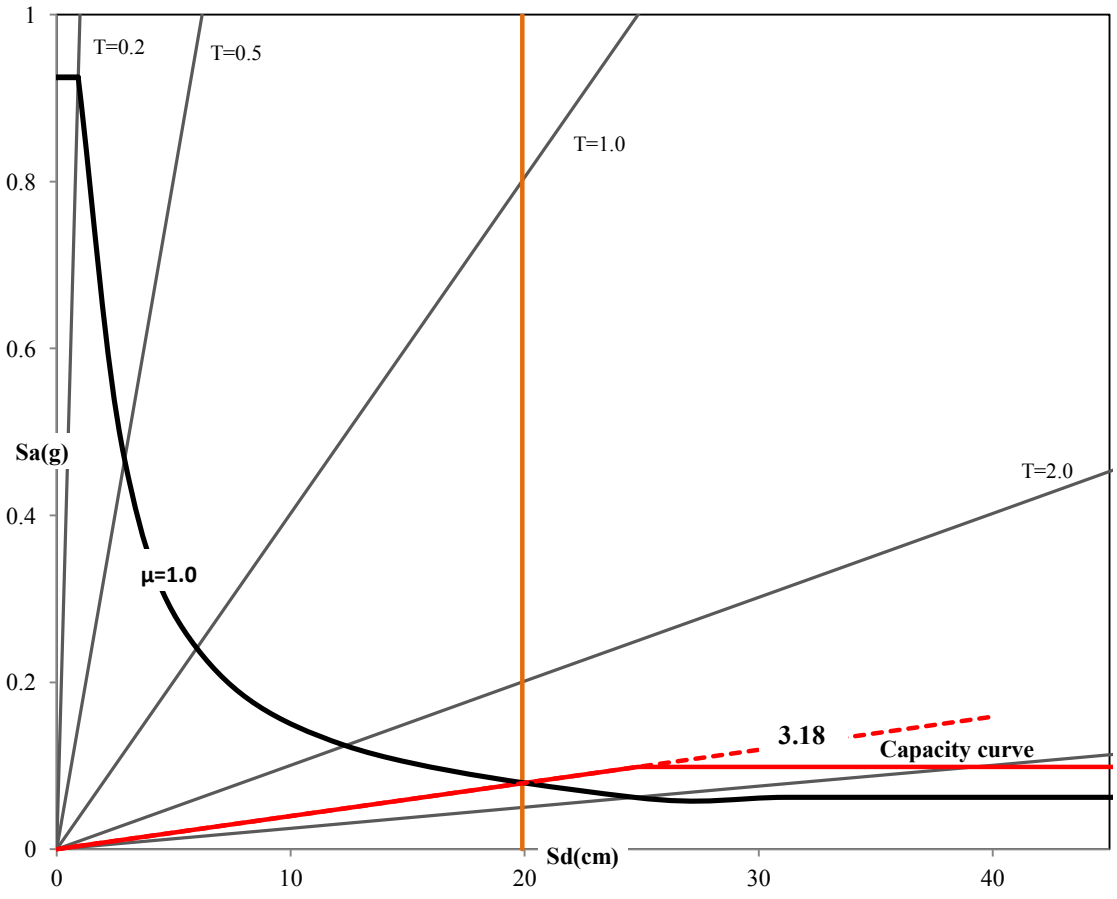


Figure 4.10: Graphical representation of CSM application on 15-storey SPSW

## 4.4 Summary

Seismic performance evaluation is one of the important step in performance based design procedure. CSM can be used as a performance evaluation tool for any structure. A simple transformation from MDOF to ESDOF system was used. Nonlinear pushover curves have been converted into capacity spectrum of ESDOF system. Vancouver design response spectrum was transferred into inelastic demand spectrum for different ductility factors. Displacement demand and ductility demand were calculated from the intersection point of the capacity curve and demand curve.

Displacement demand in CSM for 4-storey and 8-storey SPSW were close to the nonlinear time history analysis results. On the other hand, ductility demand was lower than the design consideration and nonlinear pushover analysis. Displacement demands in CSM show very close to the beam yielding point in pushover curve while it has around 6.03% and 19.4% errors in nonlinear time history analysis of 4-storey SPSW system and 8-storey system respectively. It shows 22.7% discrepancy for 15-storey SPSW system. Nonlinear pushover analysis of all SPSWs showed very high capacity of the structures in terms of displacement, stiffness and ductility. Estimated displacement demand and ductility demand of all SPSWs by CSM are lower than the capacity of these structures, which represents the satisfactory performance of these systems. Lower ductility demand in CSM is mainly due to the over strength of the structures. The structural over strength was the primary reason for this small ductility demand of the structure.

Finally, capacity-spectrum method can be used for performance evaluation and rapid design assessment for SPSW system to get a global idea of the building performance instead of nonlinear time history analysis. Capacity-spectrum method needs an assumed displacement shape and a lateral load pattern for nonlinear pushover analysis. In this method, first elastic vibration mode shape was used as an assumed mode shape. Therefore, this method cannot include higher mode contribution in the overall building performance. Therefore, this method is suitable for such structure, which is mainly dominated by its fundamental mode of vibration. By applying capacity-spectrum method, inelastic displacement demand of 4-storey SPSW predicts better than 8-storey and 15-storey SPSW. For different hazard level, CSM can be performed with different response spectrum for corresponding hazard level. So the expected performance level for different level of ground motion can be analyzed by CSM as well.

Chapter- Five

# Seismic Performance Evaluation of Steel Plate Shear Walls Using Modal Pushover Analysis

## 5.1 Introduction

A Modal Pushover Analysis (MPA) is an improved pushover analysis, which includes higher-mode contributions to seismic demands. MPA is a tool for performance-based seismic design and performance evaluation of new and existing structures. The main focus of this chapter is to estimate seismic demand considering inelastic behavior of SPSWs by applying MPA developed by Chopra and Goel (2001). Theoretical background of the MPA procedure is discussed in the beginning of this chapter. After that, applicability of MPA in the seismic demand estimation and performance evaluation of steel plate shear wall will be investigated for low-rise (4-storey), medium-rise (8-storey) and high-rise (15-storey) buildings with SPSW, which are designed according to capacity design approach. Estimated responses from the modal pushover analysis are compared with nonlinear dynamic analysis.

## 5.2 Modal Pushover Analysis

The equation of motion of an elastic multi-storey building to earthquake ground motion $\ddot{u}_g(t)$ is as follows:

$$m\ddot{u} + c\dot{u} + ku = m\iota\ddot{u}_g(t) = P_{eff}(t) \qquad 5.1$$

where, $u$ is the floor displacement vector of $N$ lateral floor displacement relative to the ground; $m$, $c$ and $k$ are the mass, classical damping and lateral stiffness matrix of the system respectively;

$\iota$ is the influence vector which represents the displacement of the mass (each elements of the influence vector is equal to the unity); $p_{eff}(t)$ is the effective earthquake forces. The spatial distribution of these effective forces over the height is vector $s = m\iota$. The force distribution can be expanded as a summation of modal inertia force distribution $S_n$.

$$m\iota = \sum_{n=1}^{N} S_n = \sum_{n=1}^{N} \Gamma_n m\phi_n \qquad 5.2$$

$\varphi_n$ is the n$^{th}$ natural vibration mode of the structure, $S_n$ is the contribution of the $n^{th}$ mode and $\Gamma_n$ is the modal perception factor.

$$\Gamma_n = \frac{L_n}{M_n}; \quad L_n = \phi_n^T m\iota; \quad M_n = \phi_n^T m\phi_n; \quad S_n = \Gamma_n m\phi_n; \quad P_{effn}(t) = -s_n \ddot{u}_g(t) \qquad 5.3$$

Where, $L_n$ and $M_n$ are the mass of the n$^{th}$-mode SDOF system and effective modal mass respectively. The response of the MDOF system to $P_{effn}(t)$ is entirely in the $n^{th}$ mode. Then the floor displacement of $n^{th}$ mode and total displacement are as follows,

$$u_n(t) = \phi_n q_n(t); \quad u(t) = \sum_{n=1}^{N} \phi_n q_n(t) \qquad 5.4$$

The modal co-ordinate $q_n(t)$ is governed by,

$$\ddot{q}_n + 2\zeta_n \omega_n \dot{q}_n + \omega_n^2 q_n = -\Gamma_n \ddot{u}_g(t) \qquad 5.5$$

Where, $\omega_n$ is the natural vibration frequency and $\xi_n$ is the damping of $n^{th}$ mode.

$$q_n(t) = \Gamma_n D_n(t) \qquad 5.6$$

Where, $D_n(t)$ is governed by the equation of motion of $n^{th}$ mode linear SDOF system and total response of the system to the lateral excitation $P_{eff}(t)$ is,

$$\ddot{D}_n + 2\xi_n \omega_n \dot{D}_n + \omega_n^2 D_n = -\ddot{u}_g(t) \qquad 5.7$$

$$u(t) = \Gamma_n \phi_n D_n(t) \tag{5.8}$$

For an inelastic multi-storey building, floor displacements u are not a single value it depends on the history of displacement, so the equation 5.1 will change in to,

$$m\ddot{u} + c\dot{u} + fs(u, sign\dot{u}) = m\ddot{u}_g(t) = P_{eff}(t) \tag{5.9}$$

Due to modal orthogonality, equation 5.5 and equation 5.7 can be written as follows;

$$\ddot{q}_n + 2\zeta_n \omega_n \dot{q}_n + \frac{F_{sn}}{M_n} = -\Gamma_n \ddot{u}_g(t) \tag{5.10}$$

$$\ddot{D}_n + 2\xi_n \omega_n \dot{D}_n + \frac{F_{sn}}{L_n} = -\ddot{u}_g(t) \tag{5.11}$$

Only the term that differs from previous equation,

$$F_{sn} = F_{sn}(q, sign\dot{q}) = \phi_n^T f_s(u, sign\dot{u}) \tag{5.12}$$

To develop a pushover analysis consistent with the response spectrum analysis value can be obtained by a static analysis of the structure subject to lateral force distribution $S_n^*$, over the building height. The structure can push up to displacement $u_{rno}$, which can be calculated from Equation 5.8, where $D_n$ is the peak value of the $D_n(t)$ which is determined by equation 5.11, as described earlier.

$$S_n^* = m\phi_n \tag{5.13}$$

From this roof displacement $u_{rno}$, all other response parameter can be calculated. All the peak modal responses are combined by any of the modal combination rule.

### 5.2.1 Modal Pushover Analysis Procedure

Step by step procedure of MPA is briefly discussed in this section. Following steps are taken from Chopra and Goel (2001).

**Step-01:** Estimate the Natural frequencies of the structures $\omega_n$, and associated normalized mode shape vectors $\phi_n$, for linearly elastic vibration modes of the structures.

**Step-02:** Compute the base shear-roof displacement ($V_{bn}$-$u_{rn}$) pushover curve for force distribution $s_n^*$ (equation 5.13) for n$^{th}$-"mode" of the structure. This force distribution is assumed to be constant during the pushover analysis. Physical basis of this force distribution is the inertial force of the structure that opposes the deformation due to the external force.

**Step-03:** Convert the regular pushover curves of each "mode" in to bilinear idealized curves according to following assumptions of FEMA 273 (FEMA 1997): (1) initial stiffness of bilinear curve is equal to original pushover curve (2) Area under the original curve and bilinear curve up to target displacement are equal (3) Two curves intersect at the force equal to 60% of the yield strength (4) post yielding stiffness is zero for the stiffness degrading pushover curve. After idealization of pushover curve, initial and post-yielding stiffness of the systems can be calculated by following equations.

$$K_{in} = \left(0.6V_{bny}\right)/u_{rn}, 0.6 \tag{5.14}$$

$$\alpha_n = \frac{\left[\left(V_{bno}/V_{bny}\right)-1\right]}{\left[\left(u_{rno}/u_{rny}\right)-1\right]} \tag{5.15}$$

Where, $V_{bny}$ and $V_{bno}$ are yield base shear and ultimate base shear; $u_{rny}$ and $u_{rno}$ are yield displacement and target displacement respectively of MDOF systems. $K_{in}$ is the initial stiffness for n$^{th}$-"mode", $\alpha_n$ is the post-yielding strain hardening. Schematic diagram of idealized pushover

curve are shown in Figure 5.1.

**Step-04:** $V_{bn}$-$u_{rn}$ pushover curve are then converted in to force-displacement relation ($F_{sn}/L_n$-$D_n$) of n$^{th}$-mode inelastic SDOF system using following two relations of force and displacement.

$$F_{sn} = \frac{V_{bn}}{\Gamma_n} \qquad D_n = \frac{u_{rn}}{\Gamma_n \phi_{rn}} \tag{5.16}$$

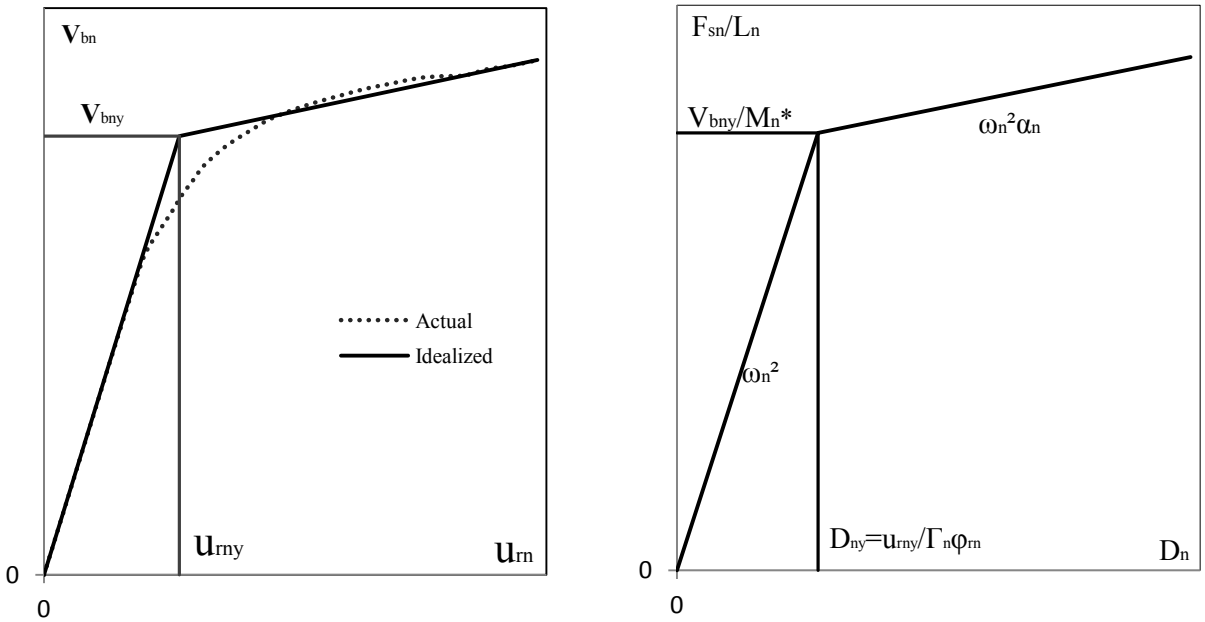


Figure 5.1: Schematic figure of actual pushover curve and idealized pushover curve (left) and $F_{sn}/L_n$-$D_n$ relation (right) (Chopra and Goel (2001))

**Step-5:** Compute the peak deformation of the n$^{th}$-mode inelastic SDOF system $D_n$ by solving equation 5.11 or from inelastic response spectrum.

**Step-6:** Calculate the peak deformation of MDOF system $u_{rno}$ by equation 5.8. Then, other properties such as floor displacement and inter-storey drift can also be calculated from $u_{rno}$.

**Step-7:** Calculate total responses of the structure by combining response of all the effective modes. Any modal combination rules may apply for this purpose.

## 5.3 Application of MPA

### 5.3.1 SPSW Systems for MPA Application

One 4-storey and one 8-storey SPSW systems have been designed according to current capacity design approach of CSA/CAN S16-09 and a finite element model in ABAQUS (Hibbitt et al. 2011) have been developed in chapter-3. Seismic performance of SPSWs has been evaluated for a set of earthquake records (chapter-3). Though these low-rise and medium-rise SPSW systems are very unlikely to have higher mode effect, a high-rise SPSW system needs to be used for MPA application. A 15-storey SPSW that has been introduced in chapter-4 is going to be used for MPA application. Same ground motion records (two real and two simulated) have been adopted in this chapter.

### 5.3.2 Seismic Demand and Performance Evaluation of SPSW

Frequency analysis was performed in the FEM for all of the SPSWs to calculate linearly elastic vibration periods and corresponding modes. In Figure 5.2, first three elastic normalized mode shapes of the SPSWs are presented. Lateral force distribution (according to equation 5.13) for SPSWs is presented in Figure 5.3 . Lateral force distribution for SPSWs calculated for inertia forces, which are applied incrementally up to the target roof displacement. Finite element software ABAQUS (Hibbitt et al. 2011) was used to perform nonlinear pushover analysis for each mode. Gravity loads were applied prior to pushover analysis. Figure 5.4, Figure 5.5 and Figure 5.6 are presenting the base shear-roof displacement curve for first three-vibration "mode" of 4-storey, 8-storey and 15-storey respectively.

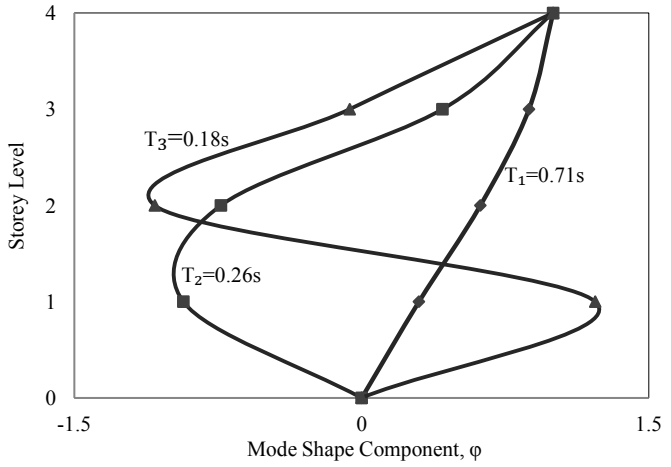


(a)

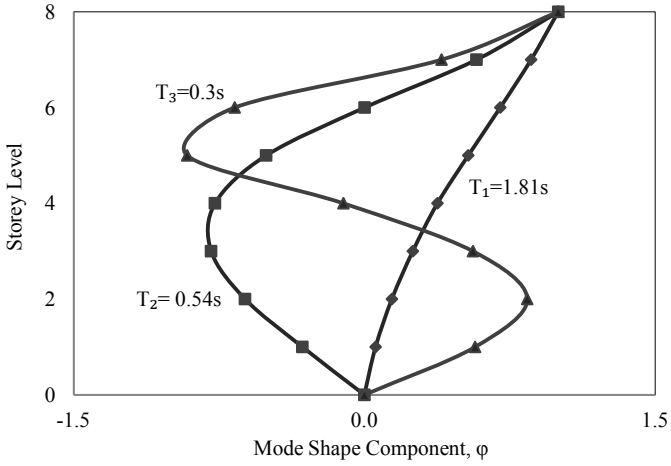


(b)

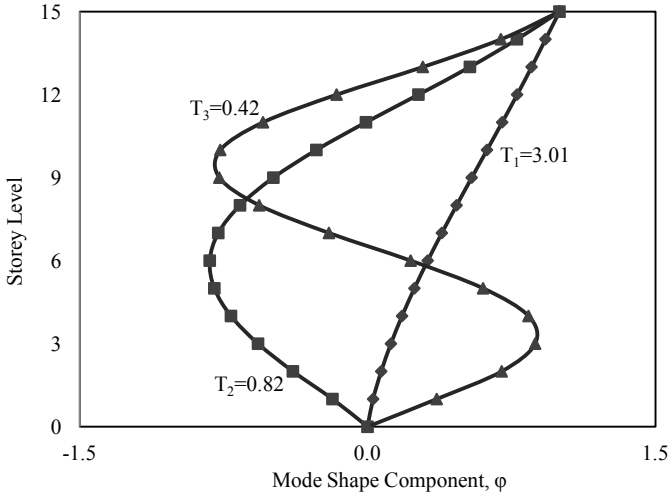


(c)

Figure 5.2: First three elastic mode of vibration and period of (a) 4-storey SPSW, (b) 8-storey SPSW and (c) 15-storey SPSW

1st "mode" pushover curve of 4-storey SPSW was "normal", where the overall roof displacement after yielding was same as its original yield mechanism. In the second and third "mode" pushover, some forces push the structure where some other pulls. 2nd "mode" force distribution creates local plastic mechanism in 2nd storey column. Even though, overall force distribution to the left was higher than right, the resultant roof displacement was to the right and base shear force was higher than 1st "mode". In the 3rd "mode" pushover curve, deformation of the roof followed its mechanism according to its mode shape. Therefore, for 4-storey SPSW all the "modal" pushover curves were "normal".

Roof deformation after yielding of 2nd "mode" pushover curve of 8-storey SPSW, was opposite to its original mechanism due to the local 4th-storey column plastic hinge formation. This type of pushover curve pattern is often called "reversal" in pushover. "Reversal" in the pushover curve arises when a local mechanism forms and roof moves opposite to its original mechanism due to the resultant storey forces.

“Reversal” in pushover was also observed in 2nd “mode” and 3rd “mode” pushover curve of 15-storey SPSW. Direct push-pull action in 2nd “mode” pushover analysis was found in 15-storey SPSW, which produced local column plastic hinge in 5th-storey. Similarly, in 3rd “mode” pushover local plastic hinge formation was found in 7th-storey column. Resultant force above these local plastic hinges pushed the structure opposite to its original mechanism. This type of "Reversal" can be avoided either by using elastic analysis of those modes or by using another reference storey above than plastic hinge

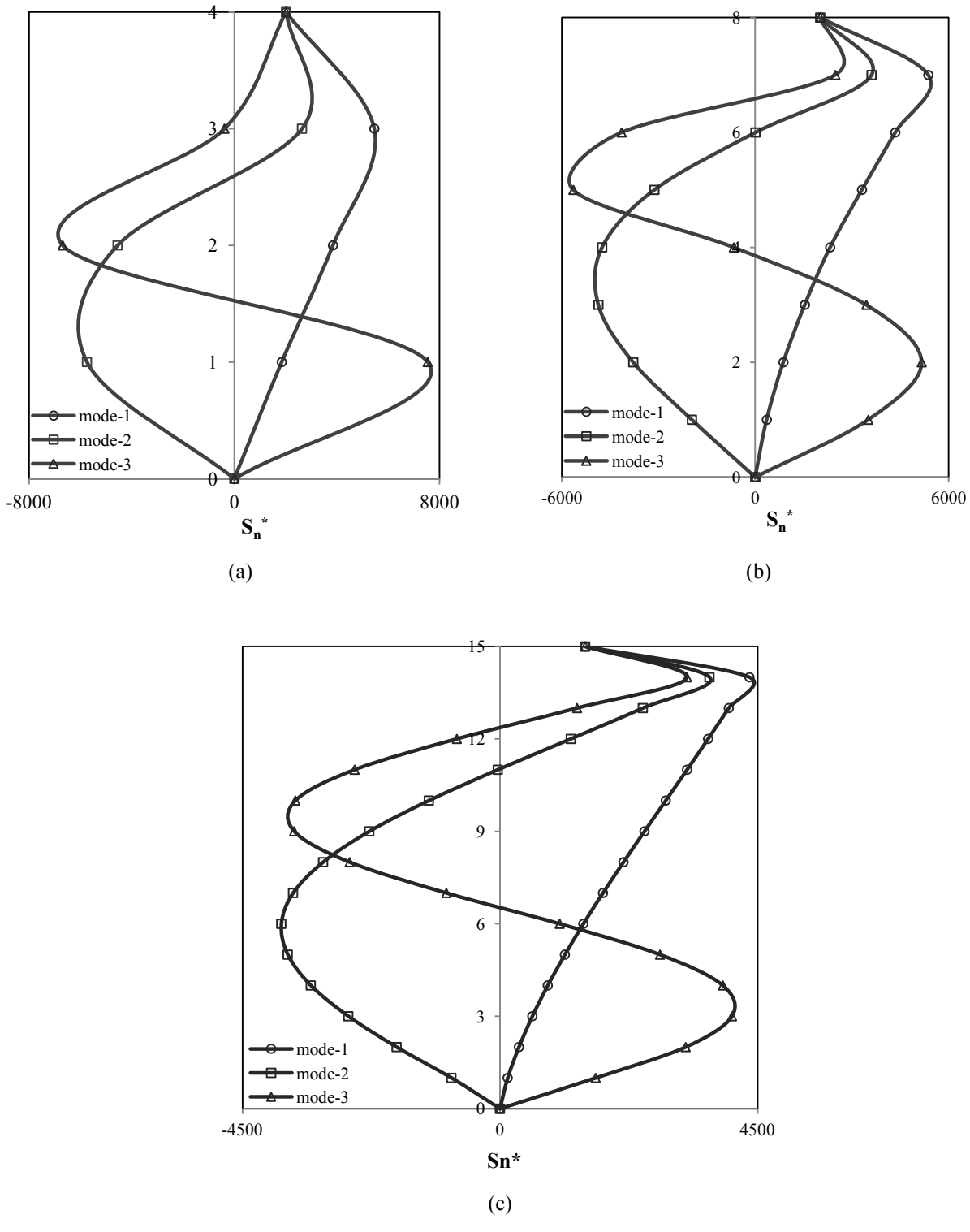


Figure 5.3: Force Distribution according to equation 5.13, first three modes for 4-storey (a), 8-storey (b) and 15-storey(c)

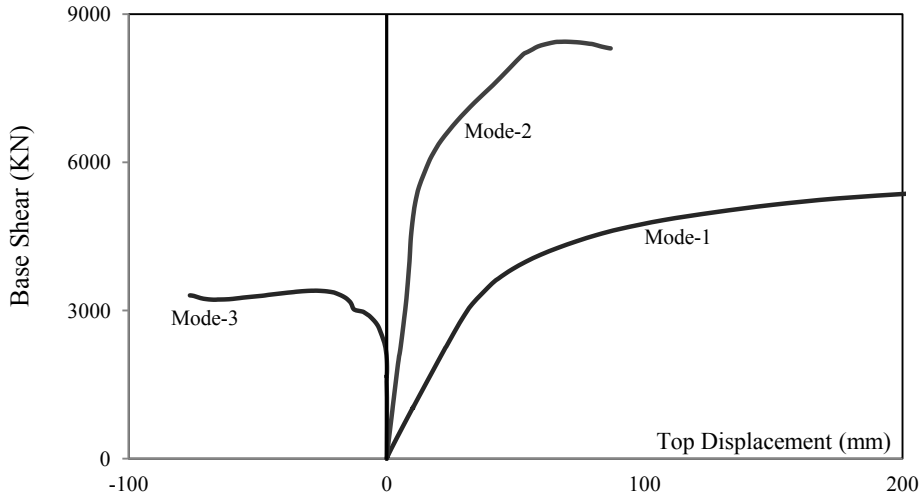


Figure 5.4: "modal" pushover curves for 4-storey SPSW system

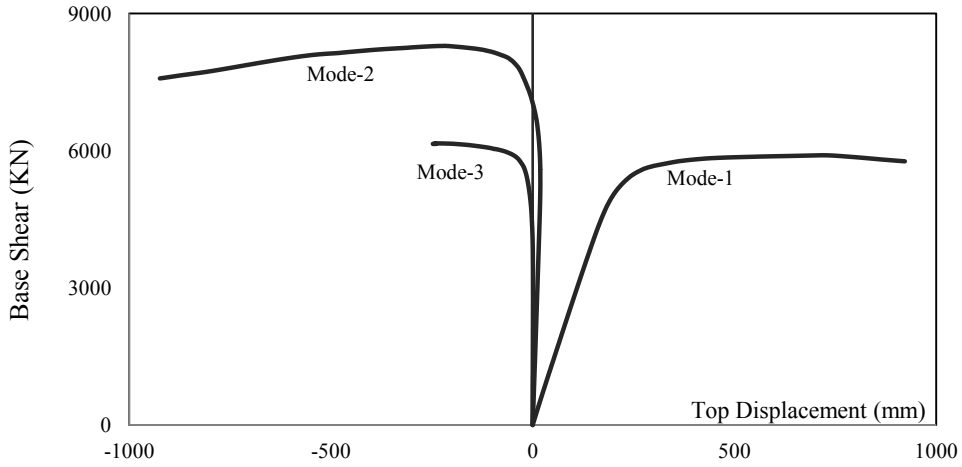


Figure 5.5 : "modal" pushover curves for 8-storey SPSW system

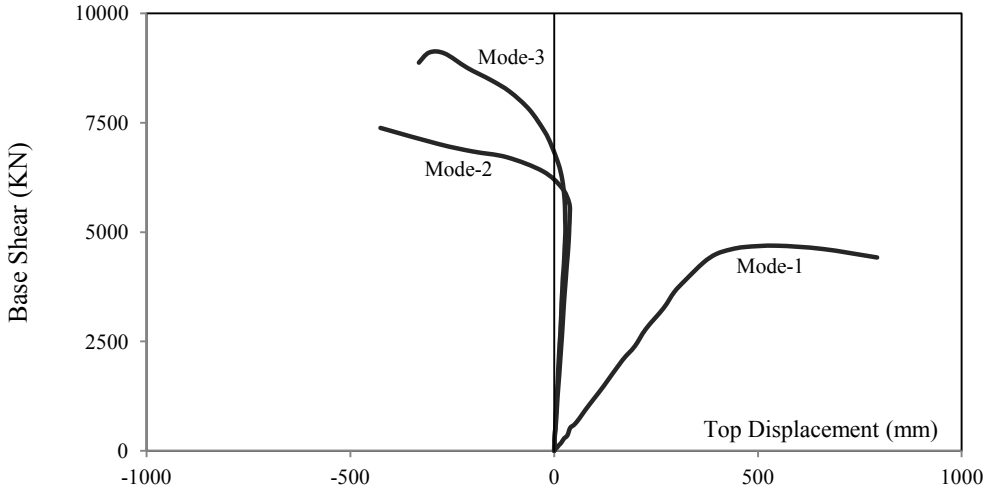


Figure 5.6: "modal" pushover curves for 15-storey SPSW system

formation for pushover curve (Goel and Chopra 2005). Elastic analysis of any higher "mode" pushover may significantly decrease computational complexity. However, nonlinear analysis may offer better prediction, if higher "mode" contribution passes the elastic range of vibration.

All of the "regular" pushover curves of each SPSW have been idealized in to bilinear curves. $V_{bn}$-$u_{rn}$ pushover curve of MDOF are then converted in to force- displacement relation ($F_{sn}/L_n$-$D_n$) of $n^{th}$-mode inelastic SDOF, which are presented in Figure 5.1. Initial slope of the curve represents the initial stiffness and second slop represents the post yielding stiffness, which is post yielding strain hardening times initial stiffness. Actual pushover curve and idealized pushover curve for MDOF and SDOF are presented in the same plot in Figure 5.7 and in Figure 5.8. Properties of "modal" inelastic SDOF systems are presented in Table 5-1.

In this study, all the SDOF system of SPSW are analysed to solve equation-5.12 for four selected ground motion records. The "modal" pushover analysis of SPSWs have both "normal" and "reversed" pushover curve. Therefore, nonlinear analysis was carried out for inelastic SDOF systems, which were associated with "normal" pushover curves. SDOF systems that have "reversal" in pushover analysis were analyzed by linear analysis. It was assumed that, structure performs elastically in the higher mode vibration (Chopra et al. 2004; Goel and Chopra 2005). Calculated peak deformations of SDOF systems $D_n$, are utilized to calculate the Peak deformation of MDOF (equation-5.8). Then, other properties such as floor displacement and inter-storey drift are also calculated

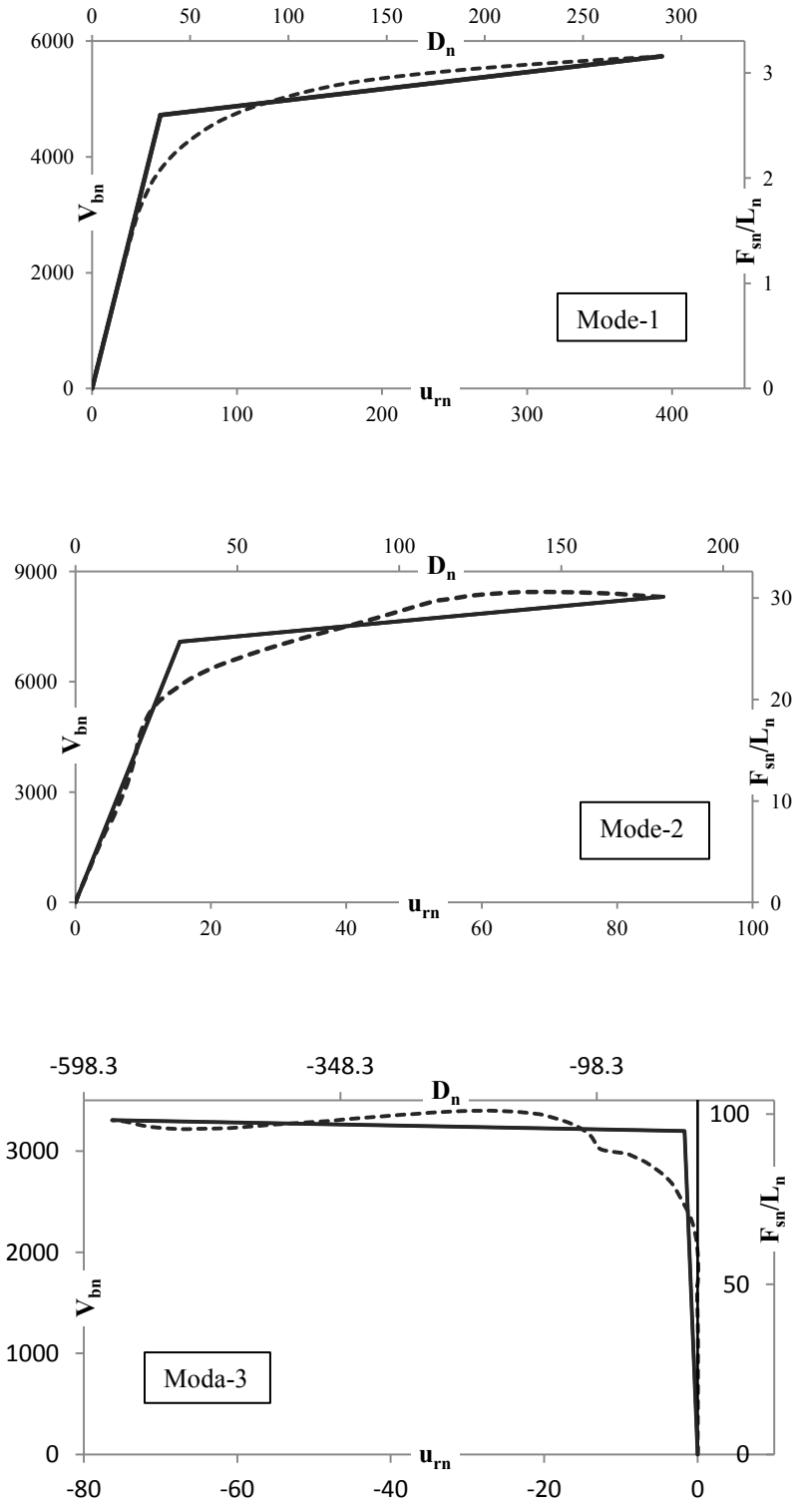


Figure 5.7: Actual, idealized pushover curve of MDOF ($V_{bn}$-$u_{rn}$) and SDOF systems ($F_{sn}/L_n$-$D_n$) for 4-storey SPSW system

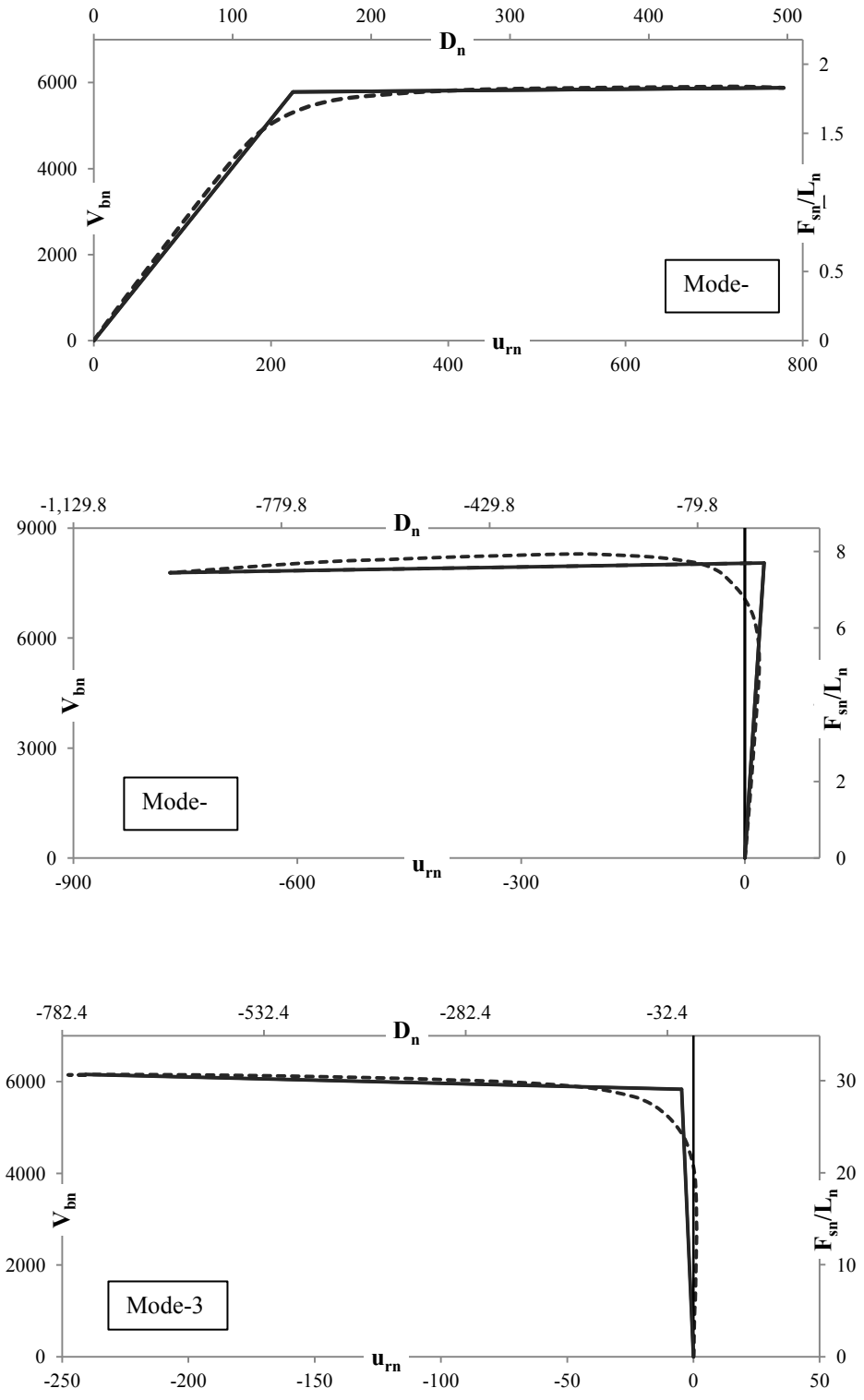


Figure 5.8: Actual, idealized pushover curve of MDOF ($V_{bn}$-$u_{rn}$) and SDOF systems ($F_{sn}/L_n$-$D_n$) for 8-storey SPSW system

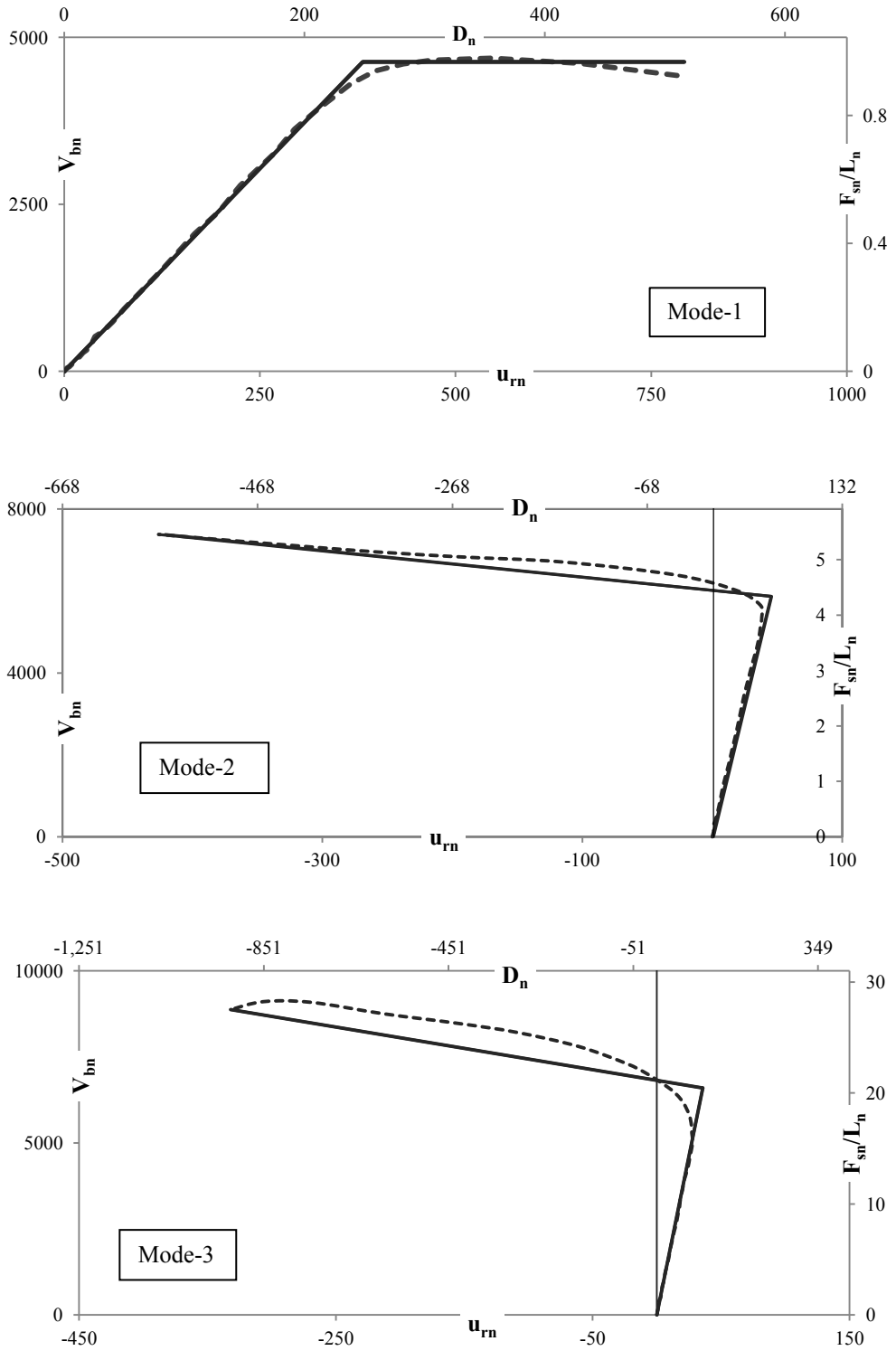


Figure 5.9: Actual, idealized pushover curve of MDOF ($V_{bn}$-$u_{rn}$) and SDOF systems ($F_{sn}/L_n$-$D_n$) for 15-storey SPSW system

Table 5-1: Properties of inelastic "$n^{th}$-mode" SDOF systems

| Mode | properties | Mode-1 | Mode-2 | Mode-3 |
|---|---|---|---|---|
| Storey-4 | $L_n$ (ton) | 1341.462 | -576.668 | 251.622 |
| | $M_n^*$ (ton) | 1816.658 | 275.8247 | 33.646 |
| | $\Gamma_n$ | 1.354 | -0.47831 | 0.134 |
| | $F_{sn}/L_n$ (m/sec$^2$) | 2.60 | 25.71561 | 95.08 |
| | $D_{ny}$ (mm) | 34.87 | 32.21985 | -12.63 |
| | $F_{sno}/L_n$ (m/sec$^2$) | 3.16 | 30.12602 | 98.25 |
| | $\alpha$ | 0.0294 | 0.03699 | 0.000756 |
| | $T_n$ (sec) | 0.72773 | 0.222405 | 0.072428 |
| | $\xi_n$ (%) | 5 | 5 | 12.13 |
| Storey-8 | $L_n$ (ton) | 2051.99 | -1312.63 | 628.02 |
| | $M_n^*$ (ton) | 3212.84 | 1045.68 | 200.68 |
| | $\Gamma_n$ | 1.57 | -0.80 | 0.32 |
| | $F_{sn}/L_n$ (m/sec$^2$) | 1.800184 | 7.699176 | 29.07565 |
| | $D_{ny}$ (mm) | 143.482 | 32.35649 | -14.6521 |
| | $F_{sno}/L_n$ (m/sec$^2$) | 1.829059 | 7.442587 | 30.68171 |
| | $\alpha$ | 0.00651 | 0.001079 | 0.001095 |
| | $T_n$ (sec) | 1.77 | 0.41 | 0.14 |
| | $\xi_n$ (%) | 5 | 5 | 11.98 |
| Storey-15 | $L_n$ (ton) | 3119.54 | -1786.571 | 896.550 |
| | $M_n^*$ (ton) | 4789.57 | 1353.048 | 322.548 |
| | $\Gamma_n$ | 1.53534 | -0.7573 | 0.3598 |
| | $F_{sn}/L_n$ (m/sec$^2$) | 0.96773 | 4.3383 | 20.46 |
| | $D_{ny}$ (mm) | 248.174 | 59.7265 | 99.66 |
| | $F_{sno}/L_n$ (m/sec$^2$) | 0.96773 | 5.454 | 27.51 |
| | $\alpha$ | 0 | 0.031 | 0.03356 |
| | $T_n$ (sec) | 3.18 | 0.73723 | 0.43851 |
| | $\xi_n$ (%) | 5 | 5 | 8.22 |

from the $u_{rno}$ and the corresponding values of base shear of MDOF system were estimated from the actual pushover curves. Total responses for all of the structures are calculated by combining all the responses of effective modes. Here, modal combination rule SRSS has been used to this modal combination.

## 5.4 Result and Discussion

Modal Pushover Analysis (MPA) was performed on low-rise (4-storey), medium-rise (8-storey) and high-rise (15-storey) SPSW systems. Two real and two simulated ground motion records have been used to solve equation- 5.11. Finally, peak displacement, inter-storey drift and base-shear force are estimated for 1-mode, 2-modes and 3-modes combination. In the result and discussion section, all types of structures are discussed here separately so that the applicability of the MPA for seismic demand calculation for different SPSW systems can be evaluated.

MPA for low-rise (4-storey) SPSW shows that, only 1$^{st}$ mode pushover analysis is enough to predict floor displacement as well as inter-storey drift. Therefore, higher mode effect is negligible for low-rise building. To include 90% of effective mass, first two modes can be used for MPA. Floor displacement pattern was close to the average result of Nonlinear Time History Analysis (NTHA) of MDOF system. 13.5% maximum error was found in 2$^{nd}$ storey displacement. Roof displacement of MPA and NTHA was much closer than intermediate floor displacement, it shows that NTHA displacement pattern are not closely following its mode shape pattern. Inter-storey drift estimated by MPA can predict close to the NTHA response. Here, inter-storey drift was underestimated in the bottom 2-storeys but overestimated for the top.

MPA for medium-rise (8-storey) SPSW shows that, 1-mode combination can predict floor displacement very well and 2-mode combination can improve the prediction. 3rd-mode contribution is negligible for medium-rise building. In addition, to include 90% of effective mass, only first two modes can be used for MPA. Floor displacement pattern of 1-mode combination was relatively close to the average result of Nonlinear Time History Analysis (NTHA) of MDOF system. After adding 2nd-mode, floor displacement of lower storeys is improved and 9.28% maximum discrepancy was observed in 2nd-storey displacement. Overall floor displacement of MPA and NTHA was very close but little underestimated. Difference of the Inter-storey drifts estimated by MPA and NTHA were variable with height of the structure. For the lower and upper level, inter-storey drifts was underestimated but overestimated for the intermediate storeys. 2-mode combination predicts very well where maximum difference was noted at the 4th-storey.

MPA for high-rise (15-storey) SPSW shows considerable higher mode contribution. 1-mode combination predicts floor displacement pretty well, where 2-mode combination improves the prediction. 3rd mode contribution is relatively smaller than 2nd mode contribution. It has been observed that "reversal" occurs in 2nd- and 3rd-mode pushover curves. Elastic analysis was performed for those modes. For this high-rise structure, maximum displacement from elastic analysis of 2nd-mode SDOF system showed that, the maximum displacement was not in elastic range. According to Goel and Chopra (2005), "reversal" in pushover can also be avoided by using another storey displacement as the reference displacement. "Reversal" in pushover curve using roof displacement can be eliminated in the base shear versus any floor above the local plastic hinge displacement. This approach was adopted for the MPA for 2nd-mode contribution of

15-storey SPSW. It was observed that, 5th storey local plastic hinge formed during the "2nd-mode" pushover analysis. Therefore, pushover curve for base-shear versus 6th-storey displacement as presented in Figure 5.10, which is a "regular" pushover curve, is considered for 15-storey 2nd mode. After that, all other MPA steps were conducted with this new pushover curve. Nonlinear analysis was performed to solve equation 5.11 with this new pushover curve. 2-mode combination of MPA shows very good prediction in terms of floor displacement and inter-storey drift.

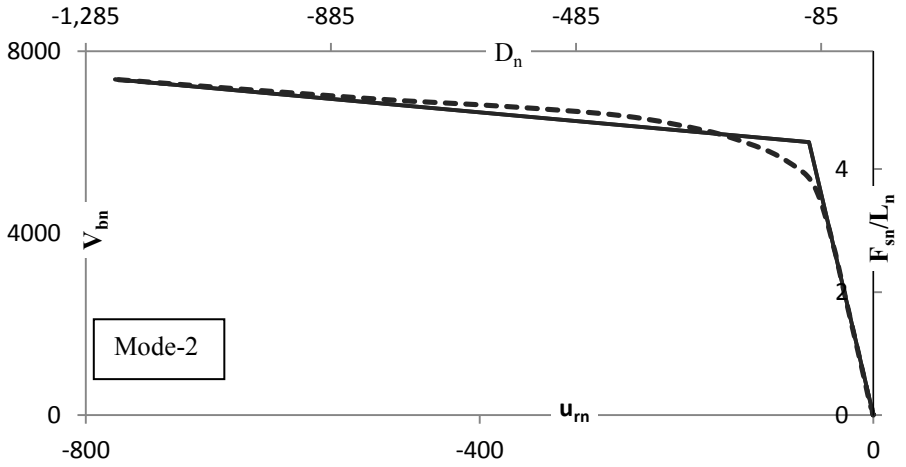


Figure 5.10 : Actual, idealized pushover curve of MDOF ($V_{bn}$-$u_{rn}$) and SDOF systems ($F_{sn}/L_n$-$D_n$) for 15-storey SPSW system for 2nd mode with 6th floor displacement

3-mode combination represents very good roof displacement and inter-storey drift. Overall Floor displacement pattern of 2-mode combination was similar to the average floor displacement of Nonlinear Time History Analysis (NTHA) of MDOF system. After adding 2nd and 3rd mode, floor displacement of lower storeys are improved while difference between MPA and NTHA for top 3-storeys are not too much affected. Overall floor displacement of MPA and NTHA was very close but little underestimated. Unlike low-rise and medium-rise building,

discrepancy between MPA and NTHA for Inter-storey drifts was variable with height of the structure.

Base shear for each mode and mode-combination are presented in Tables 5-2, 5-3 and 5-4, It has been observed that adding $2^{nd}$ and $3^{rd}$-mode base shear contribution exceeded the average base shear of NTHA. Thus, using this modal combination rule for base shear or any other force calculation cannot provide realistic estimation. This was also observed by other researchers (Chopra and Goel 2004) for ductile moment resisting frames.

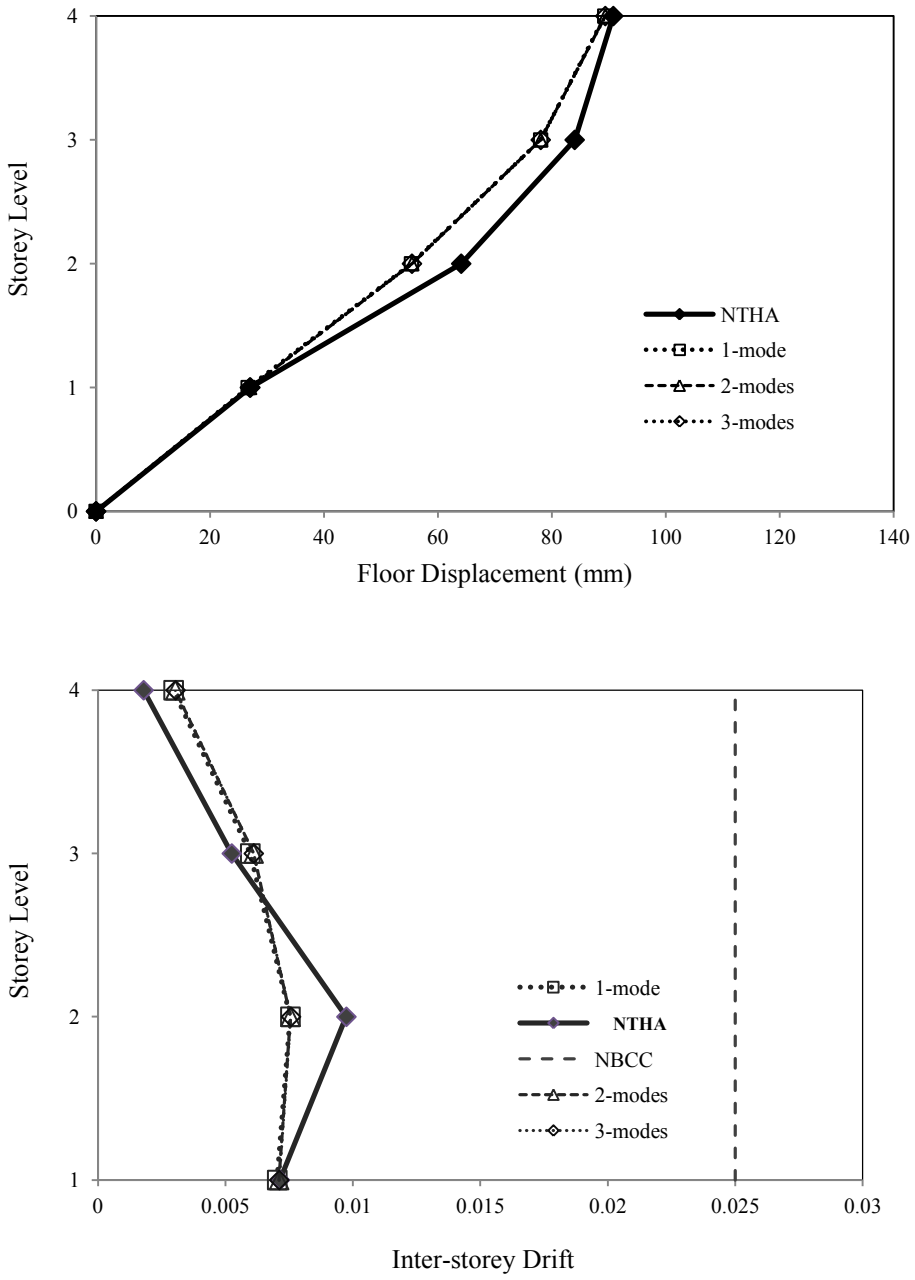


Figure 5.11: Height wise variation of floor displacements and inter-storey drift from MPA and NTHA for average response under selected ground motion records for 4-storey SPSW

Table 5-2: seismic performance evaluation of 4-storey SPSW using MPA and NTHA for average response under selected ground motion records

| Parameters | storey | Modal Response | | | MPA | | | NTHA |
|---|---|---|---|---|---|---|---|---|
| | | Mode-1 | Mode-2 | Mode-3 | 1 mode | 2 mode | 3 Mode | |
| Floor Displacement (mm) | 1st | 26.7 | -3.9 | -1.14 | 26.7 | 26.9 | 27.00 | 27.09 |
| | 2nd | 55.4 | -3.1 | 1.01 | 55. 4 | 55.4 | 55. 5 | 64.1 |
| | 3rd | 78.04 | 1.75 | 0.06 | 78.04 | 78.06 | 78.06 | 84.02 |
| | 4th | 89.3 | 4.15 | -0.93 | 89.3 | 89.4 | 89.39 | 90.8 |
| Inter-storey Drift | 1st | 0.007 | -0.001 | 3E-4 | 0.007 | 0.0071 | 0.0071 | 0.0071 |
| | 2nd | 0.008 | 0.0002 | 6E-4 | 0.008 | 0.0075 | 0.0075 | 0.0097 |
| | 3rd | 0.006 | 0.0013 | 2.5E-4 | 0.006 | 0.0061 | 0.0061 | 0.0052 |
| | 4th | 0.003 | 0.0006 | 2.6E-4 | 0.003 | 0.0030 | 0.003 | 0.0018 |
| Base Shear (KN) | | 4845.5 | 1910 | 17626 | 4845.5 | 5208.5 | 5498 | 5053 |

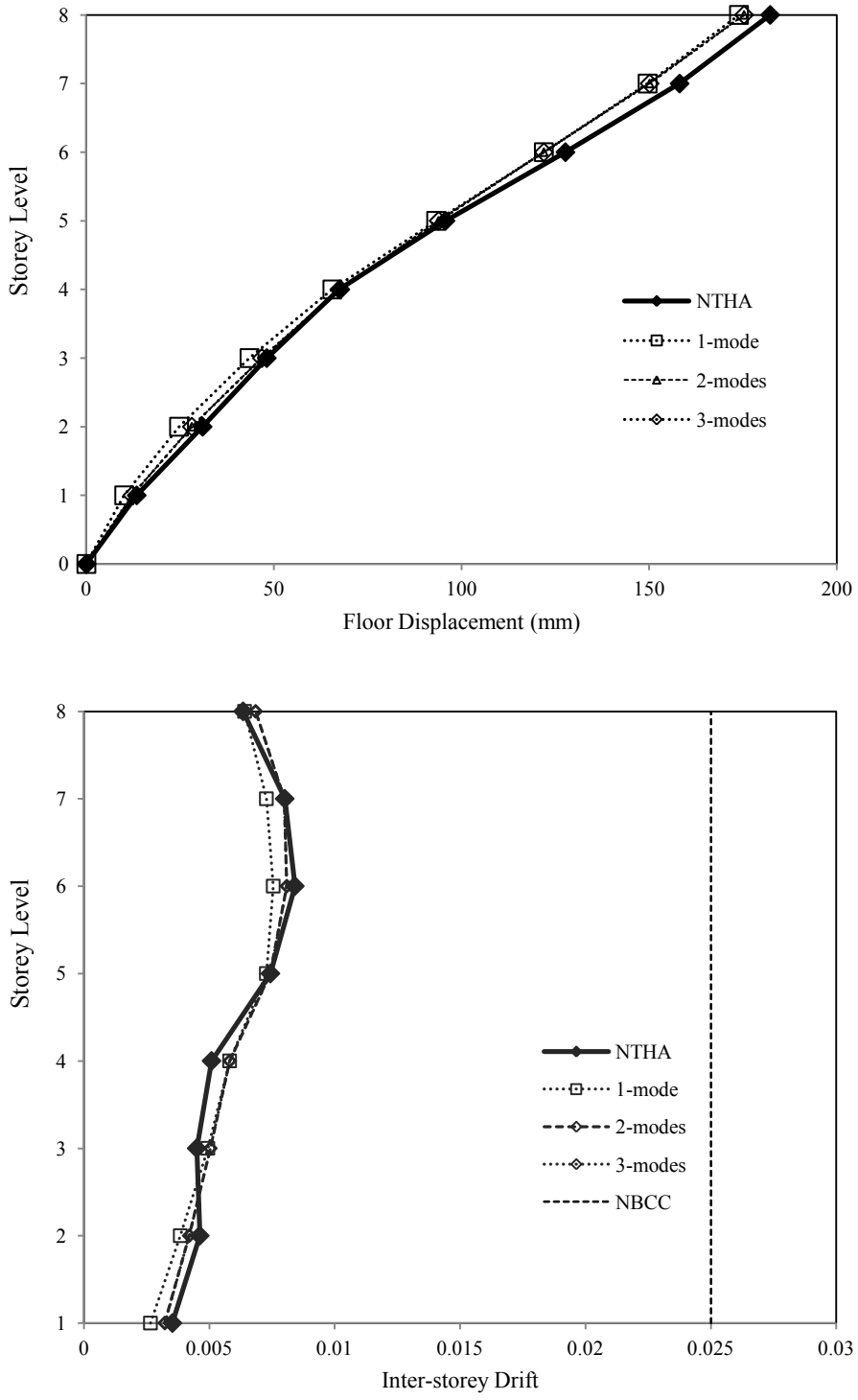


Figure 5.12: Height wise variation of floor displacements and inter-storey drift from MPA and NTHA for average response under selected ground motion records for 8-storey SPSW

Table 5-3: Seismic performance evaluation of 8-storey SPSW using MPA and NTHA for average response under selected ground motion records

| Parameters | storey | Modal Response | | | MPA | | | NTHA |
|---|---|---|---|---|---|---|---|---|
| | | Mode-1 | Mode-2 | Mode-3 | 1 mode | 2 mode | 3 Mode | |
| Floor Displacement (mm) | 1st | 0.00 | 0.00 | 0.00 | 0.00 | 0.00 | 0.00 | 13.42 |
| | 2nd | 10.09 | -6.96 | -0.41 | 10.09 | 12.25 | 12.26 | 30.98 |
| | 3rd | 24.70 | -13.40 | -0.60 | 24.70 | 28.09 | 28.10 | 48.08 |
| | 4th | 43.48 | -17.20 | -0.40 | 43.48 | 46.76 | 46.76 | 67.43 |
| | 5th | 65.56 | -16.77 | 0.08 | 65.56 | 67.67 | 67.67 | 95.70 |
| | 6th | 93.22 | -11.03 | 0.66 | 93.22 | 93.87 | 93.87 | 127.66 |
| | 7th | 121.91 | 0.02 | 0.48 | 121.91 | 121.91 | 121.91 | 158.10 |
| | 8th | 149.56 | 12.57 | -0.29 | 149.56 | 150.09 | 150.09 | 182.22 |
| Inter-storey Drift | 1st | 173.91 | 21.75 | -0.72 | 173.91 | 175.27 | 175.27 | 3.5E-3 |
| | 2nd | 3.84E-3 | -1.7E-3 | -5.1E-5 | 3.8E-3 | 4.2E-3 | 4.2E-3 | 4.6E-3 |
| | 3rd | 4.94E-3 | -1.0E-3 | 5.3E-5 | 4.9E-3 | 5.0E-3 | 5.0E-3 | 4.5E-3 |
| | 4th | 5.81E-3 | 1.1E-4 | 1.3E-4 | 5.8E-3 | 5.8E-3 | 5.8E-3 | 5.1E-3 |
| | 5th | 7.28E-3 | 1.5E-3 | 1.5E-4 | 7.3E-3 | 7.4E-3 | 7.4E-3 | 7.4E-3 |
| | 6th | 7.55E-3 | 2.9E-3 | -4.6E-5 | 7.6E-3 | 8.1E-3 | 8.1E-3 | 8.4E-3 |
| | 7th | 7.28E-3 | 3.3E-3 | -2.0E-4 | 7.3E-3 | 7.9E-3 | 7.9E-3 | 8.0E-3 |
| | 8th | 6.41E-3 | 2.4E-3 | -1.1E-4 | 6.4E-3 | 6.9E-3 | 6.9E-3 | 6.3E-3 |
| Base Shear (KN) | | 4477.3 | 6792.6 | 894.18 | 4477.3 | 8135 | 8184.5 | 6682.7 |

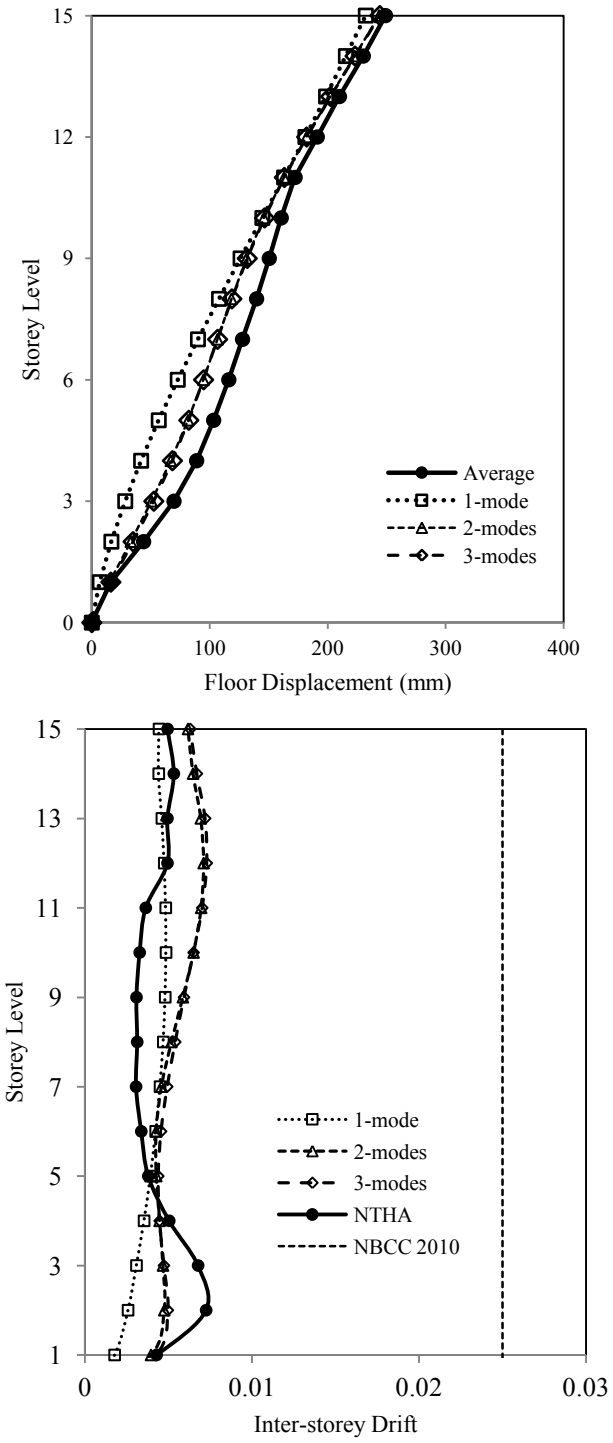


Figure 5.13: Height wise variation of floor displacements and inter-storey drift from MPA and NTHA for average response under selected ground motion records for 15-storey SPSW

Table 5-4: Seismic performance evaluation of 15-storey SPSW using MPA and NTHA for average response under selected ground motion records

| Parameters | storey | Modal Response | | | MPA | | | NTHA |
|---|---|---|---|---|---|---|---|---|
| | | Mode-1 | Mode-2 | Mode-3 | 1 mode | 2 mode | 3 Mode | |
| Floor Displacement (mm) | 1st | 6.77 | 13.43 | 5.87 | 6.77 | 15.04 | 16.15 | 16.32 |
| | 2nd | 16.59 | 28.58 | 11.38 | 16.59 | 33.05 | 34.95 | 43.9 |
| | 3rd | 28.32 | 41.93 | 14.21 | 28.32 | 50.60 | 52.56 | 69.66 |
| | 4th | 41.79 | 52.29 | 13.65 | 41.79 | 66.94 | 68.32 | 88.85 |
| | 5th | 56.74 | 58.65 | 9.80 | 56.74 | 81.61 | 82.19 | 103.3 |
| | 6th | 72.85 | 60.41 | 3.66 | 72.85 | 94.64 | 94.71 | 116.1 |
| | 7th | 89.95 | 57.14 | -3.28 | 89.95 | 106.57 | 106.62 | 127.7 |
| | 8th | 107.80 | 48.82 | -9.19 | 107.80 | 118.34 | 118.70 | 139.6 |
| | 9th | 126.08 | 36.05 | -12.57 | 126.08 | 131.13 | 131.73 | 150.4 |
| | 10th | 144.54 | 19.60 | -12.49 | 144.54 | 145.87 | 146.40 | 160.5 |
| | 11th | 162.94 | 0.60 | -8.86 | 162.94 | 162.94 | 163.18 | 172.3 |
| | 12th | 181.01 | -19.49 | -2.62 | 181.01 | 182.06 | 182.07 | 191.1 |
| | 13th | 198.53 | -39.20 | 4.69 | 198.53 | 202.36 | 202.42 | 209.9 |
| | 14th | 215.33 | -57.19 | 11.31 | 215.33 | 222.79 | 223.08 | 230.1 |
| | 15th | 232.20 | -73.48 | 16.27 | 232.20 | 243.55 | 244.09 | 248.9 |
| Inter-storey Drift | 1st | 1.8E-3 | 3.5E-3 | 1.5E-3 | 1.8E-3 | 4.0E-3 | 4.2E-3 | 4.3E-3 |
| | 2nd | 2.6E-3 | 4.0E-3 | 1.4E-3 | 2.6E-3 | 4.8E-3 | 5.0E-3 | 7.3E-3 |
| | 3rd | 3.1E-3 | 3.5E-3 | 7.5E-4 | 3.1E-3 | 4.7E-3 | 4.7E-3 | 6.8E-3 |
| | 4th | 3.5E-3 | 2.7E-3 | -1.5E-4 | 3.5E-3 | 4.5E-3 | 4.5E-3 | 5.0E-3 |
| | 5th | 3.9E-3 | 1.7E-3 | -1.0E-3 | 3.9E-3 | 4.3E-3 | 4.4E-3 | 3.8E-3 |
| | 6th | 4.2E-3 | 4.6E-4 | -1.6E-3 | 4.2E-3 | 4.3E-3 | 4.6E-3 | 3.4E-3 |
| | 7th | 4.5E-3 | -8.6E-4 | -1.8E-3 | 4.5E-3 | 4.6E-3 | 4.9E-3 | 3.1E-3 |
| | 8th | 4.7E-3 | -2.2E-3 | -1.6E-3 | 4.7E-3 | 5.2E-3 | 5.4E-3 | 3.1E-3 |
| | 9th | 4.8E-3 | -3.4E-3 | -8.9E-4 | 4.8E-3 | 5.9E-3 | 5.9E-3 | 3.1E-3 |
| | 10th | 4.9E-3 | -4.3E-3 | 2.2E-5 | 4.9E-3 | 6.5E-3 | 6.5E-3 | 3.3E-3 |
| | 11th | 4.8E-3 | -5.0E-3 | 9.5E-4 | 4.8E-3 | 7.0E-3 | 7.0E-3 | 3.6E-3 |
| | 12th | 4.8E-3 | -5.3E-3 | 1.6E-3 | 4.8E-3 | 7.1E-3 | 7.3E-3 | 4.9E-3 |
| | 13th | 4.6E-3 | -5.2E-3 | 1.9E-3 | 4.6E-3 | 6.9E-3 | 7.2E-3 | 4.9E-3 |
| | 14th | 4.4E-3 | -4.7E-3 | 1.7E-3 | 4.4E-3 | 6.5E-3 | 6.7E-3 | 5.3E-3 |
| | 15th | 4.4E-3 | -4.3E-3 | 1.3E-3 | 4.4E-3 | 6.2E-3 | 6.3E-3 | 5.0E-3 |
| Base-Shear (KN) | | 2863 | 5040 | 2895 | 2863 | 5796 | 6479 | 5749.25 |

## 5.5 Applicability of CSM and MPA

Top storey displacement demand has been estimated for low-rise, medium rise and high-rise SPSW system by conducting Capacity-spectrum method and Modal Pushover analysis. Displacement demands of all three SPSW are now presented in Figure 5.14. It is clear from this comparative study, top storey displacement demand of a low-rise building can be predicted accurately by both of the nonlinear static analysis procedure. For rapid performance evaluation, CSM can be carried out for low-rise SPSW, while it provides conservative estimation for mid-rise and high-rise SPSW system. CSM can be performed to estimate ductility demand for a given level for hazard. However, MPA estimates very close top-storey displacement for all height of SPSW systems. For all type of building, MPA can be performed to estimate top displacement, floor displacement and inter-storey drift.

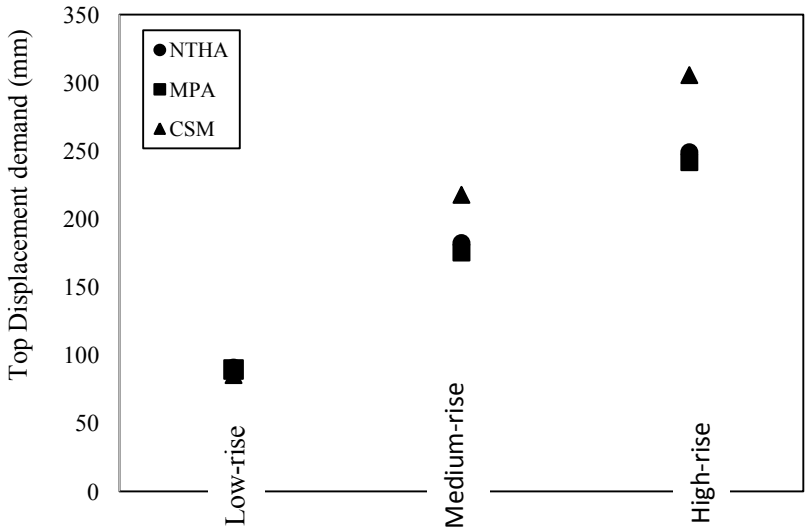


Figure 5.14: Comparison between capacity-spectrum method and modal pushover method for all SPSWs

## 5.6 Summary

Effective and relatively simple seismic performance evaluation is an important concern of performance based seismic design. Therefore, various nonlinear static procedures are used by professional engineers. MPA is one of the simple and effective nonlinear static analysis techniques for seismic performance evaluation as well seismic demand calculation. MPA was applied on law-rise, medium-rise and high-rise SPSW system to investigate its applicability and accuracy for seismic performance evaluation. "Modal" pushover analysis was performed on MDOF system with inertia force distribution of different modes of vibration. Each MDOF system was transformed into a number of SDOF systems for different modal response. Modal response of each SDOF system was combined by using SRSS.

MPA can predict seismic behavior very well when compared with nonlinear dynamic analysis results. Only the first mode in MPA method is enough to evaluate seismic performance of low-rise SPSW system. Higher mode effects are negligible for low-rise buildings with SPSWs. Local mechanism were found in higher mode pushover analysis. However, local mechanism was not observed during nonlinear dynamic analysis.

In medium-rise and high-rise SPSW building, MPA shows that only the first mode is not enough for predicting seismic performance of SPSW and the prediction can be improved when first two modes are considered. Local mechanism was also observed in higher mode pushover analysis, however, it was not observed in nonlinear dynamic analysis. "Reversal" in pushover can be found for higher mode pushover analysis which is also very unlikely to observe in seismic analysis. MPA with fundamental "mode" showed inelastic behavior. For the higher "mode" of

low-rise and medium-rise building, the displacements were within elastic limit, meaning that, the structures remained elastic when vibrated in higher modes. Only 2nd-mode of high-rise building showed inelastic behavior during the analysis.

Finally, applicability of CSM and MPA were compared for roof displacement of selected SPSW systems. It was noticed that, CSM can offer very good estimation for Low-rise SPSW where, effectiveness of MPA was consistent for all type of SPSW.

# Chapter-Six
# Summary, Conclusion and Recommendations

## 6.1 Summary

A finite element model has been developed to study the behavior of unstiffened steel plate shear walls with rigid beam-to-column connections. Material and Geometrical nonlinearities were considered for this modeling. The finite element model was validated using the results from two quasi-static experimental programs. The validated FE model was used to study seismic performance of one 4-storey and one 8-storey steel plate shear wall in Vancouver. The SPSWs were designed according to capacity design provision of CAN/CSA S16-09. Nonlinear seismic analysis was performed under real and simulated ground motion records to estimate important seismic performance parameters, such as storey displacements, inter-storey drift, and base shear of the selected steel plate shear walls.

Seismic performance evaluation of the selected SPSWs was carried out using capacity spectrum method. Capacity-spectrum method is a nonlinear static analysis procedure, which has been performed to estimate seismic displacement demand and ductility demand of previously designed steel plate shear walls. Standard design response spectrum of Vancouver was converted to inelastic demand spectrum and nonlinear pushover curve was converted in to capacity curve of an equivalent-single-degree of freedom system. Inelastic displacement demand and ductility demand of the structures were estimated to evaluate seismic performance of the selected SPSW buildings.

Another nonlinear static analysis procedure used to evaluate seismic performance of SPSWs was modal pushover analysis. Higher mode contribution of the building performance was considered in modal pushover analysis. Critical seismic performance parameters, such as inter-storey drift and floor displacement have been estimated from modal pushover analysis. Finally, applicability of these nonlinear static analysis procedures for seismic performance evaluation was determined by comparing their results with more accurate nonlinear dynamic analysis results.

## 6.2 Conclusion

Major finding of the research project are listed below:

- The finite element model developed in this study was able to provide reasonably accurate predictions of the behaviour of SPSW. Excellent agreement was observed between results from FE analysis and results from quasi-static tests of SPSW specimens with different geometry. . The finite element model was capable to capture all essential features of the test specimens, such as initial stiffness, ultimate strength.
- 4-storey and 8-storey SPSWs with moment resisting frame behaved as per the capacity design approach. Bottom storeys steel infill plates and beam-ends were yielded in most of the events. While partial yielding was observed in columns bases in some cases boundary columns were essentially elastic for all seismic analysis. Berman and Bruneau (2008) capacity design approach served well under selected ground motion records.
- Estimated inter-storey drifts for all of the seismic events were within the NBCC2010 drift limit of 2.5% of the storey height. Displacement patterns and inter-storey drift patterns were comparable to each other. Maximum dynamic base shear of SPSWs were

larger than the equivalent static base shear and probable storey shear resistance of SPSWs. A considerable amount of the shear contribution by the boundary columns was recognised.

- Excellent accuracy of capacity-spectrum method was noticed for low-rise SPSW in terms of top displacement demand and ductility demand. The disagreement between nonlinear seismic analysis and capacity-spectrum method increased with an increase in building height. This is because, for high-rise SPSW, contributions from higher modes are not considered in capacity spectrum method.
- Great efficiency of modal pushover analysis was observed for seismic performance evaluation of SPSW systems. Storey displacement and inter-storey drifts for low-rise, medium-rise and high-rise SPSWs were predicted very well. Higher mode contribution was accounted for medium-rise and high-rise SPSWs, which is not possible for conventional pushover analysis. For almost all cases, first two modes were enough to predict the response parameters accurately. That is, adding the third mode contribution did not improve the responses noticeably. This observation indicate that for SPSW, second mode compared to the third or higher modes contributes more, is similar to that observed in earlier studies for moment resisting frames.
- Capacity-spectrum method provided good prediction of seismic response parameters for 4-storey SPSW. CSM can be performed to estimate seismic behavior of low-rise SPSW as a rapid evaluation procedure. However, MPA is applicable for all type of buildings, especially for high-rise SPSW buildings, where significant higher mode contribution is expected.

## 6.3 Recommendations for Future Study

A few number of steel plate shear walls have been analysed in this research project. More steel plate shear walls with different geometry and height needed to be analyzed. To date most of the research, including current research, mainly focus on planar SPSWs. It would be interesting to examine the behaviour of SPSWs when subjected to torsional and transverse loading. A three dimensional dynamic analysis will be required for that study.

One of the limitations for the capacity spectrum method is that it only considers the initial elastic stiffness in performance estimation. Thus, future research is required to incorporate tangent stiffness of the lateral load resisting system in the capacity spectrum method.

One of the limitation for the modal pushover analysis is, it cannot ensure very consistent estimation for inter-storey drift. Discrepancy between MPA and NTHA for inter-storey drift was variable with building height. Modal combination role of MPA often fails to estimated base shear demand for structures.

This research has not included the evaluation of the accuracy of MPA procedure for SPSW buildings with unsymmetrical plans, where torsion effects will occur. Future research is required in this area. The current research on MPA did not consider steel plate shear wall with MRF (dual system). Since total lateral load in any direction is now shared by both SPSW and MRF, the behaviour of this dual system will be different from SPSW alone. Future research can be conducted on modal pushover analysis of steel shear wall-frame systems.

# References


ANSI/AISC. 2005. Seismic Provisions for Structural Steel Buildings. American Institute of Steel Construction Inc, Chicago, Illinois.

ANSI/AISC. 2010. Seismic Provisions for Structural Steel Buildings. American Institute of Steel Construction Inc, Chicago, Illinois.

Applied Technology Council. 1992. Guidelines for Cyclic Seismic Testing of Components of Steel Structures. ATC-24, Redwood City, California.

Applied Technology Council. 1996. Seismic Evaluation and Retrofit of Concrete Buildings, ATC-40. Seismic Safety Commission, State of California, California.

Army. 1986. Seismic Design Guidlines for Essential Buildings. Depatment of Army( TM 5-809-10-1); Navy (NAVFAC P355.1); Air force (AFM 88-3, Chapter 13, Section A), Washington, D.C.

ASCE. 2010. Minimum Design Loads for Buildings and Other Structures. American Society of Civil Engineers, Virginia.

Atkinson, G.M. 2009. Earthquake Time Histories Compatible with the 2005 NBCC Uniform Hazard Spectrum. www.seismotoolbox.ca .

Behbahanifard, M., Gilbert, R., Grondin, Y., and Elwi, A.E., 2003. Experimental and Numerical Investigation of Steel Plate Shear Walls. Department of Civil and Environmental Engineering, University of Alberta, Edmonton.

Berman, J.W., and Bruneau, M. 2008. Capacity design of vertical boundary elements in steel plate shear walls. ASCE, Engineering Journal, first quarter 57-71.

Berman, J.W., and Bruneau, M. 2003. Plastic Analysis and Design of Steel Plate Shear Walls. ASCE Journal of Structural Engineering 11 (129): 1448-1456.

Berman, J.W., and Bruneau, M. 2004. Steel Plate Shear Walls Are Not Plate Girders. AISC Engineering Journal, Third Quarter: 95-106.

Bhowmick, A.K., Grondin, G.Y. and Driver, R.G. 2011. Estimating Fundamental Periods Of Steel Plate Shear Walls. Journal of Engineering Structures 33: 1883-1893.

Bhowmick, A.K., Driver, R.G. and Grondin, G.Y. 2009. Seismic Analysis Of Steel Plate Shear Walls Considering Strain Rate And P–Delta Effects. Journal of Constructional Steel Research 65 (5): 1149-1159. doi:10.1016/j.jcsr.2008.08.003.

Bhowmick, A.K. 2009. Seismic Analysis and Design of Steel Plate Shear Walls. University of Alberta, Edmonton.

Blume, J.A.N., Newmark, M. and Corning, L.M. 1960. Design of Multi-story Reinforced Concrete Buildings for Earthquake Motions, Portland Cement Association, Chicago, U.S.A.

Caccese, V., Elgaaly, M. and Chen, R. 1993. Experimental Study of Thin Steel-plate Shear Walls Under Cyclic Load. ASCE Journal of Structural Engineering 199 (2): 573-587.

Chopra, A.K, and Goel, R.K. 2000. Evaluation Of NSP To Estimate Seismic Deformation: SDF Systems. Journal of Structural Engineering 126 (4): 482-490.

Chopra, A.K., and Goel, R.K. 1999. Capacity-Demand-Diagram Methods for Estimaing Seismic Deformation of Inelastic tructures: SDF Systems. Urban Earthquake Disaster Mitigation, University of California, Pacific Earthquake Engineering Research Center, California.

Chopra, A.K. 2007. Dynamics of Structures-Theory and Applications to Earthquake Engineering. 3rd. Prentice Hall, New Jersey.

Chopra, A.K., Goel, R.K. and Chintanapakdee, C. 2004. Evaluation of A Modified Mpa Procedure Assuming Higher Modes As Elastic to Estimates Seismic Demands. Earthquake Spectra 20 (3): 757-778.

Chopra, A.K., and Goel, R.K. 2001. A Modal Pushover Analysis Procedure to Estimate Seismic Demans for Buildings: Theory and Priliminary Evaluation. Pacific Earthquake Engineering Research Center, California.

CSA. 2001. Limit States Design of Steel Structures. Canadian Standards Association, Willowdale, Ontario, Canada.

CSA. 2009. Limit states design of steel structures. Canadian Standards Association. Toronto, Ontario.

Cuesta, I.M., Aschheim, A. and Fajfar, P. 2003. Simplified R-Factor Relationships for Strong Ground Motions. Earthquake Spectra (Earthquake Engineering Research Institute) 19 (1): 25-45. doi:0.1193/1.1540997.

Cui, X., Xingwen L., and Li Xin. 2009. Direct Displacement-Based Seismic Design Method of High-Rise Buildings Considering Higher Mode Effects. International Symposium on Computational Structural Engineering. 253-265. Shanghai, China. doi:10.1007/978-90-481-2822-8_29.

Driver, R.G., Kulak, G.L. Elwi, A.E. and Kennedy, D.J.L. 1998. Cyclic Tests of Four-Story Steel Plate Shear Wall. ASCE Journal of Structural Engineering 124 (2): 112-120.

Driver, R.G., Kulak, G.L., Kennedy, D.J.L. and Elwi, A.E. 1997. Seismic Behaviour of Steel Plate Shear Walls; Structural Engineering Report No. 215. Department of Civil Engineering, University of Alberta, Edmonton, Alberta, Canada.

Elgaaly, M. 1998. Thin Steel Plate Shear Walls Behaviour and Analysis. Thin-Walled Structures 32: 151-180.

Elgaaly, M., Caccese, V. and Du, C. 1993. Post-Buckling Behaviorof Steel-Plate Shear Walls under Cyclic Loads. ASCE Journal of Structural Engineering 199 (2): 588-605.

Fajfar, P. 1999. Capacity Spectrum Method Based on Inelastic Demand Spectra. Earthquake Engineering and Structural Dynamics 28 (9): 979-993.

Fajfar, P. 1996. Design Spectra for the New Generation of Codes. Eleventh World Conference on Earthquake Engineering. Elsevier Science Ltd. Paper No. 2127.

FEMA. 2005. Improvement of Nonlinear Static Seismic Analysis Procedures, FEMA-440. Applied Technology Council (ATC-55 Project), Washington, D.C.

FEMA. 1997. NEHRP Guidlines for the Seismic Rehabilitation of Buildings, FEMA-273. Applied Technology Council for the Building Seismic Safety Council, the Federal Emergency Management Agency, Washinton,D.C, USA.

FEMA. 2000. Prestandard and Commentary for the Seismic Rehabilitation of Buildings, FEMA-356. American Society of Civil Engineers. Federal Emergecy Management Agency, Washington, D.C.

Freeman, S A. 1998. Development and Use of Capacity Spectrum Method. 6th US NCEE Conference on Earthquake Engineering/ EERI, Seattle, Washington

Freeman, S.A. 2004. Review of the Development of the Capacity Spectrum Method. Journal of Earthquake Technology (ISET) 41 (1): 1-13.

Freeman, S.A., Nicoletti, J.P. and Matsumura, G. 1984. Seimic Design Guidlines for Essential Buildings. 8th World Conference on Earthquake Engineering. San Francisco, California, U.S.A. 717-722.

Freeman, S.A, Nicoletti, J.P. and Tyrell, J.V. 1975. Evaluations of Existing Buildings for Seismic Risk-A Case Study of Puget Sound Naval Shipyard. U.S. National Conference on Earthquake Engineers. EERI. Bremerton, Washington, 113-122.

Goel, R.K., and Chopra, A.K. 2003. Evaluation of Modal and FEMA pushover analysis: SAC Buildings. California: SAC, USA.

Goel, R.K., and Chopra. A.K. 2005. Role of Higher-"Mode" Pushover Analysis in Seismic Analysis of the Buildings. Earthquake Spectra 21 (5): 1027-1041.

Hibbitt, Karlsson, and Sorensen. 2011. ABAQUS/Standard User's Manual. Pawtucket, RI: HKS Inc.

Humar, J., Farrokh F., Ghorbanie-Asl, M. and Freddy E. Pina. 2011. Displacement-based seismic design of regular reinforced concrete shear wall buildings. *Canadian Journal of Civil Engineering* 38 (6): 616-626.

Jianmeng, M., Zhai., and Xie L. 2008. An improved model pushover analysis procedure for estimation seismic demans of structures. Earthquake Engineering and Engineering Vibration 7 (1): 25-31.

John, A. and Halchuk S. 2003. Fourth Generation Seismic Hazard Maps of Canada: Values for over 650 Canadian Localities Intended for the 2005 National Building Code of Canada. Geological Survey of Canada, Ottawa.

Krawinkler, H.E.L. and Nassar, A., A. 1992. Seismic design based on ductility and cumulative damage demands and capacities. In Nonlinear seismic analysis and design of reinforced concrete buildings , edited by P Fajfar and H Karwinkler, 23-39. Elsevier Applied Science, New York.

Krawinkler, H., and Seneviratna, G.D.P.K. 1998. Pros and Cons of a Pushover Analysis of Seismic Performance Evaluation. Journal of Enginering Structures 20 (4-6): 452-464.

Lamontagne, M.S., Halchuk, J.F., Cassidy, and Rogers, G.C. 2008. Significant Canadian Earthquakes of the Period 1600–2006. Seismological Research Letters 79 (2): 211-224. doi:10.1785/gssrl.79.2.211.

Lubell, A.S., Prion, H.G.L., Ventura C.E., and Rezai, M. 2000. Unstiffened Steel Plate Shear Wall Performance Under Cyclic Load. Journal of Structural Engineering, ASCE 126 (4): 453-460.

Naumoski, N., Murat S., and Kambiz, Amiri-Hormozaki. 2004. Effects of Scaling of Earthquake Excitations on the Dynamic Response of Reinforced Concrete Frame Buildings. 13th World Conference on Earthquake Engineering, Vancouver.

NBCC. 2010. National Building Code of Canada. Canadian Commission on Building and Fire Codes. National Research Council of Canada (NRCC), Ottawa, Onterio.

Newmark, N.M., and Hall, W.J. 1982. Earthquake Spectra and Design. Earthquake Engineering Research Inst. Berkeley, California.

PEER. 2010. Next Generation Attenuation of Ground Motions Project (NGA) Database. Pacific Earthquake Engineering Research Center, Berkely, California.

Rezai, M. 1999. Seismic Behavior of Steel Plate Shear Walls by Shake Table Testing. Department of Civil Engineering, Universityof British Columbia. Vancouver, Canada

Saatcioglu, M., and Humar, J. 2003. Dynamic Analysis of building for Earthquake Resistent Design. Canadian Journal od Civil Engineering 30: 338-359. doi:10.1139/L02-108.

SEAOC. 1995. Vision 2000: Performance-BAsed Seismic Engineering of Buildings. Structural Engineers Association of California, Sacramento, California.

Seilie, F.I., and John, H.D. 2005. Steel Plate Shear Walls: Practical Design and Construction. Steel Modern Steel Construction, 45.4 (2005): 37-43.) 45 (4): 37-43.

Thorburn, L.J., Kulak, G.L. and Montgomery, C.J. 1983. Analysis of Steel Plate Shear Walls, Structural Report No. 107. Department of Civil and Environmental Engineering, University of Alberta, Edmonton, Alberta.

Timler, P.A., and Kulak, G.L. 1983. Experimental Study of Steel Plate Shear Walls. Structural Engineering Report No. 114. Dept. of Civil Engineering, university of Alberta, Edmonton, AB.

Vidic, T, Fajfar, P., and Fischinger, M. 1994. Consistent Inelastic Design Spectra: Strength and Displacement. Earthquake Engineering and Structureal Dynamics 23 (5): 507-521. doi:10.1002/eqe.4290230504.

Wagner, H. 1931. Flat Sheet Metal Girders with Very Thin Webs, Part-1- General Theories and Assumptions. Technical Memo No. 604. National Advisory Committee for Aeronautics. Washington, DC.

Wang, Y., and Yang, P. 2000. A Study on Improvement of Pushover Analysis. 12th World Conference of Earthquake Engineering, New Zeland.

Yu, K., Qi-Song, Raymond P., Michael A., and Carrie B. 2004. Assessment of Modal Pushover Analysis Procedure and Its Application to Seismic Eveluation of Existing Buildings. 13th World Conference on Earthquake Engineering, Vancouver.